Federal University of Ceará
Postgraduate Program in Electrical and Computer Engineering

Tensor-Based Multiuser Detection for Cooperative Wireless Communications Systems

Master of Science Thesis

Author
Antonio Augusto Teixeira Peixoto

Advisor
Prof. Dr. Carlos Alexandre Rolim Fernandes

Sobral – Brazil
June 2017

Universidade Federal do Ceará
Programa de Pós-graduação em Engenharia Elétrica e de Computação

Detecção Multiusuário baseada em Tensores para Sistemas de Comunicação sem fio Cooperativos

Autor
Antonio Augusto Teixeira Peixoto

Orientador
Prof. Dr. Carlos Alexandre Rolim Fernandes

Dissertação apresentada à Coordenação do Programa de Pós-graduação em Engenharia Elétrica e de Computação da Universidade Federal do Ceará como parte dos requisitos para obtenção do grau de ***Mestre em Engenharia Elétrica e de Computação****. Área de concentração: Sistemas de Comunicação.*

Sobral – Brasil
Junho 2017

Antonio Augusto Teixeira Peixoto

Tensor-Based Multiuser Detection for Cooperative Wireless Communications Systems

Dissertação apresentada ao Programa de Pós-graduação em Engenharia Elétrica e de Computação da Universidade Federal do Ceará, como requisito parcial para a obtenção do título de Mestre em Engenharia Elétrica e de Computação. Área de concentração: Sistemas de Comunicação.

Aprovoda em: 28/07/2017.

BANCA EXAMINADORA

Prof. Dr. Carlos Alexandre Rolim Fernandes (Orientador)
Universidade Federal do Ceará (UFC)

Prof. Dr. André de Almeida Lima Férrer
Universidade Federal do Ceará (UFC)

Prof. Dr. Leandro Ronchini Ximenes
Universidade Estadual de Campinas (Unicamp)

Dados Internacionais de Catalogação na Publicação
Universidade Federal do Ceará
Biblioteca Universitária
Gerada automaticamente pelo módulo Catalog, mediante os dados fornecidos pelo(a) autor(a)

P43t Peixoto, Antonio Augusto Teixeira.
Tensor-Based Multiuser Detection for Cooperative Wireless Communications Systems / Antonio Augusto Teixeira Peixoto. – 2017.
115 f. : il. color.

Dissertação (mestrado) – Universidade Federal do Ceará, Campus de Sobral, Programa de Pós-Graduação em Engenharia Elétrica e de Computação, Sobral, 2017.
Orientação: Prof. Dr. Carlos Alexandre Rolim Fernandes.

1. tensor model. 2. semi-blind receiver. 3. cooperative communications. 4. MIMO. 5. PARAFAC. I. Título.

CDD 621.3

Acknowledgments

I would like to express my deepest gratitude to:
God, for everything.
Professor Carlos Alexandre Rolim Fernandes, for the time and patience.
Amanda Costa, for the love and support.
My mother, for always believing in me.
My friends Bruno and Pedro, for helping me in some results of this work.

Abstract

Signal processing applications in wireless communications may sometimes take advantage of multilinear algebra concepts. This can be done by modeling the signals as high order tensors. From this context, tensor decompositions such as the Parallel Factor analysis (PARAFAC), may be found useful. On the other hand, cooperative communications and Multiple-Input Multiple-Output (MIMO) systems are ways for granting better data rates, capacity, fading mitigation and coverage. Joining the signal processing capabilities of tensor algebra, MIMO and cooperative communications can bring great benefits in wireless communications systems. In this dissertation, two receivers are proposed for two system models that are a multiuser DS-CDMA (Direct-Sequence Code-Division Multiple-Access) uplink based on multirelay cooperative communications. The two system models are almost the same, except that in one of them, multiuser interference is considered at the relays. The Amplify-and-Forward (AF) protocol is used on all the relays, thus exploiting cooperative diversity. For the received signal of the first system model, a quadrilinear PARAFAC decomposition will be adopted and by doing so, the proposed tensor-based semi-blind receiver can jointly estimate the transmitted symbols, channel gains and spatial signatures of all users by assuming previous knowledge of the users spreading codes and a few transmitted symbols. For the second system model, multiuser interference is considered at the relays, then, a receiver based on a trilinear PARAFAC decomposition is proposed. The estimation of the second receiver is done in two phases with the first phase being a supervised stage where non-orthogonal training sequences are sent by all users. During the second phase, the users' data symbols are then estimated. Both receivers use the Alternating Least Squares (ALS) algorithm to fit the tensor models, assuming no channel state information (CSI) at the base station neither at the relays. With computational simulations, we will also provide performance evaluation of the proposed receivers for various cases and system variations.

Keywords: wireless communications, semi-blind receiver, DS-CDMA, cooperative communications, tensor model, PARAFAC, multiuser detection, alternating least squares, MIMO.

Resumo

As aplicações de processamento de sinal em sistemas de comunicações sem fio às vezes podem tirar proveito de conceitos de álgebra multilinear. Isso pode ser feito modelando os sinais como tensores de ordem elevada. Neste contexto, as decomposições tensoriais, tais como a análise de fatores paralelos (Parallel Facor - PARAFAC), podem ser úteis. Por outro lado, as comunicações cooperativas e a área de sistemas de múltiplas-entradas e múltiplas-saídas (Multiple-Input Multiple-Ouput - MIMO) são uma maneira de se alcançar melhores taxas de dados, capacidade, qualidade de transmissão e cobertura. Juntando-se as capacidades de processamento de sinal da álgebra tensorial, dos sistemas MIMO e das comunicações cooperativas, podemos obter grandes benefícios nos sistemas de comunicações sem fio. Nesta dissertação, dois receptores são propostos para dois modelos de sistema, que são o enlace reverso de um sistema DS-CDMA multiusuário baseado em comunicações cooperativas auxiliadas por múltiplos retransmissores. Os dois modelos de sistema são quase iguais, exceto que em um deles, a interferência de múltiplos usuários é considerada nos retransmissores. O protocolo Amplify-and-Forward (AF) é aplicado em cada retransmissor, explorando a diversidade cooperativa. Para o sinal recebido no primeiro modelo de sistema, uma decomposição tensorial PARAFAC quadrilinear será adotada e, ao fazê-lo, o receptor semi-cego proposto pode estimar conjuntamente os símbolos transmitidos, ganhos de canais e assinaturas espaciais de todos os usuários, assumindo o conhecimento prévio dos códigos de espalhamento dos usuários e alguns símbolos transmitidos. Para o segundo modelo de sistema, interferência multiusuário é considerada nos retransmissores dos usuários, então, um receptor baseado em uma decomposição PARAFAC trilinear é proposto. O segundo receptor realiza as estimações em duas fases, sendo a primeira fase um estágio supervisionado em que todos os usuários enviam sequências de treinamento não ortogonais. Durante a segunda fase, os símbolos de dados dos usuários são então estimados. Ambos os receptores usam o algoritmo ALS (Alternating Least

Squares) para ajustar os modelos tensoriais, assumindo nenhuma informação de estado do canal (CSI - Channel State Information) na estação base nem nos retransmissores. Com simulações computacionais, também forneceremos avaliação de desempenho dos receptores propostos para vários casos e variações do sistema.

Palavras-chave: receptor semi-cego, DS-CDMA, comunicações cooperativas, modelos tensoriais, PARAFAC, alternating least squares, MIMO.

List of Acronyms

2D	Two-Dimensional
3D	Three-Dimensional
4D	Four-Dimensional
***M*-QAM**	M-ary Quadrature Amplitude Modulation
AF	Amplify-and-Forward
ALS	Alternating Least Squares
BER	Bit Error Rate
CDMA	Code-Division Multiple-Access
CP	CANDECOMP-PARAFAC
CSI	Channel State Information
DFT	Discrete Fourier Transform
DKRST	Distributed Khatri-Rao Space Time Coding
DS-CDMA	Direct Sequence - Code-Division Multiple-Access
KRST	Khatri-Rao Space Time Coding
LS	Least Squares
MIMO	Multiple-Input Multiple-Output
NMSE	Normalized Mean Squared Error
PARAFAC	Parallel Factors
SER	Symbol Error Rate
SISO	Single-Input Single-Output
SNR	Signal-to-Noise Ratio
ZF	Zero Forcing

List of Symbols

$\jmath$	Square root of -1
$\mathbb{R}$	Field of real numbers
$\mathbb{C}$	Field of complex numbers
$(\cdot)^{\mathsf{H}}$	Hermitian operator
$(\cdot)^{\mathsf{T}}$	Transpose operator
$(\cdot)^{-1}$	Inversion operator
$(\cdot)^{\dagger}$	Pseudo-inverse operator
$diag_j[\,]$	Operator that forms a diagonal matrix from the j-th row
$\mathrm{vec}(\cdot)$	Vectorization operator
$\cdot \circ \cdot$	Outer product
$\cdot \otimes \cdot$	Kronecker product
$\cdot \diamond \cdot$	Khatri-Rao product
$\cdot \times_n \cdot$	n-mode product
$\langle \cdot, \cdot \rangle$	Inner product
$\|\cdot\|_{\mathrm{F}}$	Frobenius norm
$\|\cdot\|_2$	Euclidean norm
$\|\cdot\|_{\mathrm{F}}^2$	Squared Frobenius norm

List of Figures

Contents

Chapter 1

Introduction

The constant growth of telecommunications systems implies in constant research and improvements of the associated technologies used. Further steps are needed to enhance the efficiency of communication networks. From generation to generation we have significant improvements that include better spectrum and channel utilization, better noise protection, better signal-to-noise ratio (SNR), higher transmission rates, and so on. In recent years, wireless communications networks have come up with a new way of network transmission, where a source has to rely on the help of other network nodes to transmit or relay information to a given destination. This new decentralized topology has inspired new ideas for the design of communications systems and networks where cooperation between nodes and users can be used to improve system performance, resulting in a new communication paradigm called cooperative communications [3]. Certainly this means that we have to answer how the performance can be improved through cooperative communications.

Cooperative diversity is a recent paradigm that provides better capacity, fading mitigation, spatial diversity and coverage at wireless networks [3], [4]. The characteristics of cooperative communications systems have put the topic into research interest lately. The idea behind it is making the network nodes help each other, allowing improvements on the system performance without increasing the power at the transmitter. Cooperative diversity is now an important part of telecommunications research and is already into consideration to become a standard in wireless systems, such as in IEEE 802.16, which supports relaying in order to extend cell coverage [5].

There are some cooperative protocols available, like the amplify-and-forward (AF) [6], the decode-and-forward (DF) [7], variations of these two protocols and

others [8], [3]. In means of simplicity, the AF protocol is quite a good choice because the relay node just amplify the other users signals and forward it to the destination. Latency and complexity are then keep small on this protocol making it preferable when these factors are of importance on the system deployment.

Multiple-Input Multiple-Output (MIMO) systems, in turn, allow an improvement in the throughput by taking advantage of spatial diversity. Basically, MIMO is a method for multiplying the capacity of a radio link or to enhance the transmission quality by using multiple transmit and receive antennas to exploit rich multipath propagation [9]. MIMO systems can provide high spectral efficiencies by capitalizing on spatial multiplexing [10, 11] while also improving reliability of the link by using space-time coding [12], [13]. Space-time codes can improve the reliability of data transmission by distributing coded data over multiple antennas and multiple time-slots, thus, providing both coding gain and diversity gain [14]. An example of space-time code is the Khatri-Rao space-time (KRST) code, introduced in [15]. We will use an alternative version of KRST coding in a variation of the system model of Chapter 3.

Cooperative communications and MIMO systems can provide many benefits for telecommunications systems, as explained earlier. However, when users share these benefits, multiple-access can be a problem. A possibility to solve this problem is by adopting a multiple-access scheme. In this dissertation, we use Direct-Sequence Code-Division Multiple-Access (DS-CDMA) to handle multiple users on the system. A DS-CDMA system turns multiple access possible by means of spread spectrum modulation. In DS-CDMA systems, the transmitted symbols are spread in frequency by multiplying the narrowband symbols to be transmitted by a spreading sequence, or code. Hence, the users share the same frequency band to communicate and each user is identified by a unique spreading code [16]. At the receiver, the recovery of the users' signals uses the same spreading sequence for spreading at the transmitter, in order to perform correlation detection [16]. CDMA may be used to be obtained secrecy, multiuser separation and greater resistance to unintentional and intentional interference [17], [18]. It is also possible to increase reliability or performance by using direct-sequence spreading on the transmitted signals in order to reduce overall signal interference. The integration of multiple antennas and CDMA technologies has also been subject of several studies [19], [20]. The system models that we introduce in this dissertation are valid for both KRST coding systems and for DS-CDMA systems.

On the other hand, the application of linear and multilinear algebraic prop-

erties in signal processing has been explored for some time [21], and, with the expansion and development of communications systems, this field allowed new techniques for information processing to be developed. Currently, the use of theories of linear and multilinear algebra contributed to the development of areas such as [22], [23], [24], [25]:

- Telecommunications;
- Numerical analysis;
- Data mining;
- Signal processing;
- Big Data;
- Computer vision;
- Multilinear filtering.

But what would be the motivation to develop new information processing techniques based on multilinear algebra? More precisely, multilinear algebra allows certain areas mentioned above, such as signal processing and telecommunications, to cover a wide range of system models, e.g., MIMO, CDMA and cooperative communications. An important concept of multilinear algebra used in this work are tensor models. Tensors basically are a generalization of higher order arrays, with its use already demonstrated in several areas, as seen in [22] and in [23]. An advantage of using tensors in comparison to matrix algebra is due to the fact that tensors allows us the use of multidimensional data, which contrasts with two dimensions data represented by matrices, thus allowing a better understanding and processing for a multidimensional perspective.

Tensor representation of data signals open us possibilities to exploit tensor decompositions. The use of tensor decompositions has gained attention in some signal processing applications for wireless communication systems, as described in [26]. More precisely, in some wireless communications systems, the fact that the received signal is a third or fourth-order tensor means that each received signal sample is associated with a three or four-dimensional space, and it is represented by three or four indices, each index associated with a variation of the received signal. On a multidimensional perspective, each dimension of the received signal tensor can be interpreted as a particular form of diversity [1].

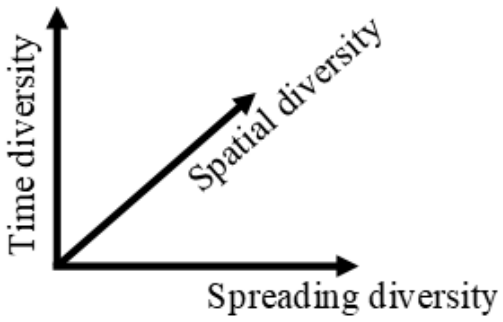

Figure 1.1: Representation of tridimensional data.

In most of the cases, two of these dimensions represent space and time. The space dimension corresponds to the number of receive antennas and the time dimension corresponds to the length of the data block to be processed. The third and four dimensions of the fourth-order tensor depends on the system itself. Thus, tensor decompositions provide the capacity of modeling wireless communications systems with multivariate data, instead of only two dimensions, as common in linear algebra. For instance, spatial diversity or spatial multiplexing can now be a dimension of the processed data alongside time, spreading and others. Fig. 1.1 illustrates tridimensional data including time, spatial and spreading diversity in one signal.

One of the motivations for using tensor models in wireless communications systems comes from the fact that is possible to perform multiuser signal separation and channel estimation under uniqueness conditions more relaxed than conventional matrix-based approaches [1]. A very popular decomposition is the Parallel Factor (PARAFAC) decomposition, proposed by Harshman [27] and Carroll & Chang [28] (Carroll & Chang's work presented the same decomposition as Canonical Decomposition). The PARAFAC has been used as a component analysis tool in many fields, for instance, psychometrics [28], chemometrics [29, 30], speech processing [31], independent component analysis (ICA) in signal processing [32], principal component analysis (PCA) and many others that are described in [22]. The main motivation for using the PARAFAC decomposition comes from its intrinsic uniqueness. In comparison to matrix decompositions, where we often have the problem of rotational freedom, the PARARAC decomposition of high order tensors is unique up to scaling and permutation ambiguity. This uniqueness property makes the PARAFAC decomposition a good solution to blind equaliza-

tion, blind multiuser detection, blind separation and so on.

Starting from the work of Sidiropoulos et al. in [2], the use of tensor decompositions in wireless communications proved to be valid and effective. In the referred work, the authors showed that a set of DS-CDMA signals received at an uniform linear array of antennas can be viewed as a third-order tensor, also admitting a PARAFAC decomposition. In [33], the PARAFAC decomposition was used in multiple invariance sensor array processing. Similar PARAFAC decompositions were proposed for Wideband CDMA, OFDMA (Orthogonal Frequency-Division Multiple-Access) systems and spatial signatures estimation in [34], [35] and [36] respectively. Other works on tensor decomposition includes generalization of tensor models for wireless communications [37, 38] and blind channel identification [39]. For the applications described above, the principal characteristic of tensor decompositions in signal processing is the following. It does not require the use of training sequences or pilot symbols, nor the knowledge of channel impulse responses and antenna array responses, with weak identifiability conditions. Moreover, the PARAFAC decomposition does not rely on statistical independence between the transmitted signals. Instead, the receiver algorithms are purely deterministic and explore the multilinear algebraic structure of the received signal (a high order tensor) [1].

The joint use of tensor decompositions and MIMO systems was proposed in the literature, as for example in [15], where a space-time coding model with blind detection was proposed for a multiple-antenna scheme. In [40], a tensor model is proposed for a MIMO-CDMA system with multiuser spatial multiplexing. We must note that MIMO systems influenced the development of constrained tensor models, as, for instance, the work presented in [41]. In [42], a new constrained tensor model called PARATUCK was proposed, providing a tensor space–time coding for MIMO wireless communication systems. An overview of some of these tensor models can be found in [43]. It is clear then that tensor models can be well exploited on modeling multiple-antenna systems.

There are also examples of tensor models in wireless cooperative communications, as in [44], where a receiver was proposed for a two-way AF relaying system with multiple antennas at the relay nodes adopting tensor based estimation. In [45], a blind receiver for an AF relaying uplink scenario was proposed, with different time slots for each relay transmission, a trilinear tensor model adopted and the destination node employing an antenna array. Based on [45], a unified multiuser receiver with a trilinear tensor model was proposed in [46] for a uplink

multiuser cooperative diversity system with different relaying schemes. In [47], receivers were based on a trilinear tensor model on a cooperative scenario exploiting spreading diversity at the relays and simultaneous transmission towards the destination. There are also recent works as the one shown in [48], where a two-hop MIMO relaying system was proposed adopting two tensor approaches (PARAFAC and PARATUCK) at the same time, and in [49], where a one-way two-hop MIMO AF cooperative scheme was employed with a nested tensor approach called nested Tucker. In [50], we proposed a generalization of some works mentioned (more specifically [45], [46] and [47]) using a fourth-order PARAFAC model in a cooperative DS-CDMA system. The results of [50] showed that a combination of four types of diversity in a PARAFAC decomposition proved to be better than other works present in the literature. In [51], the authors considered a three-hop one-way AF cooperative system and a semi-blind receiver based on the PARATUCK-3 is proposed.

In this dissertation, we use two system models. More specifically, they are based on a cooperative DS-CDMA AF relay-aided scenario where direct-sequence spreading is used at the relays and an antenna array is employed at the destination, thus taking advantage of cooperative and spatial diversities. Both systems consist in a wireless uplink, with users transmitting towards a base station with the help of relay-aided links. In the first scenario (considered in Chapter 3), interference between users is not considered at the relays. The second system model (used in Chapter 4) is similar to the previous one, however, in this case, multiuser interference is assumed at the relays, thus a more realistic scenario than the previous one. Based on these two system models, we propose two receivers, one for each model. The tensor modeling developed for both system models is also valid in the case where a distributed KRST (DKRST) coding [52] is used by the relays instead of DS-CDMA, as we show in Chapter 3.

We adopt a quadrilinear PARAFAC model for the receiver of the first system model of this dissertation (presented in Chapter 3). Indeed, we propose a semi-blind multiuser receiver that is able to jointly estimate the channel gains, antenna responses and transmitted symbols of all users, exploiting the uniqueness properties of a fourth order tensor. For the second system model (presented in Chapter 4), we use a trilinear tensor model for the receiver. By joinning the users symbols dimension with the channel gains dimension, we reduce the number of dimensions of the PARAFAC decomposition by one. The second receiver estimate the data in two phases. During the first phase (a supervised stage), all users send a

training sequence known at the receiver, thus the receiver is able to estimate the channel gains and spatial signatures of all users. Then, during the second phase, the receiver is able to estimate the users symbols in a non-supervised stage.

This dissertation lies in a research field that connects tensor decompositions, signal processing, wireless communications and cooperative communications. It extends [2] by considering a cooperative link with relays in addition to the direct link. Moreover, in comparison to [45] and [46], our work admits coding at the relays and in contrast to [47], the adopted system considers the relays transmitting in different time-slots instead of all relays transmitting simultaneously to the destination (although a variation with the relays transmitting simultaneously is presented in Chapter 3). An advantage of this work is its flexibility to system parameters, which can provide us generalizations of other works. Then, by choosing the system parameters, such as the number of relays or spreading code length, we get the models from [2], [45], [46] and [47]. It is also worth mentioning that the proposed receiver models provides better performance than the others presented above, as it will be shown by the simulations results of Chapter 3.

1.1 Dissertation Contribution

The main contributions of this dissertation will cover the following research topics:

- Multiuser signal separation/detection;
- Multiple-antenna transmission structures;
- Channel and spatial signatures estimations;
- AF relaying.

In the context of multiuser signal separation/detection, we have proposed a unified PARAFAC decomposition for DS-CDMA and DKRST coding cooperative multirelay uplinks, with the proposition of two receivers that can estimate the transmitted symbols. Moreover, in the context of multiple-antenna transmission structures and AF relaying, we covered some variations that can turn the system models more versatile and flexible, as, for instance, three different possibilities of relay setups: single antenna relays transmitting in different time-slots, single antenna relays transmitting simultaneously and a single MIMO relay case. In the

context of channel and spatial signatures estimations, the proposed receivers can also estimate the channel gains and spatial signatures of all users.

The different contributions of this work are associated with receiver processing. We focus primarily on multiuser signal separation/detection, channel estimation and spatial signatures estimations. To summarize, the major contributions of this dissertation are the following:

- Development of a unified PARAFAC decomposition for DS-CDMA and DKRST cooperative multirelay uplinks;
- Development of a PARAFAC tensor modeling for a cooperative multirelay uplink with multiuser interference at the relays;
- Study of the uniqueness conditions of the presented tensorial decompositions;
- Development of two receivers for the adopted system models;
- Presentation of the link between one used system model and others systems present in the literature;
- Simulation results that validate the performance of the proposed semi-blind receivers.

1.2 Scientific Output

One paper was produced from the results obtained in this dissertation:

– **A. A. T. Peixoto**, C. A. R. Fernandes, *"Tensor-Based Multiuser Detection for Uplink DS-CDMA Systems with Cooperative Diversity"* published in the 2017 XXXV Simpósio Brasileiro de Telecomunicações e Processamento de Sinais (SBrT 2017);

– A journal paper is being developed with the results of this dissertation.

1.3 Organization

This dissertation is structured as follows:

- Chapter 2 presents a multilinear algebra introduction, the PARAFAC decomposition and its uniqueness properties. For last, a short introduction of MIMO systems and cooperative communications is shown;
- Chapter 3 presents the adopted system model for a wireless cooperative communication system uplink, the quadrilinear tensorial decomposition for this system and the proposition of a semi-blind receiver for the system model. Simulations results showing the performance of the proposed receiver are also presented;
- Chapter 4 presents the second system model adopted for a wireless cooperative communication system uplink with multiuser interference at the relays, the trilinear PARAFAC decomposition used and the receiver proposed. Simulation results showing the performance of the proposed receiver are presented at the end of the chapter;
- Chapter 5 summarizes our conclusions and lists some research perspectives in this dissertation subject;
- The paper mentioned in Section 1.2 is attached in Appendix A.

Chapter 2

Tensor Models, MIMO and Cooperative Communications

This chapter is devoted to the presentation of a multilinear algebra introduction and to an explanation of MIMO and cooperative communications concepts, which will be essential to understand the methods proposed in this dissertation. First, we introduce a background of tensor algebra. Afterwards, the mathematical formalism, tensor representations and basic operations are shown. Then, we outline tensor decompositions, where we present the PARAFAC decomposition and its uniqueness properties are discussed. Finally, we present a short introduction of MIMO systems and cooperative communications.

2.1 Background on Tensor Algebra

Multilinear algebra is the algebra of arrays of order higher than two. These high order arrays are called tensors. The theory of tensors is nowadays known as tensor algebra. The word "tensor" was first introduced in the XIX century [1] but its use as we know nowadays was only introduced between the 60s and 70s by Kruskal [53], Richard A. Harshman [27] and L. R. Tucker [54], who were the pioneers on the development of tensor decompositions, analysis and factorizations for third order tensors. These decompositions of high order arrays can be viewed as generalizations of matrix decompositions. The analysis that Harshamn proposed in [27] and in [55] is called Parallel Factor (PARAFAC) analysis or PARAFAC decomposition, which has been extensively studied in the literature and applied on several areas [22].

But what PARAFAC has that is so attractive? The answer is simple: its

uniqueness feature. The PARARAC decomposition of tensors is unique up to permutation and scaling indeterminacies [53, 56]. A uniqueness proof was made by Kruskal in [53]. Also, a generalization of the uniqueness results of [53] to tensors of any order was given in [57] by N. Sidiropoulos and R. Bro, who also applied tensor models to telecommunications and provided the uniqueness conditions to complex tensor models in [2]. Another demonstration of the uniqueness properties of the PARAFAC was shown in [58], providing different uniqueness conditions. The use of tensor models and decompositions, more precisely the PARAFAC, was found to be useful in Independent Component Analysis (ICA) applications [59, 60]. ICA is a special case of blind source separation and is defined as a computational method used to separate a multivariate signal into additive subcomponents, contrasting to the fact that the PARAFAC decomposition can describe the basic structure of high order cumulants of multivariate data [29], [55], thus, showing that tensor decompositions can be an interesting way to deal with multidimensional data [61] .

Even not being used on this dissertation, it is worth mentioning the tensor decomposition Tucker-3, which can be used in interesting applications such as Principal Component Analysis (PCA) [62]. PCA is a statistical procedure that uses orthogonal transformations in order to convert a set of possibly correlated variables into a set of linearly uncorrelated variables called principal components, revealing the internal structure of the data in a way that best explains the variances in the data set [63]. It is mostly used as a tool in exploratory data analysis and development of predictive models. The Tucker-3 decomposition is also know as three mode PCA [54], [62] because of its intrinsic capabilities of component analysis. For instance, the Tucker-3 was used in personal perception analysis area [62], [64]. More recently, the use of tensors in neuroscience and biomedical signal processing was proposed, with its use being improved so on and different approaches being developed. For example, in [65], tensors were used in the modeling the structure of an epilepsy seizure using PARAFAC. In [66], a noninvasive technique for atrial activity extraction using tensors was proposed. There are also many other examples provided in Chapter 1. It is clear then that tensor decompositions can be applied to a wide range of disciplinary fields.

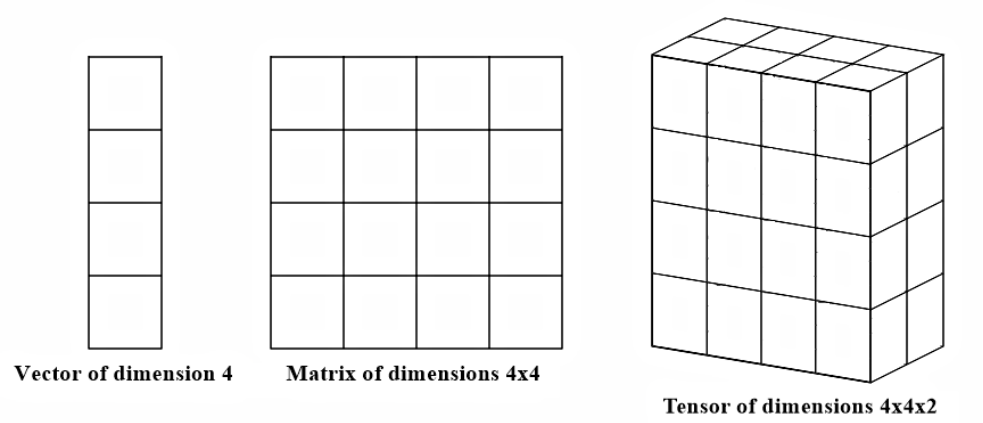

Figure 2.1: Vectors, matrices and tensors.

2.2 Basics of Tensorial Algebra

A N-th order tensor is a multilinear mapping. If the space basis associated to the mapping are fixed, then a tensor can be represented by a finite array, or table, of N coordinates. Hence, a N-th order tensor is interpreted by an array whose elements can be accessed by N indices. A tensor can be also called multidimensional array or multi-way array. The notation used in this dissertation is presented now: scalars are denoted by lower-case letters (x,y,...), vectors as lower-case boldface letters ($\mathbf{x}$,$\mathbf{y}$,...), matrices as upper-case boldface letters ($\mathbf{X}$,$\mathbf{Y}$,...) and tensors as calligraphic letters ($\mathcal{X}$,$\mathcal{Y}$,...). To retrieve the element (i,j) of $\mathbf{X}$, we use $[\mathbf{X}_{i,j}]$. We may define now:

Definition 1 (order of a tensor)**.** *$x \in \mathbb{C}$ is a scalar (order 0 tensor), $\boldsymbol{x} \in \mathbb{C}^{I_1 \times 1}$ is a vector (order 1 tensor), $\boldsymbol{X} \in \mathbb{C}^{I_1 \times I_2}$ is a matrix (order 2 tensor), $\mathcal{X} \in \mathbb{C}^{I_1 \times I_2 \times I_3}$ is an order 3, or third order, tensor and $\mathcal{X}_N \in \mathbb{C}^{I_1 \times I_2 \times I_3 \times \ldots \times I_N}$ is an order N, or N-th order, tensor.*

In Fig. 2.1 we can see a representation of vectors, matrices and third order tensors for illustrative purposes. Because a tensor is a multilinear form and has its own associated linear vector space, common linear operations that are valid and used for matrices can be extended and also used for tensors. For instance, we have:

Definition 2 (scalar notation)**.** *Let $\mathcal{X} \in \mathbb{C}^{I_1 \times I_2 \times I_3 \times \ldots \times I_N}$ be a N-th order tensor. A scalar component of $\mathcal{X}$ is denoted by:*

$$[\mathcal{X}]_{i_1,i_2,\ldots,i_N} = x_{i_1,i_2,\ldots,i_N}, \tag{2.1}$$

with i_N being the N-th dimension of $\mathcal{X}$, also being called the mode-N of $\mathcal{X}$.

Definition 3 (inner product). *Being $\mathcal{X} \in \mathbb{C}^{I_1 \times I_2 \times I_3 \times \ldots \times I_N}$ and $\mathcal{Y} \in \mathbb{C}^{I_1 \times I_2 \times I_3 \times \ldots \times I_N}$ N-th order tensors, the inner product between $\mathcal{X}$ and $\mathcal{Y}$ is given by:*

$$\langle \mathcal{X}, \mathcal{Y} \rangle = \sum_{i_1=1}^{I_1} \sum_{i_2=1}^{I_2} \ldots \sum_{i_N=1}^{I_N} x_{i_1,i_2,\ldots,i_N} y_{i_1,i_2,\ldots,i_N}, \tag{2.2}$$

where $\mathcal{X}$ and $\mathcal{Y}$ are said to be orthogonal if $\langle \mathcal{X}, \mathcal{Y} \rangle = 0$.

Definition 4 (outer product). *Being $\mathcal{X} \in \mathbb{C}^{I_1 \times I_2 \times I_3 \times \ldots \times I_N}$ and $\mathcal{Y} \in \mathbb{C}^{J_1 \times J_2 \times J_3 \times \ldots \times J_M}$ N-th and M-th order tensors, the outer product between $\mathcal{X}$ and $\mathcal{Y}$ is described as follows:*

$$[\mathcal{X} \circ \mathcal{Y}]_{i_1,i_2,\ldots,i_N,j_1,j_2,\ldots,j_M} = x_{i_1,i_2,\ldots,i_N} y_{j_1,j_2,\ldots,j_M}, \tag{2.3}$$

where "$\circ$" denotes the outer product. The result of $[\mathcal{X} \circ \mathcal{Y}]$ is a tensor with order equal to the sum of the orders of $\mathcal{X}$ and $\mathcal{Y}$ (a $(N+M)$-th order tensor).

The rank of a tensor is a concept inherited from matrix algebra. An intuitive way to describe the rank of a tensor is the following. First, let us consider that a tensor represents a physical entity characterized by magnitude and multiple directions [67]. The number of simultaneous directions R is called the rank of the tensor. In a N dimensional space, it follows that a rank-0 tensor (i.e., a scalar) can be represented by $N^0 = 1$ number since scalars represent quantities with magnitude and no direction. Similarly, a rank-1 tensor (i.e., a vector) in a N dimensional space can be represented by $N^1 = N$ numbers and a general tensor by N^R numbers. From this perspective, a rank-2 tensor (one that requires N^2 numbers to describe) is equivalent, mathematically, to an $N \times N$ matrix. The rank of a tensor is independent of the number of dimensions of the underlying space. Based on this, we have:

Definition 5 (rank-1 tensor [22]). *Let $\mathcal{X} \in \mathbb{C}^{I_1 \times I_2 \times I_3 \times \ldots \times I_N}$ be a N-th order tensor. $\mathcal{X}$ will be a rank-1 tensor if it can be represented as the outer product of N vectors $\boldsymbol{u}^{(1)} \in \mathbb{C}^{I_1}$, $\boldsymbol{u}^{(2)} \in \mathbb{C}^{I_2}$,..., $\boldsymbol{u}^{(N)} \in \mathbb{C}^{I_N}$, as follows:*

$$x_{i_1,i_2,\ldots,i_N} = u^{(1)} \circ u^{(2)} \circ \ldots \circ u^{(N)}. \tag{2.4}$$

The vectors $\boldsymbol{u}^{(N)}$ are so called the components of $\mathcal{X}$. As an example, a rank-1 matrix is given by the outer product of two vectors.

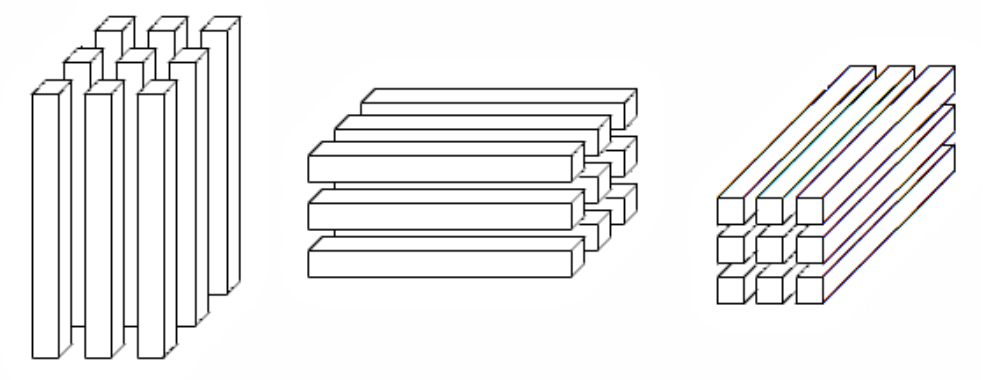

Figure 2.2: View of mode-1, mode-2 and mode-3 fibers of a third order tensor.

Definition 6 (rank of a tensor [22]). *The rank of a tensor* $\mathcal{X} \in \mathbb{C}^{I_1 \times I_2 \times I_3 \times \ldots \times I_N}$, *denoted by R, is defined as the minimum number of rank-1 components that gives* $\mathcal{X}$ *as a linear combination.*

Definition 7 (Frobenius norm). *The Frobenius norm of an N-th order tensor* $\mathcal{X} \in \mathbb{C}^{I_1 \times I_2 \times I_3 \times \ldots \times I_N}$ *is defined as:*

$$\|\mathcal{X}\|_F = \sqrt{\sum_{i_1=1}^{I_1} \sum_{i_2=1}^{I_2} \cdots \sum_{i_N=1}^{I_N} |x_{i_1,i_2,\ldots,i_N}|^2}. \tag{2.5}$$

The Frobenius norm can be also expressed in terms of the inner product $\|\mathcal{X}\|_F = \sqrt{\langle \mathcal{X}, \mathcal{X} \rangle}$.

Definition 8 (tensor fiber [22]). *The mode-n tensor fiber of a N-th order tensor* $\mathcal{X} \in \mathbb{C}^{I_1 \times I_2 \times I_3 \times \ldots \times I_N}$ *is defined as the vector formed by fixing every index but the* i_n*-th.*

For instance, consider a third order tensor $\mathcal{Y} \in \mathbb{C}^{I_1 \times I_2 \times I_3}$. Its mode-1, mode-2, and mode-3 fibers are given, respectively, by:

$$\begin{aligned} \mathbf{y}_{\cdot i_2 i_3} &\in \mathbb{C}^{I_1}, \\ \mathbf{y}_{i_1 \cdot i_3} &\in \mathbb{C}^{I_2}, \\ \mathbf{y}_{i_1 i_2 \cdot} &\in \mathbb{C}^{I_3}, \end{aligned}$$

where "$\cdot$" denotes the varying index. In Fig. 2.2 we can see an illustration of tensor fibers in different modes.

Definition 9 (tensor unfolding [22]). *The mode-n unfolding of a N-th order tensor* $\mathcal{X} \in \mathbb{C}^{I_1 \times I_2 \times I_3 \times \ldots \times I_N}$ *is a matrix* $\mathbf{X}_{(n)} \in \mathbb{C}^{I_n \times I_1 I_2 \ldots I_{n-1} I_{n+1} \ldots I_N}$ *whose elements*

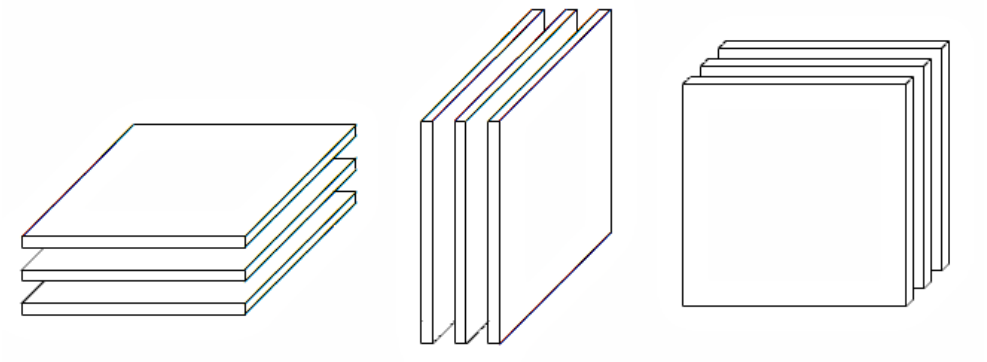

Figure 2.3: Mode-1, mode-2 and mode-3 slices of a third order tensor.

are obtained from the tensor $\mathcal{X}$ *in the following way:*

$$[\mathbf{X}_{(n)}]_{i_n,j} = [\mathcal{X}]_{i_1,\ldots,i_N}, \quad j = 1 + \sum_{\substack{u=1 \\ u\neq n}}^{N} (i_u - 1) \prod_{\substack{v=1 \\ v\neq n}}^{u-1} I_v.$$

Hence, as an example, the unfoldings of an arbitrary third order tensor $\mathcal{X} \in \mathbb{C}^{I_1 \times I_2 \times I_3}$ are

$$\mathbf{X}_{(1)} \in \mathbb{C}^{I_1 \times I_2 I_3},$$
$$\mathbf{X}_{(2)} \in \mathbb{C}^{I_2 \times I_1 I_3},$$
$$\mathbf{X}_{(3)} \in \mathbb{C}^{I_3 \times I_1 I_2}.$$

We may also note that the mode-n matrix unfolding can be seen as the concatenation of the mode-n fibers along the matrix columns. The mode-n unfolding matrices of a tensor can also be obtained by stacking the tensor slices. The tensor slices are two-dimensional sections of a tensor, defined by fixing all but two indices [22]. As Figure 2.3 shows, from left to right we have the mode-1 (or first-mode) slices, mode-2 (or second-mode) slices and mode-3 (or third-mode) slices. Thus, for the first-mode slice we have $\mathbf{Y}_{i_1..}$, for the second-mode we have $\mathbf{Y}_{.i_2.}$ and for the third mode $\mathbf{Y}_{..i_3}$. Figure 2.4 illustrates the generation of the first, second and third mode slices of a third order tensor.

Definition 10 (vectorization [68])**.** *Let* $vec(\ ) : \mathbb{C}^{I_1 \times I_2 \times I_3 \times \ldots \times I_N} \rightarrow \mathbb{C}^{I_1 I_2 I_3 \ldots I_N}$ *denote the vectorization operator, which transforms a tensor* $\mathcal{X} \in \mathbb{C}^{I_1 \times I_2 \times I_3 \times \ldots \times I_N}$ *into a vector* $vec(\mathcal{X}) \in \mathbb{C}^{I_1 I_2 I_3 \ldots I_N}$ *with components defined as:*

$$[vec(\mathcal{X})]_j = [\mathcal{X}]_{i_1,i_2,\ldots,i_N}, \quad j = i_1 + \sum_{n=2}^{N} (i_n - 1) \prod_{v=1}^{n-1} I_v. \tag{2.6}$$

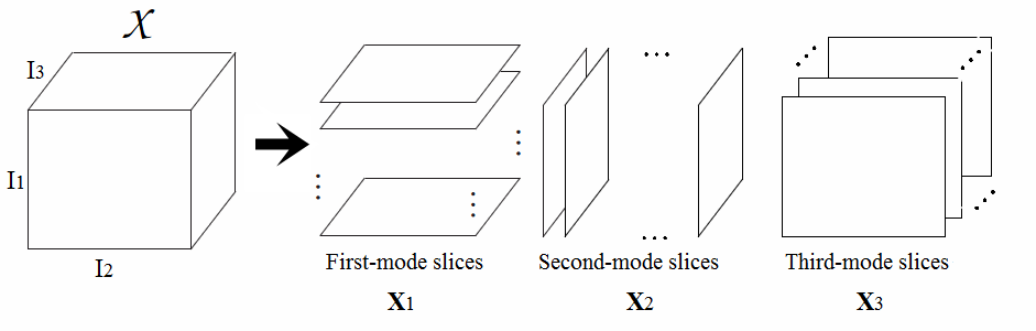

Figure 2.4: Generation of tensor slices. Adapted from [1].

The elements of the tensor are then stacked in reverse lexicographical order into a long column vector, as follows:

$$vec(\mathcal{X}) = \begin{bmatrix} x_{1,1,1} \\ \dots \\ x_{1,1,I_3} \\ \dots \\ x_{1,I_2,I_3} \\ \dots \\ x_{I_1,I_2,I_3} \end{bmatrix} \tag{2.7}$$

The inverse process (turning a vector into a tensor) is called "tensorization".

Definition 11 (mode-n product [22], [68], [1])**.** *The mode-n product between a N-th order tensor* $\mathcal{X} \in \mathbb{C}^{I_1 \times I_2 \times I_3 \times \dots \times I_N}$ *and a matrix* $\mathbf{U} \in \mathbb{C}^{J \times I_n}$ *is defined as:*

$$[\mathcal{X} \times_n \mathbf{U}]_{i_1,\dots,i_{n-1},j,i_{n+1},\dots,i_N} \coloneqq \sum_{i_n=1}^{I_n} x_{i_1,i_2,\dots,i_N} u_{j,i_n}, \quad j \in 1,\dots,J, \tag{2.8}$$

with "$\times_n$" being the mode-n product operator.

The mode-n product is a good way for representing linear transformations involving tensors.

2.3 Tensor Decompositions

In the last section, we have presented an introduction of multilinear algebra. Based on the concepts detailed, we present now the tensor decompositions that we will use in the rest of this dissertation. These decompositions, also known

as multi-way factor analysis, describes a tensor as a linear combination of outer product factors. Another important remark is that tensor decompositions can be viewed, depending on the approach and point of view, as generalizations of Principal Component Analysis (PCA) or Singular Value Decomposition (SVD) to higher order arrays. A multidimensional variable can be interpreted as a tensor, so, the analysis of a tensor in terms of its decomposed factors is useful in problems where a multilinear junction of different factors or contributions must be identified or separated from the measured data. In this context, a tensor decomposition of an observed variable modeled as a data tensor can separate the signals transmitted by different sources, allowing the development of powerful multiuser detection systems. In the following, the PARAFAC decomposition of third order and fourth order tensors (or three-way and four-way arrays) is presented, since they will be used in the applications encountered in this dissertation. We will also show the generalization of the PARAFAC to N-th order tensors.

2.3.1 Trilinear PARAFAC model

The PARAFAC (Parallel Factor) decomposition was developed and presented by Harshman [27] and Carroll & Chang [28] in the 70s. It was referred in Carroll & Chang's work as Canonical Decomposition, abbreviated to CANDECOMP, but it can be also referred by the acronym CP (Candecomp-Parafac). For signal processing, ICA, chemometrics and psychometrics purposes, the PARAFAC was a good choice and there are many applications of the PARAFAC developed for them [29]. Some examples of the use of the PARAFAC in wireless communications are [33], [2], [37], [69], [38], and [70].

The PARAFAC decomposition of an arbitrary tensor $\mathcal{Z} \in \mathbb{C}^{I_1 \times I_2 \times I_3}$ can be expressed by:

$$z_{i_1,i_2,i_3} = \sum_{q=1}^{Q} t_{i_1,q} u_{i_2,q} v_{i_3,q} \tag{2.9}$$

where $t_{i_1,q}$, $u_{i_2,q}$ and $v_{i_3,q}$ are elements of matrices $\mathbf{T}$, $\mathbf{U}$ and $\mathbf{V}$ respectively, with $\mathbf{T} \in \mathbb{C}^{I_1 \times Q}$, $\mathbf{U} \in \mathbb{C}^{I_2 \times Q}$ and $\mathbf{V} \in \mathbb{C}^{I_3 \times Q}$ being the factor matrices of $\mathcal{Z}$. Q is the rank of the tensor. We may note that z_{i_1,i_2,i_3} in (2.9) is a sum of triple products. (2.9) is also known as "the trilinear model", "trilinear decomposition" or "triple product decomposition". Using the outer product notation, the PARAFAC decomposition

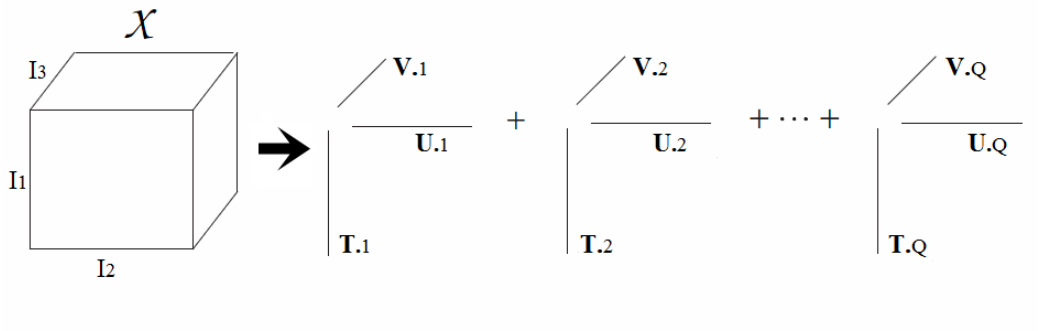

Figure 2.5: PARAFAC decomposition of a third order tensor.

of $\mathcal{Z}$ can be rewritten in the following way:

$$\mathcal{Z} = \sum_{q=1}^{Q} \mathbf{T}_{.q} \circ \mathbf{U}_{.q} \circ \mathbf{V}_{.q}. \tag{2.10}$$

Now $\mathcal{Z}$ is in function of the three factor matrices $\mathbf{T}$, $\mathbf{U}$ and $\mathbf{V}$, as Fig. 2.5 illustrates. The third mode matrix slice ($\mathbf{Z}_{..i_3}$) of the tensor $\mathcal{Z}$ is given by:

$$\mathbf{Z}_{..i_3} = \begin{bmatrix} z_{1,1,i_3} & z_{1,2,i_3} & \cdots & z_{1,I_2,i_3} \\ z_{2,1,i_3} & z_{2,2,i_3} & \cdots & z_{2,I_2,i_3} \\ \vdots & \vdots & \vdots & \vdots \\ z_{I_1,1,i_3} & z_{I_1,2,i_3} & \cdots & z_{I_1,I_2,i_3} \end{bmatrix}. \tag{2.11}$$

It can be shown that $\mathbf{Z}_{..i_3}$ admits the following factorization:

$$\mathbf{Z}_{..i_3} = \mathbf{T} diag_{i_3}[\mathbf{V}]\mathbf{U}^T, \tag{2.12}$$

where the operator "$diag_{i_3}[\,]$" is used to create a diagonal matrix by extracting the i_3-th row of $\mathbf{V}$. The first mode matrix slice of the tensor $\mathcal{Z}$ is given by:

$$\mathbf{Z}_{i_1..} = \mathbf{U} diag_{i_1}[\mathbf{T}]\mathbf{V}^T, \tag{2.13}$$

where $\mathbf{Z}_{i_1..}$ is a $I_2 \times I_3$ matrix with $\mathbf{Z}_{i_1..} = [z_{i_1,..}]$ and i_1 = 1,2,...,I_1. The second mode slice is denoted by:

$$\mathbf{Z}_{.i_2.} = \mathbf{V} diag_{i_2}[\mathbf{U}]\mathbf{T}^T, \tag{2.14}$$

where $\mathbf{Z}_{.i_2.}$ is a $I_1 \times I_3$ matrix with $\mathbf{Z}_{.i_2.} = [z_{.,i_2,.}]$ and i_2 = 1,2,...,I_2. The received data tensor $\mathcal{Z}$ can be unfolded into the form of three matrices $\mathbf{Z}_1 \in \mathbb{C}^{I_2 I_1 \times I_3}$, $\mathbf{Z}_2 \in \mathbb{C}^{I_3 I_2 \times I_1}$ and $\mathbf{Z}_3 \in \mathbb{C}^{I_1 I_3 \times I_2}$ by stacking column-wise the matrix slices as follows:

$$\mathbf{Z}_1 = \begin{bmatrix} \mathbf{Z}_{1..} \\ \vdots \\ \mathbf{Z}_{I_1..} \end{bmatrix}, \mathbf{Z}_2 = \begin{bmatrix} \mathbf{Z}_{.1.} \\ \vdots \\ \mathbf{Z}_{.I_2.} \end{bmatrix},$$

$$\mathbf{Z}_3 = \begin{bmatrix} \mathbf{Z}_{..1} \\ \vdots \\ \mathbf{Z}_{..I_3} \end{bmatrix}. \tag{2.15}$$

Hence, joining (2.12)-(2.15) we have:

$$\mathbf{Z}_1 = \begin{bmatrix} \mathbf{Z}_{1..} \\ \vdots \\ \mathbf{Z}_{I_1..} \end{bmatrix} = \begin{bmatrix} \mathbf{U}diag_1[\mathbf{T}] \\ \vdots \\ \mathbf{U}diag_{I_1}[\mathbf{T}] \end{bmatrix} \mathbf{V}^T, \tag{2.16}$$

$$\mathbf{Z}_2 = \begin{bmatrix} \mathbf{Z}_{.1.} \\ \vdots \\ \mathbf{Z}_{.I_2.} \end{bmatrix} = \begin{bmatrix} \mathbf{V}diag_1[\mathbf{U}] \\ \vdots \\ \mathbf{V}diag_{I_2}[\mathbf{U}] \end{bmatrix} \mathbf{T}^T, \tag{2.17}$$

$$\mathbf{Z}_3 = \begin{bmatrix} \mathbf{Z}_{..1} \\ \vdots \\ \mathbf{Z}_{..I_3} \end{bmatrix} = \begin{bmatrix} \mathbf{T}diag_1[\mathbf{V}] \\ \vdots \\ \mathbf{T}diag_{I_3}[\mathbf{V}] \end{bmatrix} \mathbf{U}^T. \tag{2.18}$$

These matrices admit, respectively, the following factorizations:

$$\mathbf{Z}_1 = (\mathbf{T} \diamond \mathbf{U})\mathbf{V}^T, \tag{2.19}$$

$$\mathbf{Z}_2 = (\mathbf{U} \diamond \mathbf{V})\mathbf{T}^T, \tag{2.20}$$

$$\mathbf{Z}_3 = (\mathbf{V} \diamond \mathbf{T})\mathbf{U}^T, \tag{2.21}$$

where "$\diamond$" denotes the Khatri-Rao product, which is a column-wise Kronecker product. The Khatri-Rao and Kronecker products are fairly described and explained in [71].

An interesting feature of the PARAFAC is its uniqueness property. The PARAFAC decomposition of tensors with rank > 1 can be unique up to scaling and permutation of factors, unlike matrix decompositions which are mostly not unique for rank > 1. The first studies about the uniqueness of the PARAFAC

model were done in the 70s, by Harshamn in [72] and by Kruskal in [53] for third order tensors. Later on, a generalization for N-th order tensors was proposed by Sidiropoulos and Bro in [57, 73] and more recently, a simplified proof of uniqueness was proposed by Stegeman and Sidiropoulos in [56]. Also, the uniqueness conditions were extended for the complex case by Sidiropoulos and others in [2] (which allows the use of complex modulation in telecommunications applications). The PARAFAC uniqueness conditions are based on the concept of k-rank (Kruskal-rank). To better understand the k-rank, let's review what is the rank of a matrix:

Definition 12 (rank of a matrix [2, 1])**.** *The rank of a given matrix $\boldsymbol{T} \in \mathbb{C}^{I_1 \times Q}$ is denoted by $r_{\boldsymbol{T}}$, and it is equal to r if $\boldsymbol{T}$ contains at least one set of r linearly independent columns but no set of $r + 1$ linearly independent columns.*

The k-rank concept was brought by Kruskal in [53] but the term was later coined by Harshman.

Definition 13 (Kruskal-rank [22])**.** *The Kruskal-rank, or k-rank, $k_{\boldsymbol{T}}$ of a given matrix $\boldsymbol{T} \in \mathbb{C}^{I_1 \times Q}$ is the maximum value of k such that every set of k columns of $\boldsymbol{T}$ is linearly independent. We must note that the k-rank is always less than or equal to the rank $r_{\boldsymbol{T}}$ of the matrix. Thus, we have:*

$$k_{\boldsymbol{T}} \leq r_{\boldsymbol{T}} \leq min(I_1, Q). \tag{2.22}$$

The conditions that are sufficient to guarantee uniqueness of the trilinear PARAFAC model [53] presented in (2.9), are given by:

$$k_{\mathbf{T}} + k_{\mathbf{U}} + k_{\mathbf{V}} \geq 2Q + 2. \tag{2.23}$$

If condition (2.23) is satisfied, then the set of matrices $\mathbf{T}$, $\mathbf{U}$ and $\mathbf{V}$ that generates $\mathcal{Z}$ in (2.10), are unique up to scaling and permutation ambiguity of its columns [53, 2]. It means that any set of matrices $\mathbf{T}^{'}$, $\mathbf{U}^{'}$ and $\mathbf{V}^{'}$ that satisfies condition (2.23), are related to the set $\mathbf{T}$, $\mathbf{U}$ and $\mathbf{V}$ by:

$$\mathbf{T}^{'} = \mathbf{T}\Pi\Delta_{\mathbf{T}},$$

$$\mathbf{U}^{'} = \mathbf{U}\Pi\Delta_{\mathbf{U}},$$

$$\mathbf{V}^{'} = \mathbf{V}\Pi\Delta_{\mathbf{V}}, \tag{2.24}$$

where $\Pi \in \mathbb{C}^{Q \times Q}$ is a permutation matrix and $\Delta_{\mathbf{T}}$, $\Delta_{\mathbf{U}}$ and $\Delta_{\mathbf{V}}$ are diagonal matrices that satisfies:

$$\Delta_{\mathbf{T}} \Delta_{\mathbf{U}} \Delta_{\mathbf{V}} = \mathbf{I}_Q, \tag{2.25}$$

with $\mathbf{I}_Q \in \mathbb{C}^{Q \times Q}$ being the identity matrix of order Q. Kruskal's result is non trivial and has been analyzed many times over. Let us now make some observations. It is clear that for $Q > 1$, a necessary condition for (2.23) is given by:

$$min(k_{\mathbf{T}}, k_{\mathbf{U}}, k_{\mathbf{V}}) \geq 2 \tag{2.26}$$

A matrix whose columns are drawn independently from an absolutely continuous distribution has full column rank with probability one and also has full k-rank. Thus, if we state that $\mathbf{V}$ is full column-rank, in other words, the rank of $\mathbf{V}$ is equal to Q, then, condition (2.26) turns into:

$$min(k_{\mathbf{T}}, k_{\mathbf{U}}) \geq 2, \tag{2.27}$$

which means that the trilinear PARAFAC decomposition is unique only if neither $\mathbf{T}$ nor $\mathbf{U}$ has a pair of proportional columns (note that if $\mathbf{T}$ and $\mathbf{U}$ does not have a pair of proportional columns, we can say that the values of $k_{\mathbf{T}}$ and $k_{\mathbf{U}}$ are greater than 2). This condition is shown in [74] and is a necessary, but not sufficient condition to the uniqueness of the PARAFAC decomposition.

2.3.2 Quadrilinear PARAFAC model

The PARAFAC decomposition of a fourth order tensor works the same way as for a third order tensor, but with the addition of one factor, thus one more factor matrix on the equations. Similarly to the trilinear model, for an arbitrary 4-way array $\mathcal{Z} \in \mathbb{C}^{I_1 \times I_2 \times I_3 \times I_4}$, the quadrilinear PARAFAC decomposition in scalar form turns out to [73]:

$$z_{i_1,i_2,i_3,i_4} = \sum_{q=1}^{Q} s_{i_1,q} t_{i_2,q} u_{i_3,q} v_{i_4,q}, \tag{2.28}$$

where $s_{i_1,q}$, $t_{i_2,q}$, $u_{i_3,q}$ and $v_{i_4,q}$ are elements of matrices $\mathbf{S}$, $\mathbf{T}$, $\mathbf{U}$ and $\mathbf{V}$ respectively, also with $\mathbf{S} \in \mathbb{C}^{I_1 \times Q}$, $\mathbf{T} \in \mathbb{C}^{I_2 \times Q}$, $\mathbf{U} \in \mathbb{C}^{I_3 \times Q}$ and $\mathbf{V} \in \mathbb{C}^{I_4 \times Q}$ being the

factor matrices. (2.28) can be rewritten as:

$$\mathcal{Z} = \sum_{q=1}^{Q} \mathbf{S}_{.q} \circ \mathbf{T}_{.q} \circ \mathbf{U}_{.q} \circ \mathbf{V}_{.q}, \tag{2.29}$$

which gives us similar factorizations to (2.19)-(2.21):

$$\mathbf{Z}_1 = (\mathbf{S} \diamond \mathbf{T} \diamond \mathbf{U})\mathbf{V}^T, \tag{2.30}$$

$$\mathbf{Z}_2 = (\mathbf{V} \diamond \mathbf{S} \diamond \mathbf{T})\mathbf{U}^T, \tag{2.31}$$

$$\mathbf{Z}_3 = (\mathbf{U} \diamond \mathbf{V} \diamond \mathbf{S})\mathbf{T}^T, \tag{2.32}$$

$$\mathbf{Z}_4 = (\mathbf{T} \diamond \mathbf{U} \diamond \mathbf{V})\mathbf{S}^T. \tag{2.33}$$

Any 4-way array can be unfolded into a 3-way array, much like a matrix can be unfolded into a vector via the vectorization operator, hence, the uniqueness of a quadrilinear decomposition follows from the uniqueness of a trilinear decomposition. The uniqueness conditions for a quadrilinear PARAFAC decomposition are described by Sidiropoulos et al in [57, 73] and are based on Kruskal's original trilinear conditions. Then, we have:

$$k_{\mathbf{S}} + k_{\mathbf{T}} + k_{\mathbf{U}} + k_{\mathbf{V}} \geq 2Q + 3. \tag{2.34}$$

If condition (2.34) is satisfied, then, the set of matrices $\mathbf{S}$, $\mathbf{T}$, $\mathbf{U}$ and $\mathbf{V}$ that generates $\mathcal{Z}$ in (2.29), are unique up to scaling and permutation ambiguity. It means that any set of matrices $\mathbf{S}'$, $\mathbf{T}'$, $\mathbf{U}'$ and $\mathbf{V}'$ that satisfies condition (2.34), are related to the set $\mathbf{S}$, $\mathbf{T}$, $\mathbf{U}$ and $\mathbf{V}$, similarly to the trilinear case.

2.3.3 N-th order PARAFAC model

The generalization of the PARAFAC decomposition for N-th order tensors, such as $\mathcal{Z} \in \mathbb{C}^{I_1 \times I_2 \times I_3 \times \ldots \times I_N}$, is given by:

$$z_{i_1,i_2,i_3,\ldots,i_n} = \sum_{q=1}^{Q} u^{(1)}_{i_1,q} u^{(2)}_{i_2,q} \ldots u^{(N)}_{i_N,q}, \tag{2.35}$$

where $u_{i_n,q}^{(n)}$ is an element of the matrix $\mathbf{U}^n \in \mathbb{C}^{I_n \times Q}$, with n = 1,2,...,N and i_n = 1,2,...,I_N. For this case, there will be N matrix factors and at least N matrix unfoldings. A sufficient condition for uniqueness was provided in [57] and is given by:

$$\sum_{n=1}^{N} k_{\mathbf{U}}(n) \geq 2Q + (N-1). \tag{2.36}$$

A proof for condition (2.36) was given by Sidiropoulos et al in [73] and in [57].

2.3.4 Alternating Least Squares Algorithm

The algorithm that we will use on the proposed receivers through the rest of this dissertation is explained in this subsection. Regarding the trilinear PARAFAC decomposition in (2.10), we have three factor matrices: $\mathbf{T}$, $\mathbf{U}$ and $\mathbf{V}$. The estimation of these three factor matrices is carried out by minimizing the nonlinear quadratic cost function:

$$f(\mathbf{T},\mathbf{U},\mathbf{V}) = \frac{\left\| \mathcal{Z} - \sum_{q=1}^{Q} \mathbf{T}_{.q} \circ \mathbf{U}_{.q} \circ \mathbf{V}_{.q} \right\|_{\mathrm{F}}^2}{\|\mathcal{Z}\|_F^2} \tag{2.37}$$

The Alternating Least Squares (ALS) algorithm is a possible solution to minimize this cost function. It is an iterative algorithm that alternates among the estimations of $\mathbf{T}$, $\mathbf{U}$ and $\mathbf{V}$. The ALS algorithm divides the nonlinear problem into three independent linear Least Squares (LS) problems [75, 64]. At each iteration, we have three LS estimation steps. For each step, one factor matrix, for instance, $\mathbf{T}$, is updated while the two others ($\mathbf{U}$ and $\mathbf{V}$) are fixed to their previous estimations. The algorithm makes use of the unfolded matrices $\mathbf{Z}_1$, $\mathbf{Z}_2$ and $\mathbf{Z}_3$ given in (2.19)-(2.21). The algorithm is summarized as follows:

1. Set $i = 0$; Initialize $\hat{\mathbf{U}}_{(i=0)}$ and $\hat{\mathbf{V}}_{(i=0)}$;
2. $i = i + 1$;
3. From $\mathbf{Z}_2$, find a LS estimate of $\mathbf{T}$: $\hat{\mathbf{T}}_{(i)}^T = (\hat{\mathbf{U}}_{(i-1)} \diamond \hat{\mathbf{V}}_{(i-1)})^\dagger \mathbf{Z}_2$;
4. From $\mathbf{Z}_3$, find a LS estimate of $\mathbf{U}$: $\hat{\mathbf{U}}_{(i)}^T = (\hat{\mathbf{V}}_{(i-1)} \diamond \hat{\mathbf{T}}_{(i)})^\dagger \mathbf{Z}_3$;
5. From $\mathbf{Z}_1$, find a LS estimate of $\mathbf{V}$: $\hat{\mathbf{V}}_{(i)}^T = (\hat{\mathbf{T}}_{(i)} \diamond \hat{\mathbf{U}}_{(i)})^\dagger \mathbf{Z}_1$;
6. Repeat 2-5 until convergence.

The convergence at the i-th iteration is declared when the error between two consecutive iterations is below some threshold. An error measure at the i-th iteration can be calculated from the following formula:

$$e(i) = \frac{\|\mathbf{Z}_1 - (\hat{\mathbf{T}}_{(i)} \diamond \hat{\mathbf{U}}_{(i)})\mathbf{V}^T\|_F^2}{\|\mathbf{Z}_1\|_F^2}. \tag{2.38}$$

When we have $|e(i) - e(i-1)| < \delta$, convergence is assumed (δ can be, for instance, 10^{-6}). The algorithm always converges, however, the ALS algorithm is strongly dependent on the initialization and convergence can sometimes be slow. Indeed, in some cases, a bad initialization of the matrices can affect negatively the estimations, then, the error between two consecutive iterations does not decrease and convergence takes more time.

2.4 Multiple-Input Multiple-Output Systems

In telecommunications, Multiple-Input Multiple-Output, or MIMO, is a method for multiplying the capacity or increasing the diversity of a radio link by using multiple transmit and receive antennas to exploit multipath propagation [9], contrary to SISO systems (Single-Input Single-Output), which use only one antenna both at the transmitter and receiver. The possible gains that can be achieved with MIMO systems led to its standardization in past, actual and upcoming mobile communications systems as IEEE 802.11n (Wi-Fi) [76], HSPA+ (High Speed Packet Access) [77], WiMAX and Long Term Evolution (LTE) [78]. By using MIMO, sending and receiving more than one data signal simultaneously over the same radio channel, or at different frequencies, is possible. MIMO systems are commonly used to enhance the data rates through multiplexing or to improve link quality (performance) by exploring diversity gain. A combination of both can also be used.

Figure 2.6 illustrates a configuration of N transmit antennas and M receive antennas, thus there are NM decorrelated channels. Studies that led to the development of MIMO date back to 1970s, with research papers concerning multichannel digital transmission systems, but it was only in the 1990s, with the development of methods to improve the performance of cellular radio networks, such as SDMA (Space-Division Multiple Access), that the use of multiple antennas has been proven effective. The principle of SDMA is to use directional or even smart antennas to communicate with the users on the same frequency, in

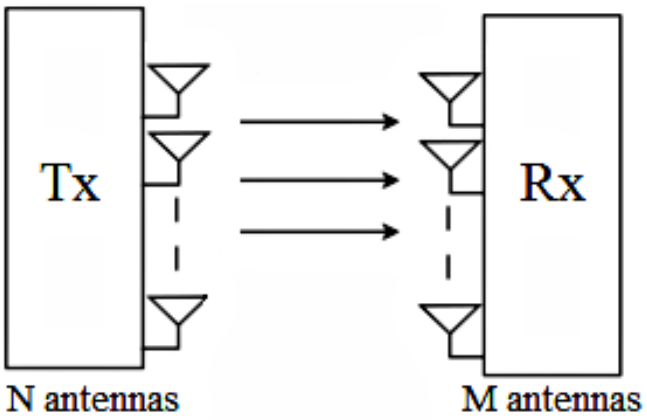

Figure 2.6: MIMO schematic.

the range of a base station, at different locations [79]. The "invention" of MIMO came in 1994 by Paulraj and Kailath [80], with the development of a SDMA based technique to multiplex broadcasts at high data rates by splitting a high rate signal into several low rate signals to be transmitted from spatially separated transmitters and recovered by the receive antenna array based on different directions of arrival. The contributions of Paulraj put MIMO systems into research interest and into use in wireless communications systems.

In this dissertation, we will use an array of antennas at the base station of the proposed system models but only one antenna on the relays and users devices, thus consisting in a multiuser SIMO (Single-Input Multiple-Output) system, which can be viewed as a multiuser MIMO (MU-MIMO) system. A variation of one proposed system model that employs a single MIMO relay will be described in the next chapter. Figures 2.7 and 2.8 depicts schematics of SISO, SIMO, MISO and MIMO systems. An example of MIMO deployment is 2x2 (2 antennas at the transmitter and 2 antennas at the receiver), 4x4 or even 8x8 (both on LTE releases). Not necessarily the number of antennas on both ends must be equal, as, for instance, a 4x2 configuration is possible. MIMO differs from smart antenna techniques developed to enhance the performance of a single data signal, such as beamforming or SDMA.

MIMO can be also used to apply space-time coding on the system. Basically, a space–time code (STC) is a method employed to improve the reliability and consequently the quality of a data transmission in wireless communication systems using multiple transmit antennas [13]. Space time codes rely on transmitting multiple and redundant copies of a data stream across a number of antennas, in order to exploit the various received versions of the data to improve the relia-

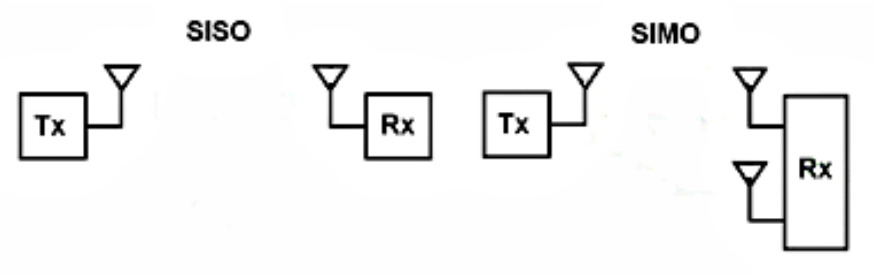

Figure 2.7: SISO and SIMO schematics.

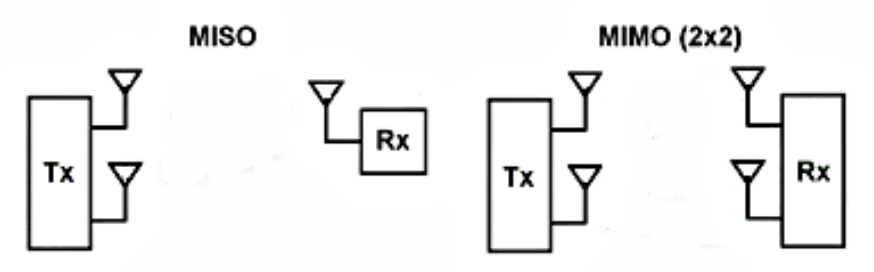

Figure 2.8: MISO and 2x2 MIMO schematics .

bility of the transmission. At the receiver, all the copies of the received signal are combined in an optimal way to extract the transmitted information. Examples of space-time codes are the Alamouti codes [12], the Khatri-Rao space-time (KRST) code [15] and its alternative version: Distributed Khatri-Rao space-time (DKRST) code [52]. The DKRST coding is used on a variation of the system model of this dissertation, as it will be detailed in Chapter 3.

2.5 Cooperative Communications

A non-cooperative communication model inside a network is described as a source node transmitting information directly to a destination node, without intervention of any other node during the transmission process. This model follows the paradigm that each device should treat only the signals addressed to itself and discards any other transmission from other devices. This approach seems simple and effective, so why bother changing this old and common paradigm? We will answer this question in a elegant manner. Let us assume that the channel in which the signals are transmitted is suddenly unavailable or its quality went down drastically. In this case, the transmission from the source node to the destination node will be severely compromised. So, the answer to que question above is: non-cooperative communications are simple, effective, but do not cover

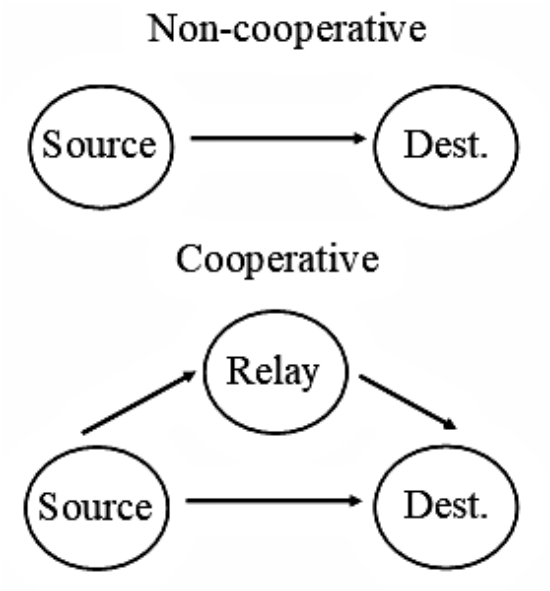

Figure 2.9: Non-cooperative and cooperative models.

all possible scenarios that may occur in a wireless communications system.

An alternative to this problem would be a scenario where a secondary link between the source and destination is available, with the help of another node acting as a repeater. This last described scenario follows the cooperative communications paradigm [3], which exploits the cooperation between nodes of the same network to achieve better transmission quality. In Fig. 2.9 we can see a schematic comparing both the non-cooperative and cooperative scenarios in wireless communications systems for a one-way half-duplex transmission. In a cooperative communications model, paths with uncorrelated fading between the destination and the source node are generated through the introduction of one or more retransmission channels [4]. Such retransmission channels are obtained through small fixed stations or through the users's own devices. Transmission commonly takes place in two phases. In the first phase, the source node sends the information simultaneously to the destination and to the relay. In the second phase, the relay retransmits the information to the destination. Both phases can also be multiplexed on frequency domain, although less common. This approach may also consider that there are no direct link between source and destination. In this case, in the first transmission phase, the source sends the information only to the relay. Another option would be a transmission from the source to the relay link only if the direct link between source and destination is shut down or compromised.

In comparison with the conventional non-cooperative model, the cooperative

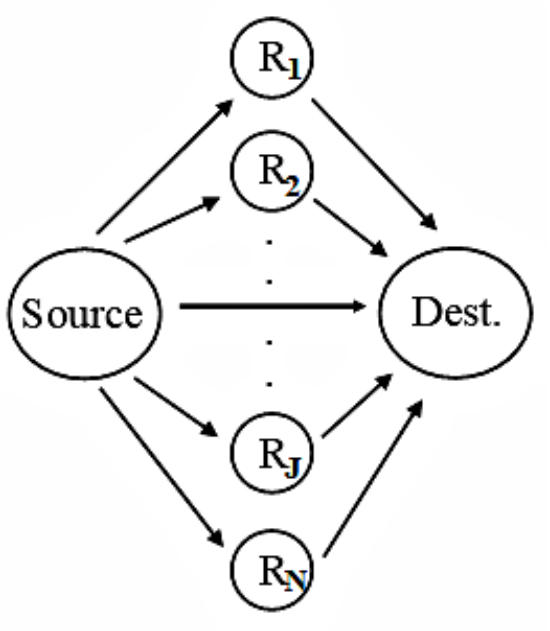

Figure 2.10: Cooperative model with N relays.

one has the following advantages [4], [3], [81]:

- Small path loss experienced;
- Increase of coverage area;
- Similar diversity to that existing in the MIMO model, without the need to insert more antennas on the same terminal;
- Costs of implementation can be reduced if the devices of the network acts as relays;
- Easier and cheaper to install relays than a base station;
- Less power required to transmissions;
- Truly uncorrelated channels (unlike MIMO).

Also, if we augment the number of relays, the coverage and link quality would greatly improves because more decorrelated alternative links would be available and, therefore, we increase the chance that at least one of the signals reach the destination with good quality. Figure 2.10 illustrates a cooperative transmission schematic with the availability of N relay-aided links.

For implementing cooperative communications, some strategies can be adopted, which are classified in: fixed and adaptive. In adaptive strategies, the use of relays

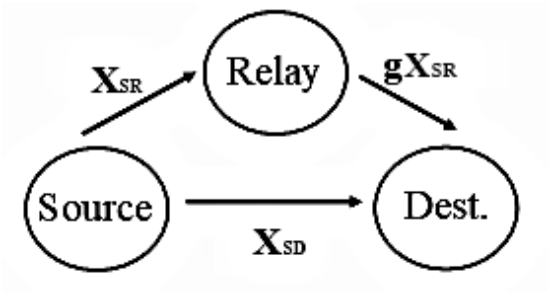

Figure 2.11: AF protocol schematic.

is controlled by some quality parameter, such as, for example, the SNR of the signal received. The implementation of these strategies becomes more complex compared to the implementation of fixed strategies, due to the need of more information about the system at the relays and due to the extra processing made. Adaptive strategies will not be used in this dissertation. More details about adaptive cooperative strategies can be found in [82] and in [3]. In fixed cooperative strategies, the relays always retransmit the information received regardless the conditions of the cooperative link. Such strategy have the advantage of being easily implemented, but, in the meantime, it has the disadvantage of low spectral efficiency. This disadvantage occurs due to the reduction of the overall rate caused by the division of the channel between the source's and relay's transmissions. The most common fixed cooperation strategies, and widely used in the literature, are the fixed amplify-and-forward (AF) and decode-and-forward (DF) protocols. In this dissertation, we will use the AF protocol on the upcoming chapters. In the AF protocol, the signal received by the relay is simply amplified by a factor g, where g is called the relay gain. Note that the amplification of the signal is intended to compensate the channel fading, so that, g is inversely proportional to the power received by the relay [3].

In Fig. 2.11 we can see a simple schematic showing the operation of a cooperative wireless communications network with AF relaying. X_{SD} denotes the signal transmitted from source to destination (source-destination link), X_{SR} denotes the signal transmitted from the source to the relay node (source-relay link) and gX_{SR} denotes the signal amplified and retransmitted from the relay node to the destination (relay-destination link). The relay gain g is, in general, given by [6]:

$$g = \sqrt{\frac{P_s}{|h_{SR}|^2 P_r + N_0}}, \tag{2.39}$$

where P_s is the source power, P_r the relay power, h_{SR} the channel coefficient of the source-relay link and N_0 is the variance of the noise present on the link. By means of simplicity, the AF protocol is of good choice because the relay node will just amplify the users signals and forwards it to the destination. Latency and complexity issues are kept small with this protocol. However, one of the disadvantages of the AF protocol is that the noise is also amplified and retransmitted to the destination. About the other fixed strategy, the decode-and-forward, the signal received by the relay will be decoded, recoded, then transmitted to the destination. The main advantage of this approach in comparison to the AF protocol is the non-propagation of noise on the transmitted signal [81], [3]. One of the main problems of this approach is the greater computational load at the relay.

Even being an interesting alternative, cooperative communications may not be the best case for every scenario. In a situation where the direct link is not subjected to much pathloss, shadowing or is close to the source, the cooperative link may not bring many improvements or may even give a worse performance. For an AF based relay link, retransmission amplifies useful signals but also amplifies the noise. Another important factor is that non-cooperative communications guarantees a high level of security and privacy of the data that travels in the network, since each device only has access to the information destined to it, instead of cooperative communications whereas information can be intercepted by other nodes of the network, which may provoke security issues.

Chapter 3

Multiuser Detection for Wireless Cooperative Uplink

In this chapter, a receiver based on a fourth-order PARAFAC tensor decomposition is proposed for a cooperative wireless communications uplink with M users transmitting to a base station with the help of relay-aided links implementing the AF protocol. The base station employs an array of antennas and the relays spreads the users signals using DS-CDMA. First, we describe the main scenario. Next we describe the tensorial model, its uniqueness conditions and properties, then we present the proposed receiver for this case. For last, the simulation results are presented and discussed.

3.1 System Model

The system model considered in this chapter is a cooperative DS-CDMA uplink. We have M users transmitting to a base station with the help of relay-aided links and there is no direct link between the users and the base station. The links between a given user and one relay are called source-relay (SR) and the ones between a relay and the base station are called relay-destination (RD). The base station has an uniform linear array of K antennas, each of the M users transmit to its R associated AF relays. The R relays of a given user will use direct-sequence spreading on the user signal, with a spreading code of length P, where the same code is used by all relays of a given user. Also, the relays and users are single antenna (SISO) devices operating in half-duplex mode.

It is assumed synchronization at chip level, frequency-flat fading is considered and all channels are independent to each other. We are considering that each

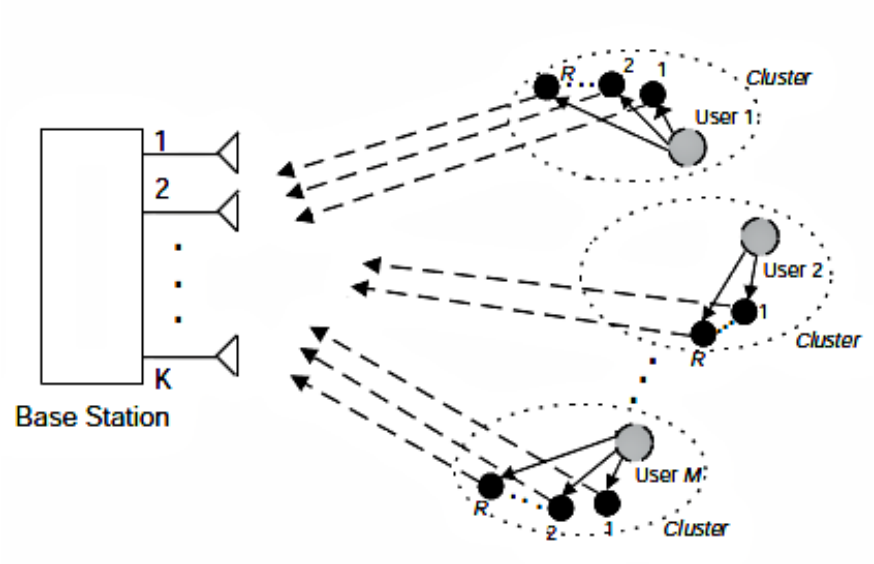

Figure 3.1: Cooperative DS-CDMA Uplink with M users and its clusters of R relays.

user communicates with its R associated relays and that each relay forwards the signal using a different time-slot. We also assume that a user and its relays are all located inside a cluster, such that the signal received at a relay located within the cluster of the m-th user contains no significant interference from the other users. This assumption was also made in [46] and [45]. An interpretation of this assumption is that a user and its relays are located in a cell, while the other users and their associated relays are located in other cells, being modeled as co-channel interferers. Fig. 3.1 illustrates the proposed system model.

The signal received by the r-th relay of the m-th user is given by:

$$u_{r,m,n}^{(SR)} = h_{r,m}^{(SR)} s_{n,m} + v_{r,m,n}^{(SR)}, \tag{3.1}$$

where $h_{r,m}^{(SR)}$ is the channel coefficient between the m-th user and its r-th relay, $s_{n,m}$ is the n-th symbol of the m-th user and $v_{r,m,n}^{(SR)}$ is the additive white gaussian noise (AWGN) component. All the data symbols $s_{n,m}$ are independent and identically distributed, with $1 \leq m \leq M$, and uniformly distributed over a Quadrature Amplitude Modulation (QAM) or a Phase-Shift Keying (PSK) alphabet. The signal received at the k-th antenna of the base station, trough the r-th time slot (relay-destination link), on the n-th symbol period and p-th chip, on the RD link is given by:

$$x_{k,r,n,p}^{(RD)} = \sum_{m=1}^{M} h_{k,r,m}^{(RD)} g_{r,m} u_{r,m,n}^{(SR)} c_{p,m} + v_{k,r,n,p}^{(RD)}, \tag{3.2}$$

where $h_{k,r,m}^{(RD)}$ is the channel coefficient between the k-th receive antenna and the r-th relay associated with the m-th user, $v_{k,r,n,p}^{(RD)}$ is the corresponding noise of the RD link, $g_{r,m}$ is the amplification factor applied by the r-th relay of the m-th user and $c_{p,m}$ is the p-th chip of the spreading code of the m-th user. Substituting (3.1) into (3.2), we get:

$$x_{k,r,n,p}^{(RD)} = \sum_{m=1}^{M} h_{k,r,m}^{(RD)} h_{r,m}^{(SR)} g_{r,m} s_{n,m} c_{p,m} + v_{k,r,n,p}^{(SRD)}, \tag{3.3}$$

$$v_{k,r,n,p}^{(SRD)} = \sum_{m=1}^{M} h_{k,r,m}^{(RD)} g_{r,m} v_{r,m,n}^{(SR)} c_{p,m} + v_{k,r,n,p}^{(RD)}. \tag{3.4}$$

The term $v_{k,r,n,p}^{(SRD)}$ is the total noise component through the source-relay-destination (SRD) link, from user to base station.

We assume that all links are subject to multipath propagation and all possible scatters are located far away from the base station, so that all the signals transmitted by the relays of a given user arrive at the destination with approximately the same angle of arrival. This means that, considering the signals transmitted from a given cluster of relays, the angle spread is small compared to the spatial resolution of the antenna array at the base station, as Figure 3.2 shows. This is truly valid when the user and its relays are close to each other and the base station experiences no scattering around its antennas. This is very common in suburban areas where the base station is on the top of a tall building or in a tower [83]. The channel coefficient $h_{k,r,m}^{(RD)}$ may then be expressed as:

$$h_{k,r,m}^{(RD)} = \sum_{l=1}^{L_{r,m}^{(RD)}} a_k(\theta_m) \beta_{l,r,m}^{(RD)}, \tag{3.5}$$

where θ_m is the mean angle of arrival of the m-th scattering cluster, $a_k(\theta_m)$ is the response of the k-th antenna of the m-th scattering cluster, defined as $a_k(\theta_m) = \exp(j{\theta_m}^{k-1})$, where θ_m is a uniform random variable with zero mean and variance of 2π, $\beta_{l,r,m}^{(RD)}$ is the fading envelope of the l-th path between the r-th relay of the m-th user and the base station. $L_{r,m}$ is the total number of multipaths. (3.5) can be rewritten as follows:

$$h_{k,r,m}^{(RD)} \approx a_k(\theta_m) \gamma_{r,m}^{(RD)}, \tag{3.6}$$

where $\gamma_{r,m}^{(RD)}$ is defined as $\gamma_{r,m}^{(RD)} = \sum_{l=1}^{L_{r,m}^{(RD)}} \beta_{l,r,m}^{(RD)}$.

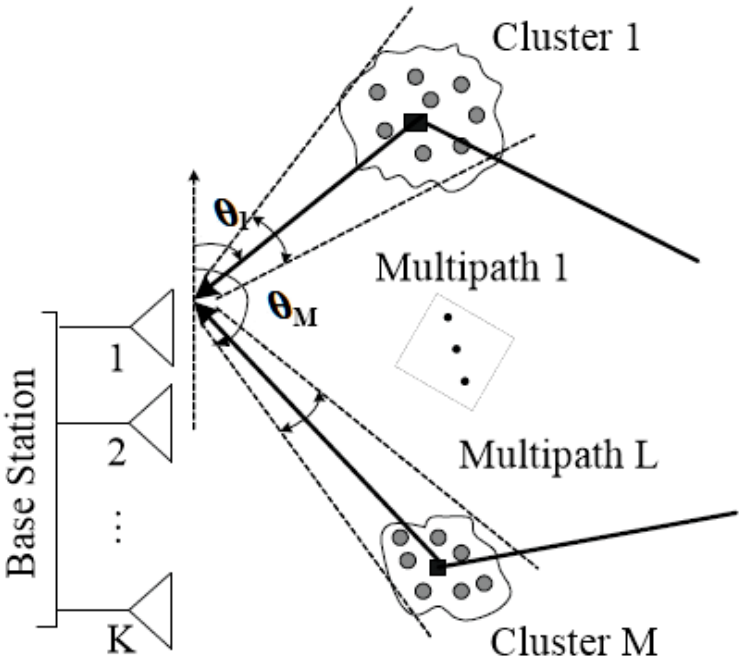

Figure 3.2: Representation of the multipath propagation scenario. Adapted from [1]

.

Now, by substituting (3.6) into (3.3), we get:

$$x_{k,r,n,p}^{(RD)} = \sum_{m=1}^{M} a_k(\theta_m)\gamma_{r,m}^{(RD)} h_{r,m}^{(SR)} g_{r,m} s_{n,m} c_{p,m} + v_{k,r,n,p}^{(SRD)} \tag{3.7}$$

and again, substituting (3.6) into (3.4), we get:

$$v_{k,r,n,p}^{(SRD)} = \sum_{m=1}^{M} a_k(\theta_m)\gamma_{r,m}^{(RD)} g_{r,m} v_{r,m,n}^{(SR)} c_{p,m} + v_{k,r,n,p}^{(RD)}. \tag{3.8}$$

The transmission rate for each user is given by $1/(R{+}1)$, thus, the total transmission rate on the system is $M/(R{+}1)$.

3.2 Variations of the System Model

Here we present some variations and considerations that can be incorporated or changed in the adopted system model. We compare some of these variations with the main model (presented on Section 3.1) in the simulation results section.

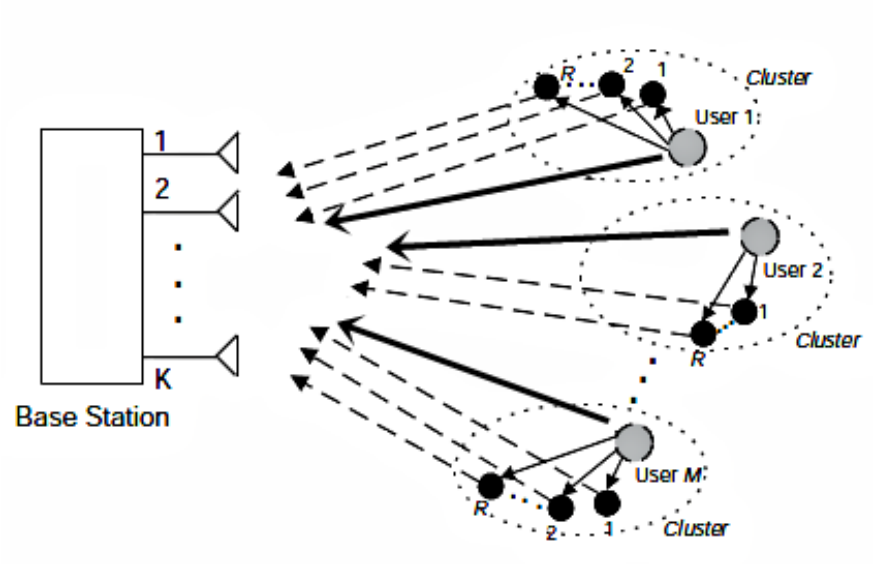

Figure 3.3: Addition of a direct link between user and base station, among the relay aided links.

3.2.1 Direct Link

The addition of a direct link between the users and the base station provides another possible scenario, as Figure 3.3 illustrates, so we have now the direct link and the cooperative links available. The direct link is called source-destination (SD) link. So, the discrete-time baseband received signal trough the SD link at the k-th base station antenna and n-th symbol period is described as follows:

$$x_{k,n}^{(SD)} = \sum_{m=1}^{M} h_{k,m}^{(SD)} s_{n,m} + v_{k,n}^{(SD)}, \tag{3.9}$$

where $h_{k,m}^{(SD)}$ is the channel coefficient between the m-th user and the k-th receive antenna, $s_{n,m}$ is the n-th symbol of the m-th user and $v_{k,n}^{(SD)}$ is the additive white gaussian noise at the k-th antenna and n-th symbol. The channel coefficient $h_{k,m}^{(SD)}$ may be also defined as:

$$h_{k,m}^{(SD)} = \sum_{l=1}^{L_m^{(SD)}} a_k(\theta_m) \beta_{l,m}^{(SD)}, \tag{3.10}$$

where $\beta_{l,m}^{(SD)}$ is the rayleigh fading envelope for the l-th path between the m-th user and the base station and $L_m^{(SD)}$ is the total number of multipaths on the SD

link. There is also a approximation for $h_{k,m}^{(SD)}$ as follows:

$$h_{k,m}^{(SD)} \approx a_k(\theta_m)\gamma_m^{(SD)}, \tag{3.11}$$

where $\gamma_m^{(SD)}$ is:

$$\gamma_m^{(SD)} = \sum_{l=1}^{L_m^{(SD)}} \beta_{l,m}^{(SD)}. \tag{3.12}$$

We can rewrite (3.9) this way:

$$x_{k,n}^{(SD)} = \sum_{m=1}^{M} a_k(\theta_m)\gamma_m^{(SD)} s_{n,m} + v_{k,n}^{(SD)}. \tag{3.13}$$

The direct link implementation presented above can be used alongside CDMA, thus giving us the system model of [2] if we do not consider the relay aided links. In Section 3.5 we compare the receiver of [2] with the proposed technique. The total transmission rate of the system for this case is M.

3.2.2 Simultaneous Transmission of the Relays

If we consider that all R relays of the system transmits at the same time instead of a transmission in R time-slots, then (3.7) turns into:

$$x_{k,n,p}^{(RD)} = \sum_{m=1}^{M}\sum_{r=1}^{R} a_k(\theta_m)\gamma_{r,m}^{(RD)} h_{r,m}^{(SR)} g_{r,m} s_{n,m} c_{p,m} + v_{k,n,p}^{(SRD)} \tag{3.14}$$

and (3.8) turns out to:

$$v_{k,n,p}^{(SRD)} = \sum_{m=1}^{M}\sum_{r=1}^{R} a_k(\theta_m)\gamma_{r,m}^{(RD)} g_{r,m} v_{r,m,n}^{(SR)} c_{p,m} + v_{k,n,p}^{(RD)}. \tag{3.15}$$

This approach was proposed in [47]. The transmission rate of the system is $M/2$. In fact, this alternative model increases the transmission rate but the model presented in Section 3.1 explores cooperative diversity by transmitting in different time-slots, which brings performance advantages, contrarily to the model presented in this subsection.

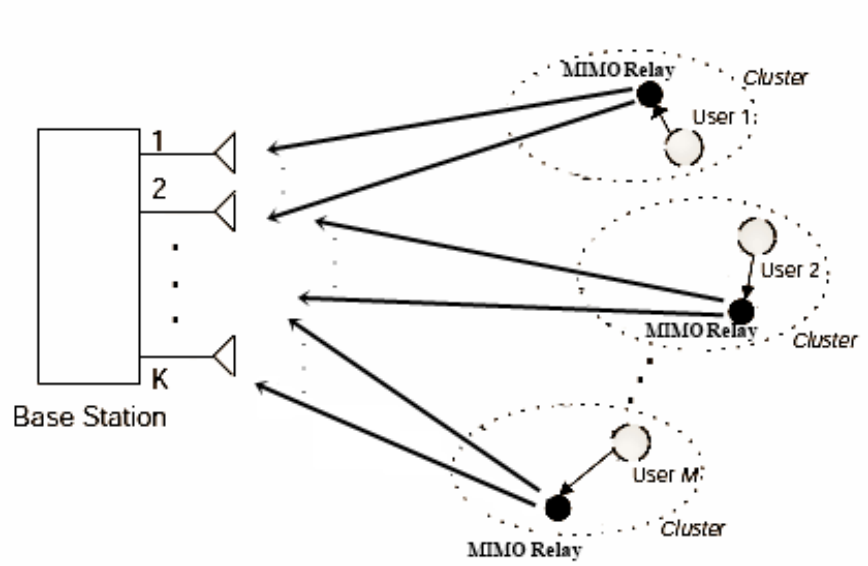

Figure 3.4: Variation of the system model by substituting R relays by a single MIMO $R \times R$ relay.

3.2.3 Distributed Khatri-Rao Space Time Coding

Instead of using direct-sequence spreading at the relays, we could use Distributed Khatri-Rao space-time (DKRST) coding, as presented in [15, 52]. In this case, the transmission of the data stream by the relays is done in blocks. By adopting DKRST coding at the relays, the model of Section 3.1 does not change, it is exactly the same. The term $c_{p,m}$ was represented as the p-th chip of the spreading sequence of the m-th user. Now, with DKRST coding, $c_{p,m}$, with $p = 1,...,P$, denotes the time-spreading code of the m-th user, with P being the length of the transmission block. By considering DKRST coding at the relays, we do not need to consider synchronization at chip level. The transmission rate for this case is $M/(R+1)$.

3.2.4 Single MIMO Relay

On this alternative model, we have only one MIMO relay for each user, totalizing M users and M relays. The same propagation scenario can be assumed here. The difference is that instead of R relays transmitting in different time-slots towards the base station, the users will have only one MIMO relay with R antennas, each antenna transmitting in different time-slots.

The index r no more represents the r-th relay, but the r-th transmit or r-th receive antenna of the MIMO relay. Hence, the mathematical model of Section

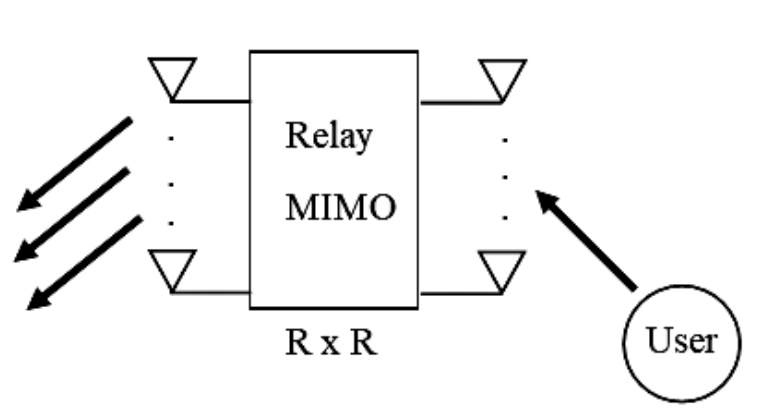

Figure 3.5: Alternate scenario where a user transmits to a single MIMO relay.

3.1 does not change. Fig. 3.5 shows the single MIMO relay schematic.

3.3 Proposed Tensor Model

The RD link described in Section 3.1 can be viewed as a four-way array with its dimensions directly related to space (receive antennas at base station), cooperative slots (cooperative channels), time (symbols) and spreading codes (chip). At this section, we model the received signal as a 4-th order tensor using a PARAFAC decomposition. For some variations of the system presented on Section 3.2, such as the direct link scenario and the simultaneous transmissions of the relays, we do not show their respective tensor models. For the system configurations using DKRST coding or a single MIMO relay per user, the following tensor model can be used with no changes.

Let $\mathcal{Y}$ be a quadrilinear PARAFAC model, so that $\mathcal{Y} \in \mathbb{C}^{K \times R \times N \times P}$ is a 4-th order tensor representing the baseband RD data signals at the base station:

$$[\mathcal{Y}]_{k,r,n,p} = x^{(RD)}_{k,r,n,p} \tag{3.16}$$

for $k = 1,...,K$, $r = 1,...,R$, $n = 1,...,N$ and $p = 1,...,P$. In order to simplify presentation we are going to omit the AWGN terms and assume that the channel is constant for N symbol periods throughout the rest of this section. A typical element of $\mathcal{Y}$, denoted by $y_{k,r,n,p} = [\mathcal{Y}_{k,r,n,p}]$ is given by:

$$y_{k,r,n,p} = \sum_{m=1}^{M} a_k(\theta_m) h_{r,m} s_{n,m} c_{p,m}, \tag{3.17}$$

where the channel coefficient $h_{r,m}$ is defined as:

$$h_{r,m} = \gamma_{r,m}^{(RD)} h_{r,m}^{(SR)} g_{r,m}. \tag{3.18}$$

(3.17) corresponds to a PARAFAC model with spatial, cooperative slots, time and code indices, in other words, a quadrilinear data tensor, as the one presented in (2.28). The data tensor $\mathcal{Y}$ can be expressed in another way:

$$\mathcal{Y} = \sum_{m=1}^{M} \mathbf{A}_{.,m} \circ \mathbf{H}_{.,m} \circ \mathbf{S}_{.,m} \circ \mathbf{C}_{.,m}, \tag{3.19}$$

where $\circ$ denotes the outer product, $\mathbf{A} \in \mathbb{C}^{K \times M}$ is the antenna array response matrix with $[\mathbf{A}]_{k,m} = a_k(\theta_m)$, $\mathbf{H} \in \mathbb{C}^{R \times M}$ is the channel matrix with $[\mathbf{H}]_{r,m} = h_{r,m}$, $\mathbf{S} \in \mathbb{C}^{N \times M}$ is the symbol matrix with $[\mathbf{S}]_{n,m} = s_{n,m}$ and $\mathbf{C} \in \mathbb{C}^{P \times M}$ is the spreading code matrix with $[\mathbf{C}]_{p,m} = c_{p,m}$. In (3.19), we have the CP decomposition of the data tensor $\mathcal{Y}$ as a sum of M rank-1 components and $\mathbf{A}$, $\mathbf{H}$, $\mathbf{S}$ and $\mathbf{C}$ are the factor matrices of the decomposition. This PARAFAC model is irreducible in the sense that $y_{k,r,n,p}$ cannot be represented using less than M components (this is the same to say that the 4-way array with typical element $y_{k,r,n,p}$ has rank M) [73].

3.3.1 Unfolding Matrices

We can rewrite (3.19) in an unfolding matricial form. The unfoldings can be obtained from the slices of the data tensor. The slices are defined by fixing all but two indices, resulting in a matrix. In this work, the 4-th order array is sliced in 4 different ways. The following slices are used:

$$\mathbf{Y}_{k,r,.,.} = \mathbf{S}\, diag_r[\mathbf{H}]\, diag_k[\mathbf{A}]\, \mathbf{C}^T, \tag{3.20}$$

$$\mathbf{Y}_{k,.,.,p} = \mathbf{H}\, diag_k[\mathbf{A}]\, diag_p[\mathbf{C}]\, \mathbf{S}^T, \tag{3.21}$$

$$\mathbf{Y}_{.,.,n,p} = \mathbf{A}\, diag_p[\mathbf{C}]\, diag_n[\mathbf{S}]\, \mathbf{H}^T, \tag{3.22}$$

$$\mathbf{Y}_{.,r,n,.} = \mathbf{C}\, diag_n[\mathbf{S}]\, diag_r[\mathbf{H}]\, \mathbf{A}^T, \tag{3.23}$$

with $\mathbf{Y}_{k,r,.,.} \in \mathbb{C}^{N\times P}$, $\mathbf{Y}_{k,.,.,p} \in \mathbb{C}^{R\times N}$, $\mathbf{Y}_{.,.,n,p} \in \mathbb{C}^{K\times R}$ and $\mathbf{Y}_{.,r,n,.} \in \mathbb{C}^{K\times P}$, where the operator $diag_j[\ \ ]$ denotes the diagonal matrix formed with the j-th row of the matrix argument. The unfolded matrices, denoted by $\mathbf{Y}_1$-$\mathbf{Y}_4$ are obtained by stacking the slices above, as follows:

$$\mathbf{Y}_1 = \begin{bmatrix} \mathbf{Y}_{1,1,.,.} \\ . \\ . \\ . \\ \mathbf{Y}_{K,R,.,.} \end{bmatrix}, \mathbf{Y}_2 = \begin{bmatrix} \mathbf{Y}_{1,.,.,1} \\ . \\ . \\ . \\ \mathbf{Y}_{K,.,.,P} \end{bmatrix},$$

$$\mathbf{Y}_3 = \begin{bmatrix} \mathbf{Y}_{.,.,1,1} \\ . \\ . \\ . \\ \mathbf{Y}_{.,.,N,P} \end{bmatrix}, \mathbf{Y}_4 = \begin{bmatrix} \mathbf{Y}_{.,1,1,.} \\ . \\ . \\ . \\ \mathbf{Y}_{.,R,N,.} \end{bmatrix}. \tag{3.24}$$

We have that $\mathbf{Y}_1 \in \mathbb{C}^{KRN\times P}$ is the tensor $\mathcal{Y} \in \mathbb{C}^{K\times R\times N\times P}$ unfolded into a matrix, as follows:

$$\mathbf{Y}_1 = (\mathbf{A} \diamond \mathbf{H} \diamond \mathbf{S})\mathbf{C}^T, \tag{3.25}$$

The other unfolding matrices are defined as:

$$\mathbf{Y}_2 = (\mathbf{C} \diamond \mathbf{A} \diamond \mathbf{H})\mathbf{S}^T, \tag{3.26}$$

$$\mathbf{Y}_3 = (\mathbf{S} \diamond \mathbf{C} \diamond \mathbf{A})\mathbf{H}^T, \tag{3.27}$$

$$\mathbf{Y}_4 = (\mathbf{H} \diamond \mathbf{S} \diamond \mathbf{C})\mathbf{A}^T, \tag{3.28}$$

with $\mathbf{Y}_2 \in \mathbb{C}^{PKR\times N}$, $\mathbf{Y}_3 \in \mathbb{C}^{NPK\times R}$ and $\mathbf{Y}_4 \in \mathbb{C}^{RNP\times K}$.

3.3.2 Uniqueness Properties

One of the most important properties of the tensor model obtained in (3.17) and (3.19) is its essential uniqueness under certain conditions [73, 57]. The uniqueness properties of the quadrilinear PARAFAC model presented by Kruskal and described in [73, 57] are given as follows:

$$k_{\mathbf{A}} + k_{\mathbf{H}} + k_{\mathbf{S}} + k_{\mathbf{C}} \geq 2M + 3, \tag{3.29}$$

where $k_{\mathbf{A}}$ is the Kruskal rank of the matrix $\mathbf{A}$, (similarly to $\mathbf{H}$, $\mathbf{S}$ and $\mathbf{C}$). If the condition (3.29) is satisfied, the factor matrices $\mathbf{A}$, $\mathbf{H}$, $\mathbf{S}$ and $\mathbf{C}$ are essentially unique, hence, each factor matrix can be determined up to column scaling and permutation. This uniqueness properties of the PARAFAC decomposition means that any other set of matrices ($\mathbf{A}^{'}$, $\mathbf{H}^{'}$, $\mathbf{C}^{'}$ and $\mathbf{S}^{'}$) that satisfies (3.19), is related with the original matrix set ($\mathbf{A}$, $\mathbf{H}$, $\mathbf{C}$ and $\mathbf{S}$) by $\mathbf{A}^{'} = \mathbf{A}\Pi\Delta_{\mathbf{A}}$, $\mathbf{H}^{'} = \mathbf{H}\Pi\Delta_{\mathbf{H}}$, $\mathbf{C}^{'} = \mathbf{C}\Pi\Delta_{\mathbf{C}}$ and $\mathbf{S}^{'} = \mathbf{S}\Pi\Delta_{\mathbf{S}}$, where $\Pi \in \mathbb{C}^{M\times M}$ is a permutation matrix and $\Delta_{\mathbf{A}}$, $\Delta_{\mathbf{H}}$, $\Delta_{\mathbf{C}}$ and $\Delta_{\mathbf{S}}$ are diagonal matrices that meet $\Delta_{\mathbf{A}}\Delta_{\mathbf{H}}\Delta_{\mathbf{C}}\Delta_{\mathbf{S}} = \mathbf{I}_M$.

Now, let us assume that $\mathbf{A}$, $\mathbf{H}$, $\mathbf{C}$ and $\mathbf{S}$ are all full k-rank (a matrix is said to have full k-rank if its k-rank is equal to minimum between the number of rows and columns), thus, condition (3.29) becomes:

$$min(K, M) + min(R, M) + min(N, M) + min(P, M) \geq 2M + 3. \qquad (3.30)$$

Given that a matrix whose elements are drawn independently from an continuous distribution has full k-rank with probability one [2], then matrix $\mathbf{H}$ has full k-rank with probability one. Such assumption is valid when the user signals undergo independent fading channels which is one of the propagation scenario assumptions made earlier. Also, the matrix $\mathbf{A}$ is full k-rank because we are modeling it as a Vandermonde matrix with distinct generators, as the different users signals arrives at the base station array with different angles of arrival. The symbols matrix $\mathbf{S}$ is full k-rank with high probability if N is sufficiently large in comparison to the modulation cardinality and the number of users. At last, for the matrix $\mathbf{C}$, full k-rank is possible if a certain length of spreading codes are used. Fig. 3.6 depicts the boundary of the identifiability region of condition (3.30) for $M = 8$ and $N = 16$.

With the assumptions above made, we can determine some parameters of the adopted system, for example, the number of users that the proposed receiver can handle and the minimum acceptable parameters (number of antennas at base station, length of the spreading code, number of relays or the data block length) that match a target number of users channels to be detected. Hence, we have flexibility when choosing K, R, N and P, which is the one of the main reasons for considering the tensor approach. It provides different tradeoffs for the system model based on the parameters. We may note that the adoption of CDMA codes when the relays do not transmit simultaneously may seem unnecessary, but the addition of one more index to the data tensor may provide more flexibility when

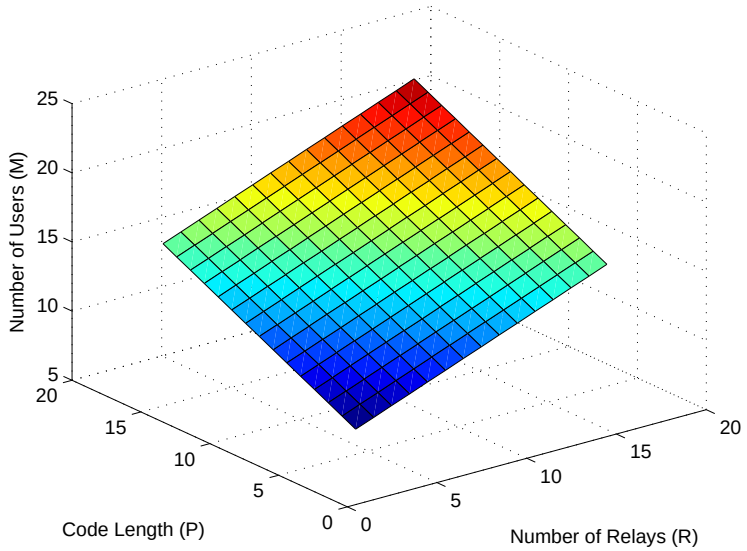

Figure 3.6: Boundary of identifiability region for $K = 4$ antennas and $N = 16$.

exploiting the uniqueness of condition (3.30). Indeed, we have:

- If $P \geq M$, $N \geq M$, then $\min(K,M) + \min(R,M) \geq 3$. For example, if $K = 2$ and $R = 1$, we satisfy condition (3.30), which means that 1 relay per user and 2 antennas at the base station (or 2 relay per user and 1 antenna at the base station) are sufficient for M users. Thus the system supports more users than relays and sensors.

- If $P \geq M$, $N \geq M$ and $K \geq 2$, then we may set $R = 1$, which can give us a possible scenario of [47], a cooperative DS-CDMA uplink with one relay per user. In this scenario, there is no cooperative diversity.

- If $K \geq M$, $N \geq M$, then $R = 2$ and $P = 1$ is sufficient for M users. Setting $P = 1$ is equivalent to no spreading at the relays, thus a non-CDMA scenario. Therefore, we get the models from [45] and [46].

- If $K \geq M$, $P \geq M$, then $R = 1$ and $N = 2$ are enough to guarantee uniqueness. It means that a short block length is sufficient for detection.

Based on the assumptions above, we can conclude that the proposed tensor model gives us flexibility about many parameters and different kinds of diversity tradeoffs. For example, let $M = 8$, $K \leq M$, $R \leq M$, $N \leq M$ and $P \leq M$, then

condition (3.30) turns into:

$$K + R + N + P \geq 19. \tag{3.31}$$

So, when modeling the system parameters to handle 8 users, the number of antennas at the base station, number o relays, lengths of the spreading codes and data blocks will have to match condition (3.31) in order to guarantee uniqueness. We can then design the system based on the number of users and then distribute the parameters according to availability (number of antennas, relays and etc).

3.4 Receiver Algorithm

Assuming that there is no channel information at the receiver or transmitter, the algorithm presented in this section is based on the ALS (Alternating Least Squares) method, which consists in fitting the quadrilinear model to the received data tensor [75, 64]. The idea behind the ALS procedure is very simple: at each time, update one of the factor matrices by using the least squares estimation technique with the previous estimations of the other factor matrices. Each factor matrix is estimated, in an alternate way, always using the previous estimations of the other factor matrices. This procedure goes on until convergence. Two factor matrices are randomly initialized before the first iteration. The unfolding matrices in (3.25)-(3.28) will be used to estimate $\mathbf{A}$, $\mathbf{H}$ and $\mathbf{S}$ for the proposed semi-blind receiver, where we are assuming knowledge of the spreading codes (matrix $\mathbf{C}$) at the receiver and the first row of matrix $\mathbf{S}$, which are pilot symbols.

Let us consider the noisy data tensor $\tilde{\mathcal{Y}}$, then $\tilde{\mathcal{Y}}$ is unfolded into the matrices $\tilde{\mathbf{Y}}_1$-$\tilde{\mathbf{Y}}_4$, the noisy versions of $\mathbf{Y}_1$-$\mathbf{Y}_4$. From (3.28), the Least Squares update for $\mathbf{A}$ is given by:

$$\hat{\mathbf{A}} = [\tilde{\mathbf{Y}}_4(\hat{\mathbf{H}} \diamond \hat{\mathbf{S}} \diamond \mathbf{C})^{\dagger}]^T, \tag{3.32}$$

where $\hat{\mathbf{H}}$ and $\hat{\mathbf{S}}$ are the Least Squares updates previously obtained for $\mathbf{H}$ and $\mathbf{S}$ respectively and $(.)^{\dagger}$ denotes the pseudo-inverse. Similarly, we have:

$$\hat{\mathbf{S}} = [\tilde{\mathbf{Y}}_2(\mathbf{C} \diamond \hat{\mathbf{A}} \diamond \hat{\mathbf{H}})^{\dagger}]^T, \tag{3.33}$$

$$\hat{\mathbf{H}} = [\tilde{\mathbf{Y}}_3(\hat{\mathbf{S}} \diamond \mathbf{C} \diamond \hat{\mathbf{A}})^{\dagger}]^T. \tag{3.34}$$

The Quadrilinear ALS algorithm is shown in Algorithm 1. The error at the end of the i-th iteration is given by:

$$e(i) = \frac{\|\tilde{\mathbf{Y}}_1 - (\hat{\mathbf{A}}_{(i)} \diamond \hat{\mathbf{H}}_{(i)} \diamond \hat{\mathbf{S}}_{(i)})\mathbf{C}^T\|_F^2}{\|\tilde{\mathbf{Y}}_1\|_F^2}. \tag{3.35}$$

where $\|.\|_F$ denotes the Frobenius norm. The convergence of the algorithm is obtained when $|e(i) - e(i-1)| < 10^{-6}$.

Algorithm 1 ALS FITTING - Semi-Blind Receiver

1)*Initialization* : *Set* $i = 0$; *Initialize* $\hat{\mathbf{A}}_{(i=0)}$ *and* $\hat{\mathbf{H}}_{(i=0)}$;
2)$i = i + 1$;
3)*Using* $\tilde{\mathbf{Y}}_2$, *find a LS estimate of* $\mathbf{S} : \hat{\mathbf{S}}_{(i)}^T = (\mathbf{C} \diamond \hat{\mathbf{A}}_{(i-1)} \diamond \hat{\mathbf{H}}_{(i-1)})^\dagger \tilde{\mathbf{Y}}_2$;
4)*Using* $\tilde{\mathbf{Y}}_3$, *find a LS estimate of* $\mathbf{H} : \hat{\mathbf{H}}_{(i)}^T = (\hat{\mathbf{S}}_{(i)} \diamond \mathbf{C} \diamond \hat{\mathbf{A}}_{(i-1)})^\dagger \tilde{\mathbf{Y}}_3$;
5)*Using* $\tilde{\mathbf{Y}}_4$, *find a LS estimate of* $\mathbf{A} : \hat{\mathbf{A}}_{(i)}^T = (\hat{\mathbf{H}}_{(i)} \diamond \hat{\mathbf{S}}_{(i)} \diamond \mathbf{C})^\dagger \tilde{\mathbf{Y}}_4$;
6)*Repeat steps* $2 - 5$ *until convergence*;

After obtaining the estimation of $\mathbf{A}$, $\mathbf{H}$ and $\mathbf{S}$, it is necessary to remove scaling ambiguity. Permutation ambiguity is not present on the semi-blind receiver because one matrix is assumed known (matrix $\mathbf{C}$). The scaling ambiguity of $\hat{\mathbf{A}}$ is removed by considering that the first row of $\mathbf{A}$ is known (the first row of $\mathbf{A}$ is composed of 1's). Then, the scaling matrix $\Delta_{\mathbf{A}}$ of $\hat{\mathbf{A}}$ is obtained by dividing the first row of $\hat{\mathbf{A}}$ by the first row of $\mathbf{A}$. To remove the scaling ambiguity of $\hat{\mathbf{A}}$, we have:

$$\hat{\mathbf{A}} = \hat{\mathbf{A}}\ \mathit{diag}\ [(\Delta_{\mathbf{A}})^-1]. \tag{3.36}$$

The same can be done to remove scaling ambiguity from $\hat{\mathbf{S}}$. Is assumed the first row of $\mathbf{S}$ as known (one pilot symbol per user) and the scaling ambiguity is removed as follows:

$$\hat{\mathbf{S}} = \hat{\mathbf{S}}\ \mathit{diag}\ [(\Delta_{\mathbf{S}})^-1], \tag{3.37}$$

where $\Delta_{\mathbf{S}}$ is the scaling matrix of $\hat{\mathbf{S}}$. After obtaining the scaling matrix of $\hat{\mathbf{A}}$ and $\hat{\mathbf{S}}$, we can find the scaling matrix $\Delta_{\mathbf{H}}$ of $\hat{\mathbf{H}}$ by:

$$\Delta_{\mathbf{A}}\Delta_{\mathbf{S}}\Delta_{\mathbf{H}} = \mathbf{I}_M \tag{3.38}$$

and again, we can remove the scaling ambiguity of $\hat{\mathbf{H}}$:

$$\hat{\mathbf{H}} = \hat{\mathbf{H}}\ \mathit{diag}\ [(\Delta_{\mathbf{H}})^-1]. \tag{3.39}$$

If the knowledge of matrix $\mathbf{C}$ is not possible, the ALS algorithm will have one step added, as shown in Algorithm 2. In terms of convergence, Algorithm 1 converges in much less time than Algorithm 2. Convergence of Algorithm 2 is obtained when $|e(i) - e(i-1)| < 10^{-6}$, with the error $e(i)$ given by (3.35). After the estimation, scaling ambiguity of matrix $\mathbf{C}$ can be removed by assuming that the first row of $\mathbf{C}$ is known. This is possible because $\mathbf{C}$ is a Hadamard matrix with the first row composed only by 1's. Then, scaling ambiguity of matrix $\hat{\mathbf{C}}$ is removed the same way showed earlier for matrix $\hat{\mathbf{A}}$.

Algorithm 2 ALS FITTING - Semi-Blind Receiver with $\mathbf{C}$ Estimation

1)*Initialization* : *Set* $i = 0$; *Initialize* $\hat{\mathbf{A}}_{(i=0)}$, $\hat{\mathbf{C}}_{(i=0)}$ *and* $\hat{\mathbf{H}}_{(i=0)}$;
2)$i = i + 1$;
3)*Using* $\tilde{\mathbf{Y}}_2$, *find a LS estimate of* $\mathbf{S} : \hat{\mathbf{S}}_{(i)}^{T} = (\hat{\mathbf{C}}_{(i-1)} \diamond \hat{\mathbf{A}}_{(i-1)} \diamond \hat{\mathbf{H}}_{(i-1)})^{\dagger}\tilde{\mathbf{Y}}_2$;
4)*Using* $\tilde{\mathbf{Y}}_3$, *find a LS estimate of* $\mathbf{H} : \hat{\mathbf{H}}_{(i)}^{T} = (\hat{\mathbf{S}}_{(i)} \diamond \hat{\mathbf{C}}_{(i-1)} \diamond \hat{\mathbf{A}}_{(i-1)})^{\dagger}\tilde{\mathbf{Y}}_3$;
5)*Using* $\tilde{\mathbf{Y}}_4$, *find a LS estimate of* $\mathbf{A} : \hat{\mathbf{A}}_{(i)}^{T} = (\hat{\mathbf{H}}_{(i)} \diamond \hat{\mathbf{S}}_{(i)} \diamond \hat{\mathbf{C}}_{(i-1)})^{\dagger}\tilde{\mathbf{Y}}_4$;
6)*Using* $\tilde{\mathbf{Y}}_1$, *find a LS estimate of* $\mathbf{C} : \hat{\mathbf{C}}_{(i)}^{T} = (\hat{\mathbf{A}}_{(i)} \diamond \hat{\mathbf{H}}_{(i)} \diamond \hat{\mathbf{S}}_{(i)})^{\dagger}\tilde{\mathbf{Y}}_1$;
7)*Repeat steps* $2-6$ *until convergence*;

3.5 Simulation Results

This section presents computer simulations results for performance evaluation purposes with the following scenario. The wireless links have frequency-flat Rayleigh fading with path loss exponent equal to 3, the base station antenna array is composed by K antennas, 16-QAM modulation is used and Hadamard orthogonal codes are considered for spreading sequences. The signals transmitted by the relays of a given user arrive at the destination with the same angle of arrival and the angle spread is zero. Also, the number of multipaths $L_{r,m}^{(RD)}$ was considered 30. The symbol error rate (SER), bit error rate (BER) and channel normalized mean square error (NMSE) curves are shown in function of the mean signal-to-noise ratio (SNR) of the RD link. The mean results were obtained using 10000 independent Monte Carlo samples with each run corresponding to a different realization of channel's gains, spatial signatures, modulation symbols and noise. The AF gain used at simulations is given by:

$$g_{r,m} = \sqrt{\frac{P_s}{|h_{r,m}^{(SR)}|^2 P_r + N_0}}, \tag{3.40}$$

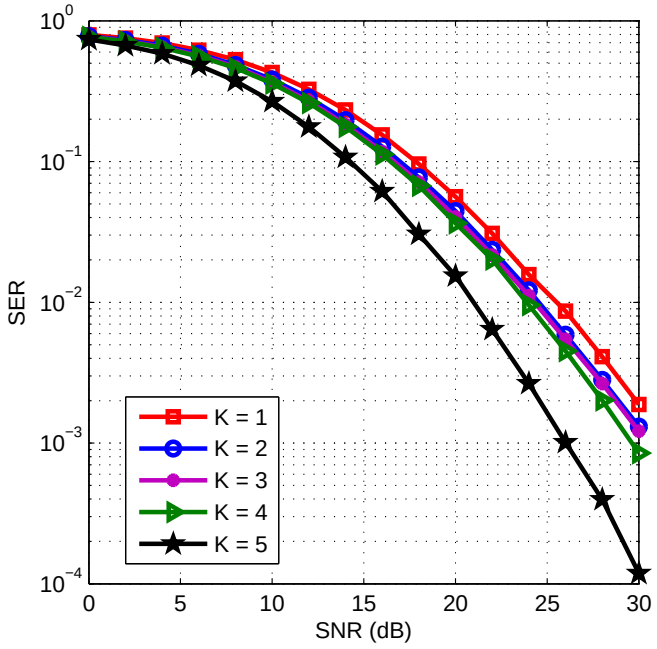

Figure 3.7: SER versus SNR performance of the proposed semi-blind receiver for different values of K (number of receive antennas).

where P_s is the source power, P_r the relay power and N_0 the noise variance. We considered $P_s = P_r = 1$.

In Fig. 3.7, we assume a datablock of $N = 16$ symbols, $M = 4$ users, $P = 8$ chips and $R = 2$ relays. This figure shows the performance of the SER for different values of K (number of receive antennas). From this figure, it can be viewed that the SER performance improves when the number of antennas at the base station is increased. We can then affirm that the proposed receiver exploits spatial diversity at the receiver.

Figure 3.8 shows the SER versus SNR for the proposed technique with $P = 8$ chips, a datablock of $N = 16$ symbols, $K = 2$ receive antennas and $M = 4$ users. Then we have curves for various values of R (number of relays on the cluster). From Fig. 3.8 we can observe a better SER performance when we increase the number of relays on the system. This happens because when the number of relays is augmented, the model turns to a more cooperative scenario, exploiting cooperative diversity and resulting in better link quality. Comparing Figures 3.7 and 3.8, we can conclude that an increase in the number of relays per user R provides a high performance gain than an increase in the number

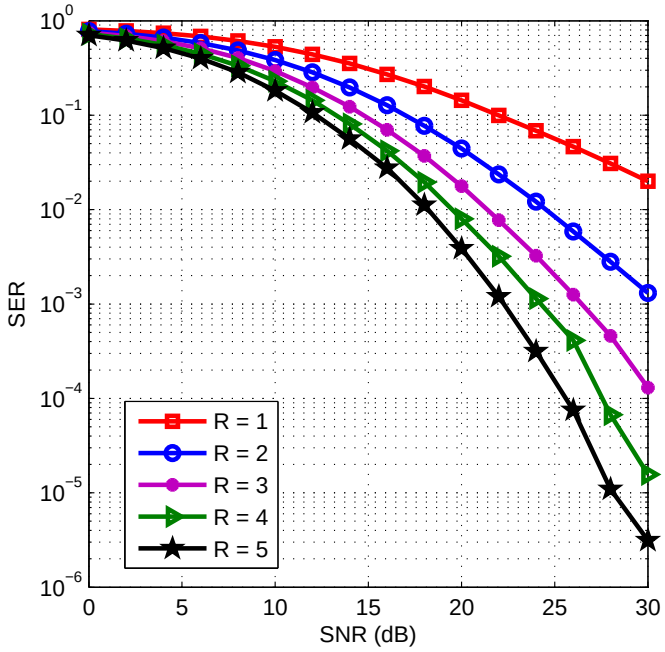

Figure 3.8: SER versus SNR performance of the proposed semi-blind receiver for a different number of relays on the system.

of receive antennas K. However, when we increase the number of relays we also decrease the spectral efficiency of the system and latency is increased.

Figure 3.9 shows the influence of the spreading code length P on the SER, where we assumed $R = 2$ relays, $K = 3$ antennas, $N = 16$ symbols and $M = 2$ users. In this figure it is possible to see a slightly decrease on the SER as the length of the spreading code is augmented. Comparing Figs. 3.7, 3.8 and 3.9, we can view that an increase in P provides a smaller performance gain than an increase in K and R. This happens because the considered communication system does not exploit frequency diversity, due to the fact that we are considering frequency-flat fading. In addition, if we assume a DKRST coding at the relays, it can be viewed as a time-spreading operation, without time diversity. Generally, the introduction of CDMA codes waives the successive transmission of the relays, since they can transmit simultaneously and share the same channel.

Fig. 3.10 depicts the SER performance for several values of the data block length N, where we have $P = 8$ chips, $K = 2$ receive antennas, $R = 2$ relays and $M = 4$ users. It is observed from Figure 3.10 that there is little change on SER for different data block lengths. Starting from a small length of 2, we note a

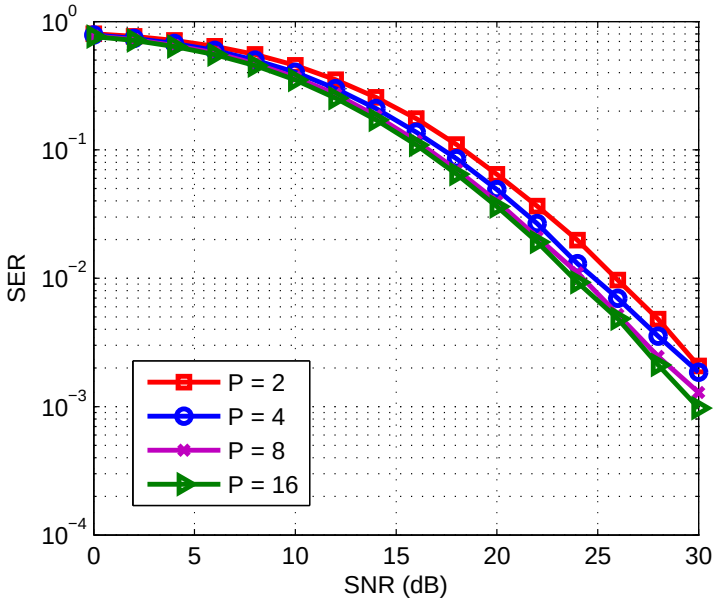

Figure 3.9: SER versus SNR performance of the proposed semi-blind receiver for different values of P (spreading code length).

small decrease of the SER performance as N is increased to 8. From a datablock length change of 8 to 256 there is almost no variation on the SER. As we increase N, we have more symbols to estimate, which explains the better performance for a short symbol block of 2. Moreover, as above explained, because the system does not exploit time diversity, we should not expect significant variations on the SER when the value of N is changed. We may also note that we assume knowledge of the first row of matrix $\mathbf{S}$, thus, smaller values of N, such as 2 or 3 means knowledge of half or one third of the matrix $\mathbf{S}$, respectively. Hence, for small values of N, the receiver should perform better than for greater values such as 32 or 256.

For Figure 3.11, we have the SER performance for different values of M (users on the system), where we consider $P = 16$, $K = 2$, $R = 2$ and $N = 16$. From Fig. 3.11, we can see that the number of users has no impact on the SER. This can be explained by the fact that multiuser interference at the relays is not considered, then, when M is increased, the error rate does not change. Also, the total number of relays is also increased when M is augmented (total number of relays is MR).

Now we compare the SER performance of the proposed semi-blind receiver for four different coding sequences. For Fig. 3.12, we considered $K = 2$ receive antennas, $R = 3$ relays, $N = 16$ and $M = 8$ users. We compared the Hadamard orthogonal code matrix, a DFT (Discrete Fourier Transform) matrix, a random

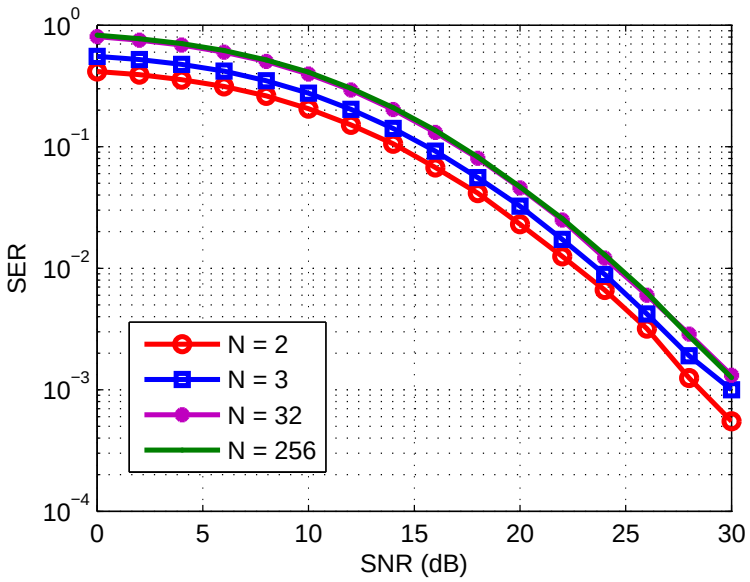

Figure 3.10: SER versus SNR performance of the proposed semi-blind receiver for different values of N (data block length).

code matrix (generated by a normal distribution with mean 0 and unitary variance) and a PN (Pseudo-Noise) sequence [84]. We set $P = 8$ for each configuration. From Fig. 3.12 we can see that the performance of the semi-blind receiver operating under direct-sequence orthogonal spreading or using the DFT coding scheme is almost identical. This happens because the DFT matrix and the orthogonal Hadamard codes provides orthogonal decorrelation. For the Random matrix and the PN sequences, performance went worse because there is noise amplification. In a practical system, Hadamard codes would be the best option as spreading sequences.

On Figure 3.13, we compare the SER of the proposed receiver with the ones of the following techniques: Zero Forcing (ZF) receiver that works under complete knowledge of $\mathbf{A}$, $\mathbf{H}$ and $\mathbf{C}$, the semi-blind DS-CDMA receiver proposed in [2] (non-cooperative DS-CDMA), the receiver proposed in [46] using AF (same cenario of the present work, but without spreading codes) and the receiver shown in [47], where the relays transmit at the same time. The ZF receiver estimates $\mathbf{S}$ as follows:

$$\hat{\mathbf{S}}_{ZF} = [(\mathbf{C} \diamond \mathbf{A} \diamond \mathbf{H})^{\dagger}\mathbf{Y}_2]^T. \tag{3.41}$$

For Figure 3.13, we set $N = 16$, $P = 2$, $M = 4$, $K = 3$ and $R = 2$ for both the ZF and the proposed receiver. For the receiver proposed in [46], only one relay is

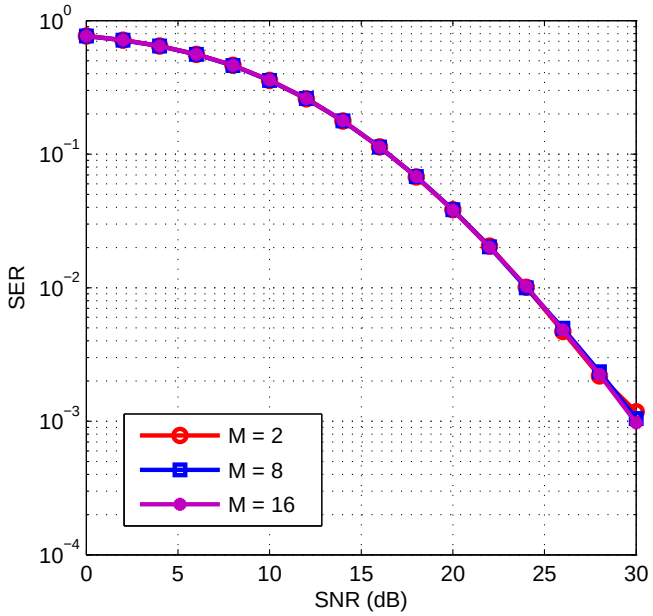

Figure 3.11: SER versus SNR performance of the proposed semi-blind receiver for different values of M (users on the system).

used and we set $K = 3$, $N = 16$ and $M = 2$. P is not considered because there is no CDMA in [46]. For [2], we set $P = 4$, $K = 3$, $N = 16$ and $M = 4$. The last receiver, the one of [47], we set $N = 16$, $P = 2$, $M = 4$, $K = 3$ and $R = 1$). These simulations parameters were chosen to give us the same or similar spectral efficiency for all the receivers. The spectral efficiency for each configuration is: $M \,/\, (PR + 1)$ for the proposed receiver and the ZF, $M \,/\, (R + 1)$ for the receiver described in [46], $M \,/\, P$ for [2] and $M \,/\, 2P$ for [47]. The link between user and base station used on [2] has three times the distance than the SR link (user to relay) with path loss coefficient equal to 3. We see in Fig. 3.13 that the ZF receiver went better in comparison with the proposed model, which is expected. However, the proposed receiver still showed good performance even without knowing the factor matrices ($\mathbf{A}$, $\mathbf{H}$ and $\mathbf{S}$). Both the ZF and the proposed receiver went better than the non-cooperative CDMA semi-blind receiver described in [2], the receiver of [46], and the one of [47].

The addition of one dimension to the received signal tensor (chip dimension) makes the proposed receiver to have a better performance in comparison to [46]. The proposed model also went better than [2] due to the cooperative scenario (short relay-aided links instead of extended direct links) and showed better performance than the receiver presented in [47] because the proposed receiver ex-

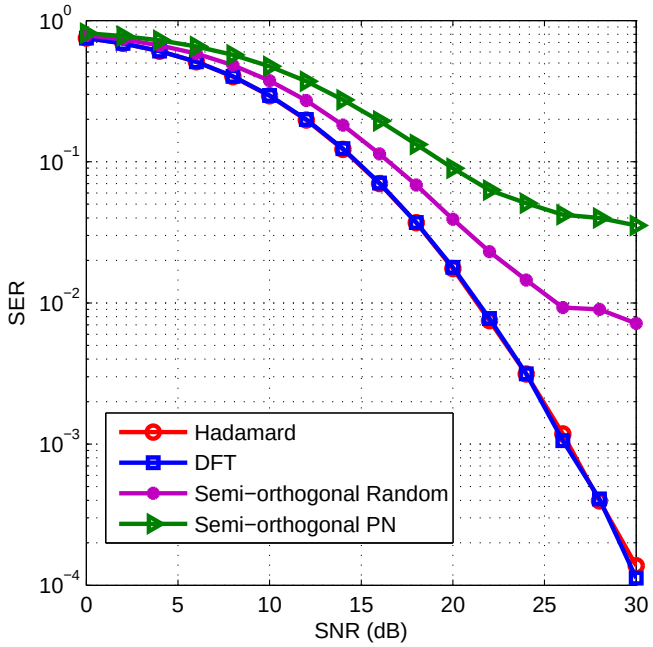

Figure 3.12: SER versus SNR performance of the proposed semi-blind receiver for four possible coding schemes.

ploits cooperative diversity. On the next result we provide another comparison of the receivers (except [2] and the ZF), but this time with the same configurations for each one, independently of spectral efficiency or transmission rate.

In Fig. 3.14 we set $K = 3$, $R = 3$, $P = 8$, $N = 16$ and $M = 4$ for all the receivers. As we can see from Figure 3.14, the proposed receiver showed better SER performance in comparison to the ones of [46] and [47]. Even with the same number of relays and spreading code length, the proposed receiver was able to surpass the other two in SER performance. This is due to the fact that the proposed receiver exploits transmission in different time slots and spreading at the relays, characteristics of the receivers of [46] and [47] respectively. Thus we can say the proposed receiver may act as junction of both [46] and [47].

Now, we compare the semi-blind receiver with the MMSE receiver [85]. The MMSE receiver works under complete knowledge of the matrix $\mathbf{A}$ and $\mathbf{H}$. Figure 3.15 presents the bit error rate (BER) performance for the proposed semi-blind and MMSE receivers. It is shown from Fig. 3.15 that the proposed receiver has performance equal to the one of the MMSE receiver. This means that the proposed receiver is able to obtain the same performance as if it had previous knowledge of the spatial signatures and channel matrices.

We show on the next figures the NMSE performance of the semi-blind receiver

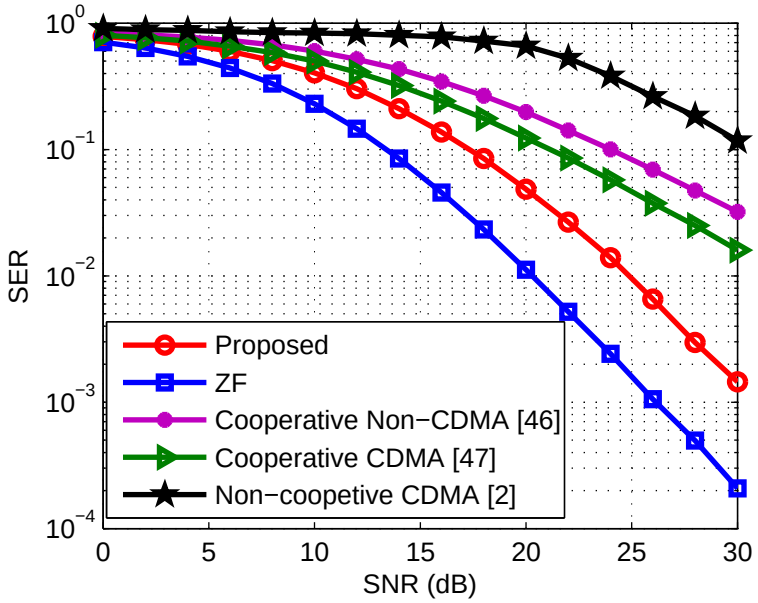

Figure 3.13: SER versus SNR performance for different receivers with the same spectral efficiency.

for the estimation of matrices $\mathbf{A}$ and $\mathbf{H}$. The NMSE of matrix $\mathbf{A}$ can be obtained by:

$$NMSE_{\mathbf{A}} = \frac{1}{M_C}\left(\frac{1}{\|\mathbf{A}_{(l)}\|_F^2}\left(\sum_{l=1}^{M_C}\|\mathbf{A}_{(l)} - \hat{\mathbf{A}_{(l)}}\|_F^2\right)\right), \tag{3.42}$$

where M_C is the number of Monte Carlo runs, $\mathbf{A}_{(l)}$ is the matrix $\mathbf{A}$ generated during the l-th Monte Carlo run and $\hat{\mathbf{A}_{(l)}}$ represent the estimation of $\mathbf{A}$ on the l-th Monte Carlo run. A similar expression was used to find the NMSE of the matrix $\mathbf{H}$. Figures 3.16 and 3.17 shows the NMSE performance versus SNR of the matrices $\mathbf{H}$ and $\mathbf{A}$ for a variation of the number of relays on the system. For this result, we set $K = 3$, $P = 8$, $M = 4$ and $N = 16$. As we can see from Figures 3.16 and 3.17, when we increase the number of relays the NMSE diminishes. The explanation for this behavior is the same as for Fig. 3.8, that is, when we increase the number of relays, we take advantage a higher degree of cooperative diversity.

In Figure 3.18, we have the NMSE of matrix $\mathbf{H}$ in function of the SNR for a variation in the number of users on the system. We set $K = 2$, $R = 2$, $P = 16$ and $N = 16$. It is possible to see that an increase on M from 2 to 8 decreases the NMSE. This happens because of the same motives as for Fig. 3.11. Increasing the number of users also increases the number of relays on the system. As the number of users is increased from 8 to 16, there is no change in the NMSE of

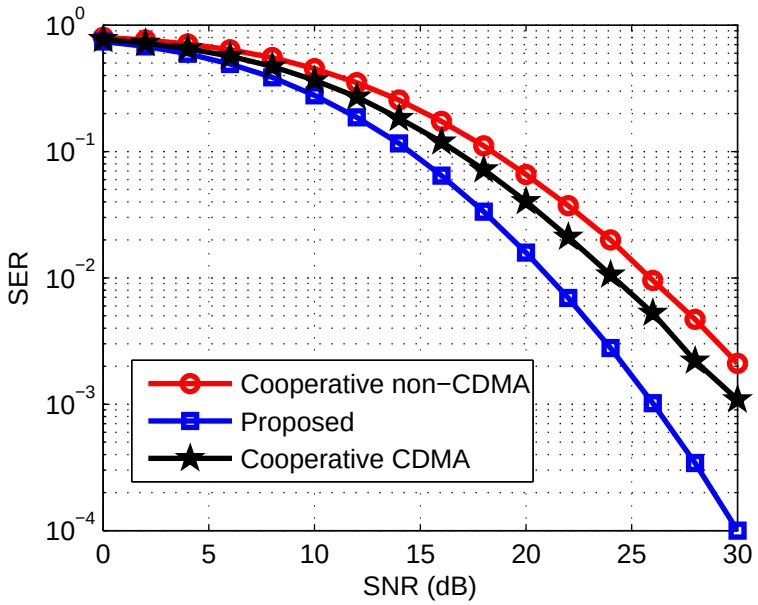

Figure 3.14: SER versus SNR performance for different receivers with similar configurations.

matrix $\mathbf{H}$, as multiuser interference at the relays is not considered. In Figure 3.19 we have the NMSE performance versus SNR of matrix $\mathbf{A}$ for a variation of the number of users M. For Fig. 3.19 we set $K = 2$, $R = 2$, $P = 8$ and $N = 16$. It is observed from Figure 3.19 that there is almost no change on the NMSE for a different number of users. As we increase M, we have more data to estimate, however, with the behavior of the proposed semi-blind receiver on Fig. 3.11, we can see that increasing the number of users do not interfere neither on the SER nor on the NMSE of $\mathbf{A}$, as said earlier, multiuser interference at the relays is not considered.

Fig. 3.20 shows the NMSE of the matrix $\mathbf{A}$ for a variation of K. The configuration for this result is $R = 2$, $P = 8$, $M = 4$ and $N = 16$. By increasing the number of receive antennas at the base station we also increase the number of spatial signatures that we have to estimate, thus, the proposed semi-blind receiver provides little better NMSEs for small values of K.

Figures 3.21 and 3.22 shows the NMSE of matrices $\mathbf{A}$ and $\mathbf{H}$ for a variation of N. We can see from Fig 3.21 that an increase on N decreases the NMSE of matrix $\mathbf{A}$. It means that an increase on the data block length does not interfere negatively on the spatial signatures estimation. This happens because larger datablocks allows better estimations of the spatial signatures. Figure 3.22 shows that an increase on the data block length provides almost no change on the NMSE

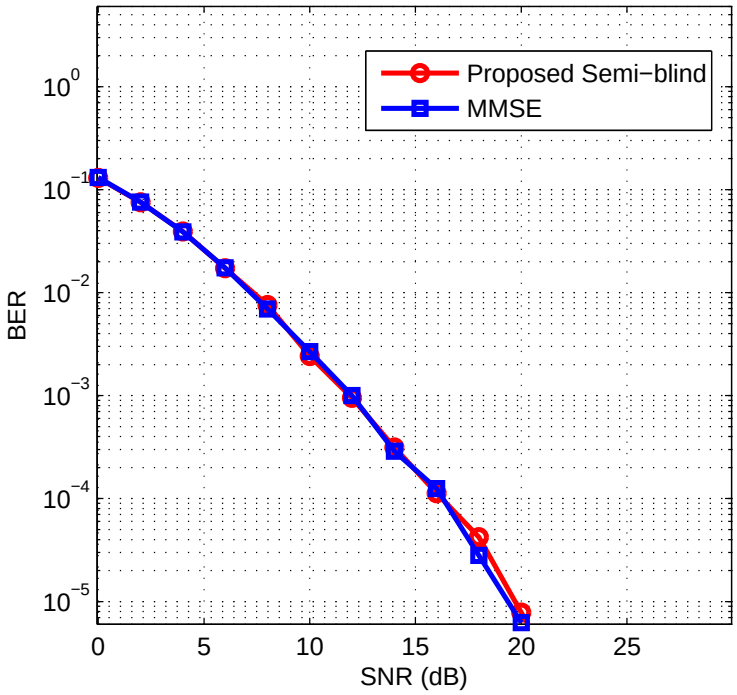

Figure 3.15: BER versus SNR performance for the proposed semi-blind receiver and the MMSE receiver.

of matrix $\mathbf{H}$. By augmenting the data block length N, the NMSE of matrix $\mathbf{H}$ does not increase, thus, the proposed receiver is able to estimate the channel gains of all users independently of the number of symbols sent.

The next results shows the number of iterations for convergence of the ALS algorithm versus the SNR of the proposed semi-blind receiver for computational complexity evaluation purposes. In Fig. 3.23 we have the number of iterations for convergence of the ALS algorithms of the proposed semi-blind receiver in function of the SNR. We compare the Algorithms 1 and 2 (presented on Section 3.4). The configuration that was set for this result is $K = 2$, $R = 2$, $P = 8$, $M = 4$, $N = 16$. We can see from Figure 3.23 that Algorithm 2 takes many more iterations to converge in comparison to Algorithm 1. The explanation for this result is simple: more data to estimate means more iterations for the receiver to run. The simple knowledge of the spreading codes matrix increases the convergence by many iterations.

Figure 3.24 shows the number of iterations for convergence of Algorithm 1 versus the SNR for a variation on the datablock length N. For Figure 3.24 we set $K = 2$, $R = 3$, $M = 8$, and $P = 8$. By increasing N, we increase the data block

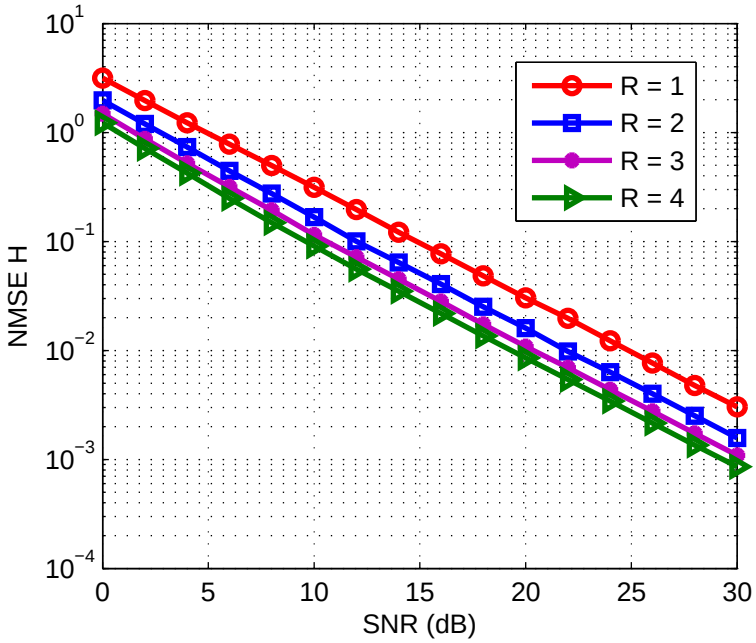

Figure 3.16: NMSE of matrix **H** versus SNR performance for a different number of relays.

length, thus, the quantity of data symbols to be estimated. We explain the result of Figure 3.24 as we explained the result of Figure 3.23: more data to estimate means more iterations for convergence.

Fig. 3.25 shows the number of iterations for convergence of Algorithm 1 of the proposed semi-blind receiver and the receiver algorithm of [2] (non-cooperative CDMA). For Figure 3.25, we set $K = 2$, $R = 3$, $P = 8$, $M = 4$ and $N = 16$. The result presented in Figure 3.25 shows us that the proposed receiver algorithm converges in fewer iterations than the receiver algorithm of [2]. The algorithm used on [2] is based on a trilinear PARAFAC decomposition while the proposed algorithm is based on a quadrilinear PARAFAC decomposition. The addition of one dimension (cooperative dimension) to the quadrilinear decomposition implies in more data to be estimated during the iterations. Even so, the proposed receiver algorithm is able to estimate more data with fewer iterations, due to the higher number of received signals.

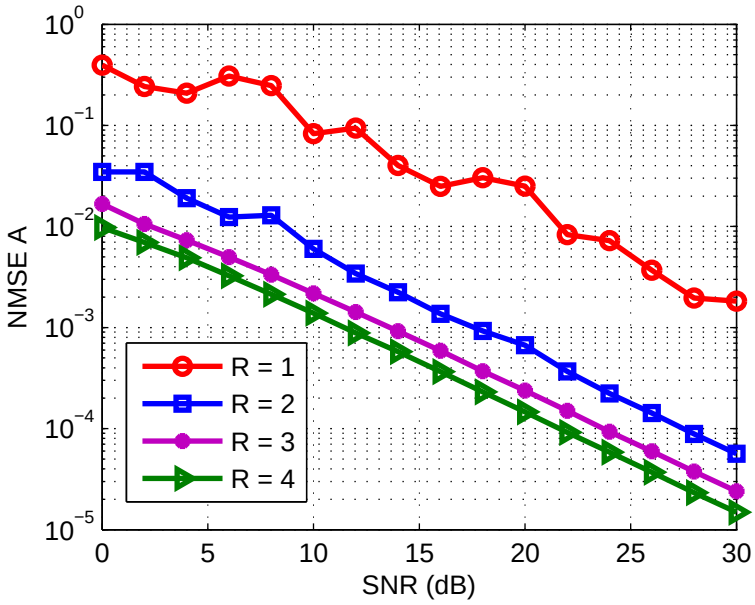

Figure 3.17: NMSE of matrix **A** versus SNR performance for a different number of relays.

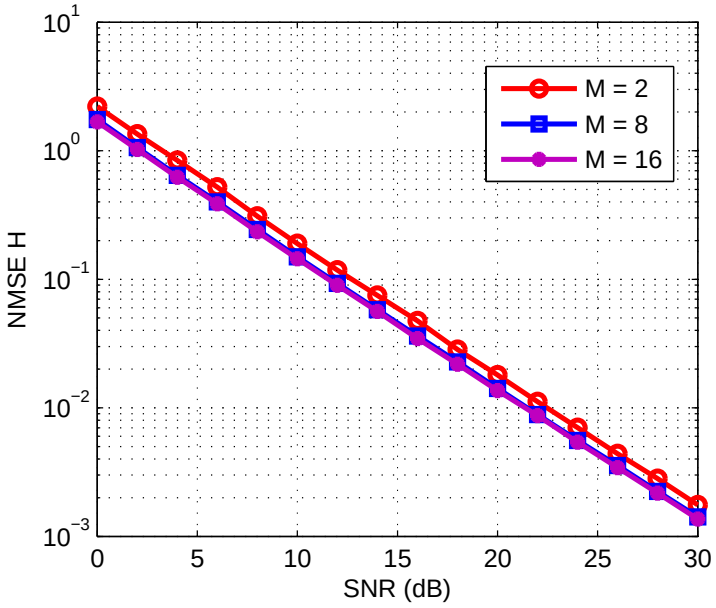

Figure 3.18: NMSE of matrix **H** versus SNR performance for a different number of users.

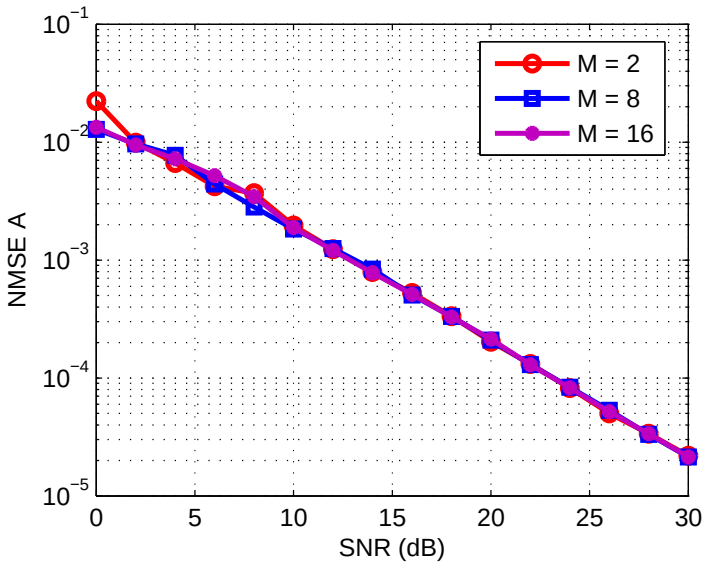

Figure 3.19: NMSE of matrix $\mathbf{A}$ versus SNR performance for a different number of users.

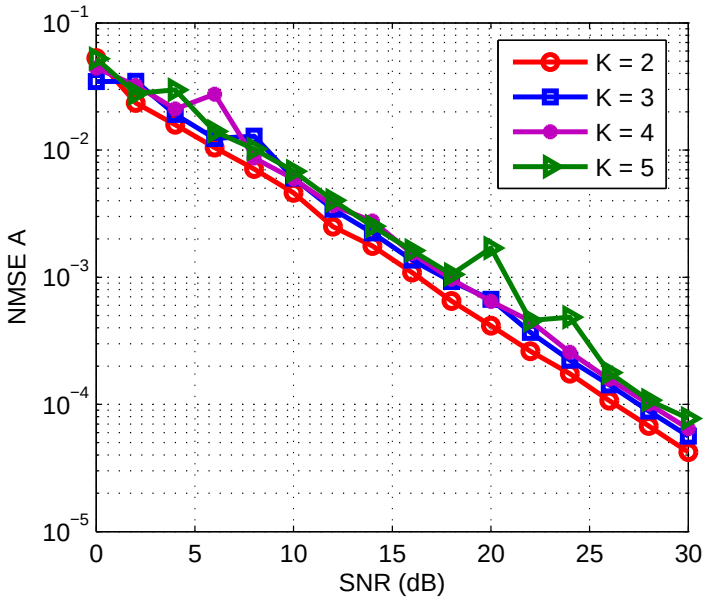

Figure 3.20: NMSE of matrix $\mathbf{A}$ versus SNR performance for a different number of receive antennas.

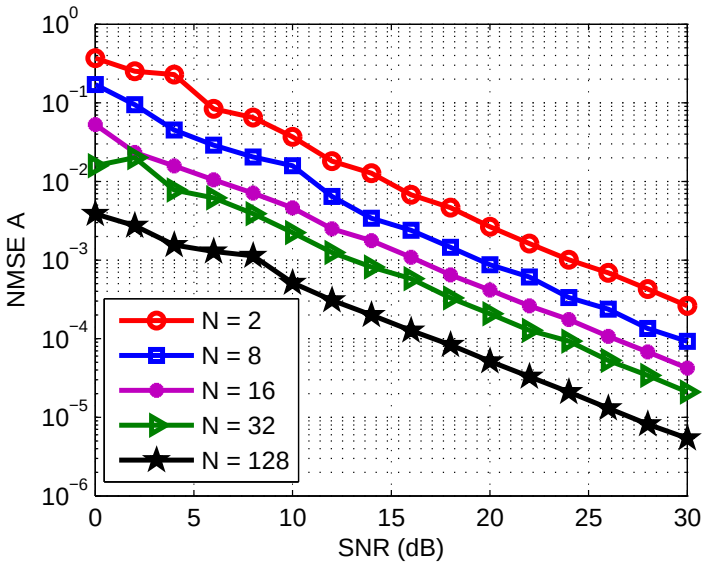

Figure 3.21: NMSE of matrix **A** versus SNR performance for a variation of N (data block length).

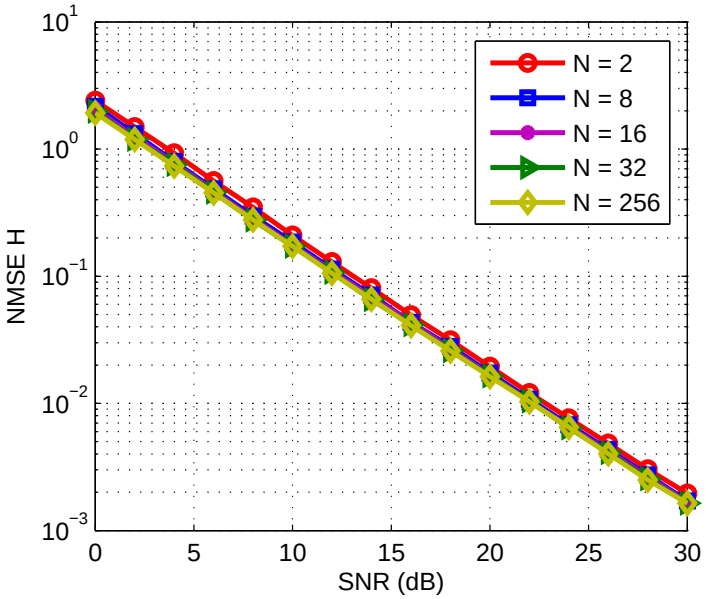

Figure 3.22: NMSE of matrix **H** versus SNR performance for a variation of N (data block length).

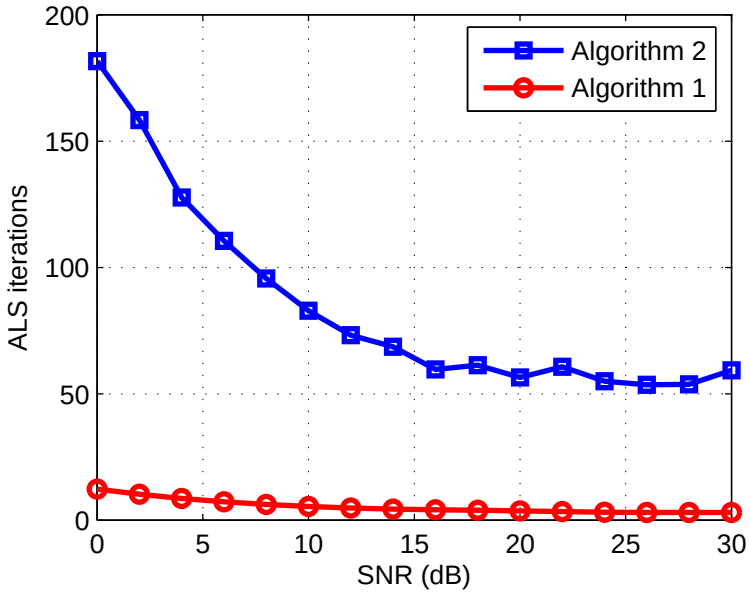

Figure 3.23: Number of ALS iterations versus SNR for the proposed semi-blind receiver algorithms.

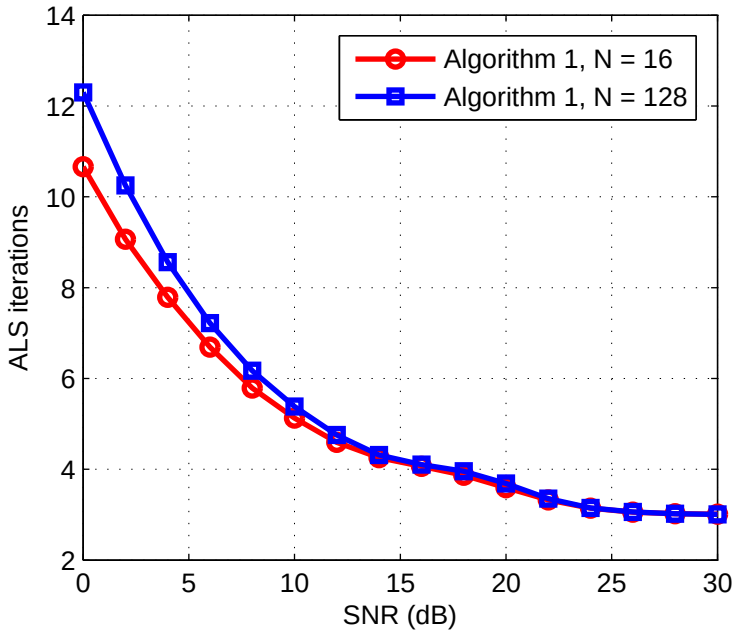

Figure 3.24: Number of ALS iterations versus SNR for Algorithm 1 with N varying.

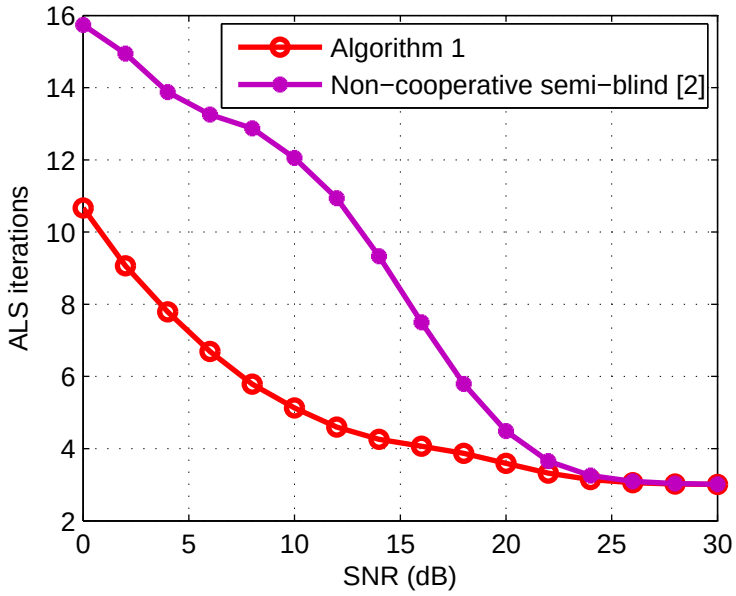

Figure 3.25: Number of ALS iterations versus SNR for the proposed semi-blind receiver and the semi-blind receiver of [2].

Chapter 4

Multiuser Detection for Wireless Cooperative Uplink with Multiuser Interference at the Relays

In this chapter, we present the second system model of this dissertation as well as a receiver for this communication system. The model is similar to the one presented on the previous chapter: a cooperative DS-CDMA uplink with M users transmitting to a base station with the help of AF relay-aided links. The base station employs an array of antennas and direct-sequence spreading is used at the relays. On this scenario, a trilinear PARAFAC decomposition is proposed to represent the received signal. The difference between the system model of Chapter 3 and the one we present here is that multiuser interference is considered at the relays, thus a more realistic scenario. The receiver will estimate the parameters in two phases: a supervised phase with a training sequence sent by all users for the estimation of channel gains and spatial signatures, then a non-supervised second phase where the users symbols are then estimated. First, we describe the system model itself, then we describe the tensorial decomposition adopted, its uniqueness conditions and properties. Next, we show the proposed receiver algorithm for this case and for last, the simulation results are shown and discussed.

4.1 System Model

On the system model considered in this chapter, we also adopt the fact that each user communicates with its R associated relays and that each relay forwards

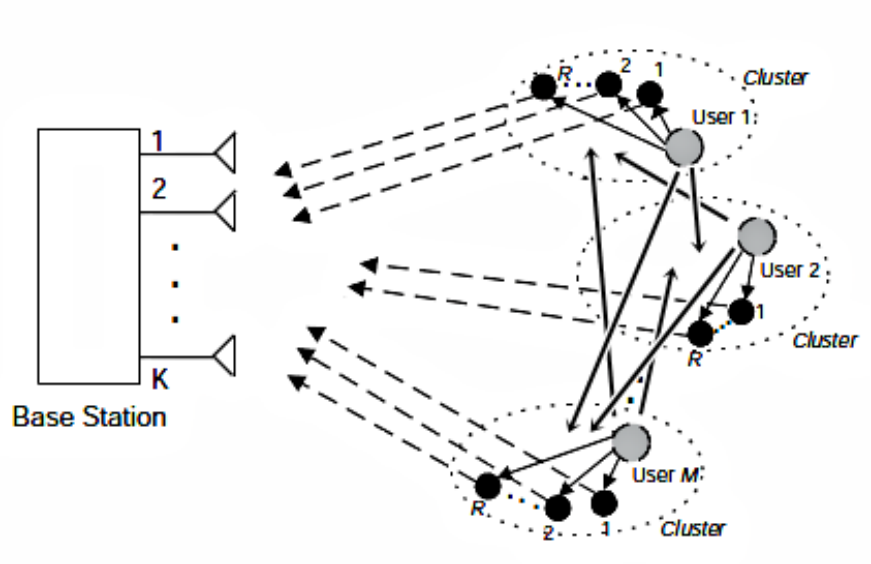

Figure 4.1: Cooperative uplink with M users and multiuser interference at the relays.

the signal using a different time-slot, but now, the signal sent by a user to its associated cluster of relays will act as interference to the relays of other users on the system (as Fig. 4.1 shows), being a more realistic scenario than the previous one. This means that we no longer make the assumption that the signal received at a relay located within the cluster of a user contains no significant interference from the other users. The R relays of a given user will use direct-sequence spreading on the user signal with a spreading code of length P, where the same code is used by all relays of a given user. It is worth mentioning that, as well as in Chapter 3, the system model presented in also holds when the DS-CDMA spread carried out by the relays is replaced by a DKRST coding, with P being the number of transmission blocks of the coding. Then, the signal received by the r-th relay of the m-th user is given by:

$$u_{r,m,n}^{(SR)} = \sum_{f=1}^{M} h_{r,m,f}^{(SR)} s_{n,f} + v_{r,m,n}^{(SR)}, \tag{4.1}$$

where $h_{r,m,f}^{(SR)}$ is the channel coefficient between the f-th user and the r-th relay of the m-th user. Thus, the signal of the m-th user will be added with the signals of the other users on the system, leading to a more realistic and challenging scenario. Note that in (3.1) there is no summation in the variable f, contrarily to 4.1. For the RD link, the signal received at the k-th antenna of the base station, trough the r-th time slot, on the n-th symbol period and p-th chip of

the spreading code is given by:

$$x_{k,r,n,p}^{(RD)} = \sum_{m=1}^{M} h_{k,r,m}^{(RD)} g_{r,m} c_{p,m} u_{r,m,n}^{(SR)} + v_{k,r,n,p}^{(RD)}, \tag{4.2}$$

which, by substituting (4.1) into (4.2), gives us:

$$x_{k,r,n,p}^{(RD)} = \sum_{m=1}^{M} h_{k,r,m}^{(RD)} g_{r,m} c_{p,m} \left(\sum_{f=1}^{M} h_{r,m,f}^{(SR)} s_{n,f} + v_{r,m,n}^{(SR)} \right) + v_{k,r,n,p}^{(RD)}. \tag{4.3}$$

Reorganizing (4.3), we get:

$$x_{k,r,n,p}^{(RD)} = \sum_{m=1}^{M} \sum_{f=1}^{M} h_{k,r,m}^{(RD)} g_{r,m} c_{p,m} h_{r,m,f}^{(SR)} s_{n,f} + v_{k,r,n,p}^{(SRD)}. \tag{4.4}$$

The same assumptions made about the propagation scenario on Chapter 3 will be considered on this system model, hence, from (3.6) we have:

$$x_{k,r,n,p}^{(RD)} = \sum_{m=1}^{M} \sum_{f=1}^{M} a_k(\theta_m) \gamma_{r,m}^{(RD)} g_{r,m} c_{p,m} h_{r,m,f}^{(SR)} s_{n,f} + v_{k,r,n,p}^{(SRD)}, \tag{4.5}$$

where $v_{k,r,n,p}^{(SRD)}$ is given by (3.8). The total transmission rate of the system is $M/(R{+}1)$.

4.2 Proposed Tensor Model

In this section, we represent the received signal presented in (4.5) as trilinear PARAFAC decomposition. To simplify presentation, we are going to omit the AWGN terms and assume that the channels are constant for N symbol periods. So let $\mathcal{Y}$ be a M-component, quadrilinear model, so that $\mathcal{Y} \in \mathbb{C}^{K \times R \times N \times P}$ is a 4-th order tensor collecting the baseband RD data signals at the base station:

$$[\mathcal{Y}]_{k,r,n,p} = x_{k,r,n,p}^{(RD)} \tag{4.6}$$

A typical element of $\mathcal{Y}$, denoted by $y_{k,r,n,p} = [\mathcal{Y}_{k,r,n,p}]$ is given by:

$$y_{k,r,n,p} = \sum_{m=1}^{M} \sum_{f=1}^{M} a_k(\theta_m) h_{r,m}^{(RD)} c_{p,m} h_{r,m,f}^{(SR)} s_{n,f} \tag{4.7}$$

for k = 1,...,K, r = 1,...,R, n = 1,...,N, p = 1,...,P, where the relay-destination channel coefficient $h_{r,m}^{(RD)}$ is defined as :

$$h_{r,m}^{(RD)} = \gamma_{r,m}^{(RD)} g_{r,m}. \tag{4.8}$$

Now, let us define a global channel coefficient, denoted by $h_{r,m,f}^{G}$, accounting for the channel coefficients of both SR and RD links, defined as follows:

$$h_{r,m,f}^{G} = h_{r,m,f}^{(SR)} h_{r,m}^{(RD)}, \tag{4.9}$$

then, (4.7) turns out to:

$$y_{k,r,n,p} = \sum_{m=1}^{M} \sum_{f=1}^{M} a_k(\theta_m) h_{r,m,f}^{G} c_{p,m} s_{n,f}. \tag{4.10}$$

To generate a trilinear model from a quadrilinear model, we have to join two dimensions into one, in order to obtain 3 dimensions. Thus, we merge indices r and n into one index, l, where $l = (n\text{-}1)R + r$ and l = 1,...,L, with $L = NR$. To accomplish that, we define a third order tensor $\mathcal{Z} \in \mathbb{C}^{R \times M \times N}$ given by:

$$\mathcal{Z} = \mathcal{H}^{G} \times_3 \mathbf{S}, \tag{4.11}$$

where $\mathcal{H}^{G} \in \mathbb{C}^{R \times M \times F}$ is a third order tensor with $[\mathcal{H}^{G}]_{r,m,f} = h_{r,m,f}^{G}$, $\mathbf{S} \in \mathbb{C}^{N \times M}$ is the users symbols matrix and "$\times_3$" is the mode-3 product. $\mathcal{Z}$ follows a Tucker-1 model [1]. The tensor $\mathcal{Z}$ can also be expressed as follows:

$$z_{r,m,n} = \sum_{f=1}^{M} h_{r,m,f}^{G} s_{n,f}, \tag{4.12}$$

where $[\mathcal{Z}]_{r,m,n} = z_{r,m,n}$. Two of the unfoldings of $\mathcal{Z}$, $\mathbf{Z}_1 \in \mathbb{C}^{NR \times M}$ and $\mathbf{Z}_2 \in \mathbb{C}^{RM \times N}$, are obtained as follows:

$$\mathbf{Z}_1 = (\mathbf{S} \otimes \mathbf{I}_R)\mathbf{H}_1^{G}, \tag{4.13}$$

$$\mathbf{Z}_2 = \mathbf{H}_2^{G}\mathbf{S}^{T}, \tag{4.14}$$

where $\mathbf{I}_R \in \mathbb{C}^{R \times R}$ is the identity matrix, "$\otimes$" denotes the kronecker product and $\mathbf{H}_1^{G} \in \mathbb{C}^{MR \times M}$ and $\mathbf{H}_2^{G} \in \mathbb{C}^{RM \times M}$ are matrix unfoldings of $\mathcal{H}^{G}$. Then, let $\mathcal{X}$ be a M-component trilinear model, so that $\mathcal{X} \in \mathbb{C}^{K \times P \times L}$ is a third order tensor collecting the baseband RD signals at the base station, with $[\mathcal{X}]_{k,p,l} = y_{k,r,n,p}$,

where $l = (n-1)R + r$. By using $\mathbf{Z}_1$ as a factor matrix of (4.7), we get the trilinear PARAFAC model of $\mathcal{X}$ (with $x_{k,p,l} = [\mathcal{X}]_{k,p,l}$):

$$x_{k,p,l} = \sum_{m=1}^{M} a_k(\theta_m) c_{p,m} z_{1l,m}, \tag{4.15}$$

where $z_{1l,m}$ denotes the elements of matrix $\mathbf{Z}_1$. (4.15) can be represented with a matricial notation, as follows:

$$\mathcal{X} = \sum_{m=1}^{M} \mathbf{A}_{.,m} \circ \mathbf{C}_{.,m} \circ \mathbf{Z}_{1.,m}, \tag{4.16}$$

where $\mathbf{A}$, $\mathbf{C}$ and $\mathbf{Z}_1$ are the factor matrices of the decomposition, and, similarly to the previous system model presented in Chapter 3, this trilinear PARAFAC decomposition is irreducible in the sense that $x_{k,p,l}$ cannot be represented using less than M components, such that the 3-way array with typical element $x_{k,p,l}$ has rank M). We may also note that we reduced the model of (4.10), which is a four order tensor, to a third order tensor in (4.15) that follows a PARAFAC decomposition with the factor matrix $\mathbf{Z}_1$ given by (4.13).

4.2.1 Tensor unfoldings

The tensor $\mathcal{X}$ unfoldings that we will use are obtained as follows:

$$\mathbf{X}_1 = (\mathbf{A} \diamond \mathbf{C})\mathbf{Z}_1^T, \tag{4.17}$$

$$\mathbf{X}_2 = (\mathbf{Z}_1 \diamond \mathbf{A})\mathbf{C}^T, \tag{4.18}$$

$$\mathbf{X}_3 = (\mathbf{C} \diamond \mathbf{Z}_1)\mathbf{A}^T, \tag{4.19}$$

with $\mathbf{X}_1 \in \mathbb{C}^{KP \times L}$, $\mathbf{X}_2 \in \mathbb{C}^{LK \times P}$ and $\mathbf{X}_3 \in \mathbb{C}^{PL \times K}$. By moving from a quadrilinear model to a trilinear model we reduced the number of factor matrices and tensor unfoldings by one.

4.2.2 Uniqueness Properties

For this case, the trilinear PARAFAC decomposition has uniqueness granted if the condition below is satisfied:

$$k_{\mathbf{A}} + k_{\mathbf{C}} + k_{\mathbf{Z1}} \geq 2M + 2, \tag{4.20}$$

where $k_{\mathbf{Z1}}$ is the Kruskal rank of matrix $\mathbf{Z}_1$. Again, if condition (4.20) is satisfied, the factor matrices $\mathbf{A}$, $\mathbf{C}$, and $\mathbf{Z}_1$ are essentially unique, meaning these matrices can be determined up to column scaling and permutation. Thus, any other set of matrices ($\mathbf{A}^{'}$, $\mathbf{C}^{'}$ and $\mathbf{Z}_1^{'}$) that satisfies (4.16) is related to the original matrix set ($\mathbf{A}$, $\mathbf{C}$ and $\mathbf{Z}_1$) by $\mathbf{A}^{'} = \mathbf{A}\Pi\Delta_{\mathbf{A}}$, $\mathbf{C}^{'} = \mathbf{C}\Pi\Delta_{\mathbf{C}}$ and $\mathbf{Z}_1^{'} = \mathbf{Z}_1\Pi\Delta_{\mathbf{Z1}}$, where $\Delta_{\mathbf{A}}\Delta_{\mathbf{C}}\Delta_{\mathbf{Z1}} = \mathbf{I}_M$. If we assume that $\mathbf{A}$, $\mathbf{C}$ and $\mathbf{Z}_1$ are all full k-rank, we have:

$$min(K, M) + min(P, M) + min(L, M) \geq 2M + 2. \tag{4.21}$$

The matrix $\mathbf{A}$ is full k-rank because we are modeling it as a Vandermonde matrix with distinct generators because the different users signals arrives at the base station array with different angles of arrival. Matrix $\mathbf{C}$ can be full k-rank if a certain length of spreading codes are used. For $\mathbf{Z}_1$ to be full k-rank, a certain data block length and a continuous distribution for the channels coefficients is necessary. With the assumptions made above, we can determine some parameters of the adopted system, as the number of users the proposed receiver can handle and the minimum acceptable parameters that match a predefined target. So, we are interested in exploiting the uniqueness of condition (4.21). Based on this, we have:

- If $K \geq M$ and $P \geq M$ then min(L,M) ≥ 2. It means that $RN \geq 2$, which could give us, for example, $R = 1$ and $N = 2$, thus a short block length and a single relay simultaneously would be sufficient to handle M users.

- If $L \geq M$, then we go back to the other cases presented in Chapter 3 where K or $P \leq M$, thus showing similarities between the uniqueness conditions of the two proposed system models.

For instance, if we have $M = 8$ users, $K \leq M$, $P \leq M$ and $L \leq M$, then condition (4.21) turns into:

$$K + P + RN \geq 18. \tag{4.22}$$

Condition (4.22) shows us system requirements for choosing the parameters to handle 8 users. The number of antennas at the base station, number of relays, spreading code length and data block length will have to match condition (4.22) in order to guarantee uniqueness. With condition (4.22) we can design the system according to availability (number of antennas, relays and etc).

4.3 Receiver Algorithm

In this section we present the proposed receiver for the system model of Section 4.1. The receiver estimates the parameters of the system in two phases. The first phase is a supervised stage where a short non-orthogonal training sequence is transmitted from all users to help the receiver estimate the channel information. On the second phase, the users' data symbols are transmitted (non-supervised stage), then the receiver is able to estimate the symbols using the channel gains obtained during the first phase. It is assumed previous knowledge of the spreading codes matrix $\mathbf{C}$. During the supervised stage (first phase) we do not use the $\mathbf{Z}_1$ defined in (4.13), instead, it is used $\mathbf{Z}_{1t}$, which is obtained by:

$$\mathbf{Z}_{1t} = (\mathbf{S}_t \otimes \mathbf{I}_R)\mathbf{H}_1^G, \tag{4.23}$$

where the matrix $\mathbf{S}_t \in \mathbb{C}^{W \times M}$ is composed of training sequences, known at the receiver. The dimension W (with $w = 1,...,W$) of matrix $\mathbf{S}_t$ is usually smaller than dimension N of matrix $\mathbf{S}$, and it represents the number of pilot symbols per data stream. Thus, during the supervised stage we have $\mathbf{Z}_{1t} \in \mathbb{C}^{WR \times M}$. With $\mathbf{Z}_{1t}$, the tensor unfoldings are generated, as follows:

$$\mathbf{X}_{1t} = (\mathbf{A} \diamond \mathbf{C})\mathbf{Z}_{1t}^T, \tag{4.24}$$

where $\mathbf{X}_{1t} \in \mathbb{C}^{KP \times L}$ and

$$\mathbf{X}_{3t} = (\mathbf{C} \diamond \mathbf{Z}_{1t})\mathbf{A}^T. \tag{4.25}$$

where $\mathbf{X}_{3t} \in \mathbb{C}^{PL \times K}$. During the first phase, the ALS algorithm is used and the factor matrices $\mathbf{A}$ and $\mathbf{Z}_{1t}$ will be estimated, as follows:

$$\hat{\mathbf{A}} = [\tilde{\mathbf{X}}_{3t}(\mathbf{C} \diamond \hat{\mathbf{Z}_{1t}})^{\dagger}]^T, \tag{4.26}$$

where $\hat{\mathbf{Z}_{1t}}$ is the Least Squares update previously obtained for $\mathbf{Z}_{1t}$ and the matrix $\tilde{\mathbf{X}}_{3t}$ is the noisy version of $\mathbf{X}_{3t}$. The estimation of $\mathbf{Z}_{1t}$ is given by:

$$\hat{\mathbf{Z}_{1t}} = [\tilde{\mathbf{X}}_{1t}(\hat{\mathbf{A}} \diamond \mathbf{C})^{\dagger}]^{T}, \tag{4.27}$$

with $\hat{\mathbf{A}}$ being the Least Squares update obtained for $\mathbf{A}$ and $\tilde{\mathbf{X}}_{1t}$ being the noisy version of $\mathbf{X}_{1t}$. Algorithm 3 depicts the two phases of estimation of the proposed semi-blind receiver for the adopted system model. The ALS is used in steps 1-5 of Algorithm 3 (during the first phase).

Algorithm 3 Proposed Receiver - Two Phase Estimation

First Phase (Supervised Stage)
1)*Initialization* : *Set* $i = 0$; *Initialize* $\hat{\mathbf{A}}_{(i=0)}$;
2)$i = i + 1$;
3)*Using* $\tilde{\mathbf{X}}_{1t}$, *find a LS estimate of* $\mathbf{Z}_{1t} : \hat{\mathbf{Z}_{1t(i)}}^{T} = (\hat{\mathbf{A}}_{(i-1)} \diamond \mathbf{C})^{\dagger}\tilde{\mathbf{X}}_{1t}$;
4)*Using* $\tilde{\mathbf{X}}_{3t}$, *find a LS estimate of* $\mathbf{A} : \hat{\mathbf{A}}_{(i)}^{T} = (\hat{\mathbf{Z}_{1t(i)}} \diamond \mathbf{C})^{\dagger}\tilde{\mathbf{X}}_{3t}$;
5)*Repeat steps* $3-5$ *until convergence*;
6)*Reorganize* $\hat{\mathbf{Z}_{1t}}$ *into* $\hat{\mathbf{Z}_{2t}}$;
7)*From* $\hat{\mathbf{Z}_{2t}}$, *estimate* $\mathbf{H}_2^G : \hat{\mathbf{H}_2^G} = \hat{\mathbf{Z}_{2t}}(\mathbf{S}_t^T)^{\dagger}$;
Second Phase (End of Supervised Stage)
8)*Using* $\tilde{\mathbf{X}}_1$, *find a estimate of* $\mathbf{Z}_1 : \hat{\mathbf{Z}_1}^{T} = (\hat{\mathbf{A}_{(i)}} \diamond \mathbf{C})^{\dagger}\tilde{\mathbf{X}}_1$;
9)*Reorganize* $\hat{\mathbf{Z}}_1$ *into* $\hat{\mathbf{Z}}_2$;
10)*From* $\hat{\mathbf{Z}}_2$, *estimate* $\mathbf{S} : \hat{\mathbf{S}} = ((\hat{\mathbf{H}_2^G})^{\dagger}\hat{\mathbf{Z}}_2)^{T}$;

The measured error at the end of the i-th iteration is given by:

$$e(i) = \frac{\|\tilde{\mathbf{X}}_1 - (\hat{\mathbf{A}}_{(i)} \diamond \mathbf{C})\hat{\mathbf{W}}_{(i)}^{T}\|_F^2}{\|\tilde{\mathbf{X}}_1\|_F^2}. \tag{4.28}$$

The criteria to stop the ALS is when $|e(i) - e(i-1)| < 10^{-6}$. After estimating matrices $\mathbf{A}$ and $\mathbf{Z}_{1t}$, we remove the scaling ambiguity of matrix $\hat{\mathbf{A}}$ by assuming that the first row of $\mathbf{A}$ is known. To remove the scaling ambiguity of matrix $\hat{\mathbf{Z}}_{1t}$ we use the following identity: $\Delta_{\mathbf{A}}\Delta_{\mathbf{Z1t}} = \mathbf{I}_M$, where $\Delta_{\mathbf{Z1t}}$ is the scaling matrix of $\mathbf{Z}_{1t}$. As we know $\Delta_{\mathbf{A}}$, it is easy to find $\Delta_{\mathbf{Z1t}}$. We can then estimate the global channel tensor $\mathcal{H}^G$. To do so, we must reorganize $\hat{\mathbf{Z}}_{1t}$ into $\hat{\mathbf{Z}}_{2t}$ (the estimated version of $\mathbf{Z}_2$ during the supervised stage) by folding $\hat{\mathbf{Z}}_{1t}$ into $\hat{\mathcal{Z}}_t$ (the estimated version of $\mathcal{Z}$ during the supervised stage) then unfold $\hat{\mathcal{Z}}_t$ into $\hat{\mathbf{Z}}_{2t}$. This is done by reorganizing the elements of $\hat{\mathbf{Z}}_{1t}$ as follows:

$$[\hat{\mathcal{Z}}_t]_{r,m,w} = [\hat{\mathbf{Z}}_{1t}]_{(w-1)R+r,m}, \tag{4.29}$$

and

$$[\hat{\mathbf{Z}}_{2t}]_{(r-1)M+m,w} = [\hat{\mathcal{Z}}_t]_{r,m,w}. \tag{4.30}$$

Hence, $\hat{\mathbf{H}}_2^G$ (the estimation of $\mathbf{H}_2^G$) is obtained as follows:

$$\hat{\mathbf{H}}_2^G = \hat{\mathbf{Z}}_2(\mathbf{S}_p^T)^\dagger. \tag{4.31}$$

Now we can just rearrange $\hat{\mathbf{H}}_2^G$ to get $\hat{\mathcal{H}}^G$, the estimation of $\mathcal{H}^G$, as follows:

$$[\hat{\mathcal{H}}^G]_{r,m,f} = [\hat{\mathbf{H}}_2^G]_{(r-1)M+m,f}, \tag{4.32}$$

With $\hat{\mathbf{H}}_2^G$ obtained, the supervised stage is over and the second phase starts. During the second phase, the estimation of $\mathbf{Z}_1$ is done as follows:

$$\hat{\mathbf{Z}}_1 = [\tilde{\mathbf{X}}_1(\hat{\mathbf{A}} \diamond \mathbf{C})^\dagger]^T, \tag{4.33}$$

where the matrix $\tilde{\mathbf{X}}_1$ is the noisy version of $\mathbf{X}_1$ and $\hat{\mathbf{A}}$ is the estimation of $\mathbf{A}$ obtained during the first phase of the algorithm. After obtaining $\hat{\mathbf{Z}}_1$, we simply reorganize it into $\hat{\mathcal{Z}}$ (the estimated version of $\mathcal{Z}$) then we unfold $\hat{\mathcal{Z}}$ into $\hat{\mathbf{Z}}_2$, as follows:

$$[\hat{\mathcal{Z}}]_{r,m,n} = [\hat{\mathbf{Z}}_1]_{(n-1)R+r,m}, \tag{4.34}$$

$$[\hat{\mathbf{Z}}_2]_{(r-1)M+m,n} = [\hat{\mathcal{Z}}]_{r,m,n}. \tag{4.35}$$

Then we can estimate $\mathbf{S}$ using the channel coefficients estimated during the supervised stage. The estimation of $\hat{\mathbf{S}}$ is obtained by:

$$\hat{\mathbf{S}} = ((\hat{\mathbf{H}}_2^G)^\dagger \hat{\mathbf{Z}}_2)^T. \tag{4.36}$$

Assuming no knowledge of the spreading codes will add another step to the ALS estimation of Algorithm 3. After the estimations, scaling ambiguity of matrix $\mathbf{C}$ can be removed the same way as in Chapter 3.

4.4 Simulation Results

In this section we present the computer simulations results for performance evaluation purposes for the system model adopted in this chapter. We are considering the following assumptions: the wireless links have frequency-flat Rayleigh

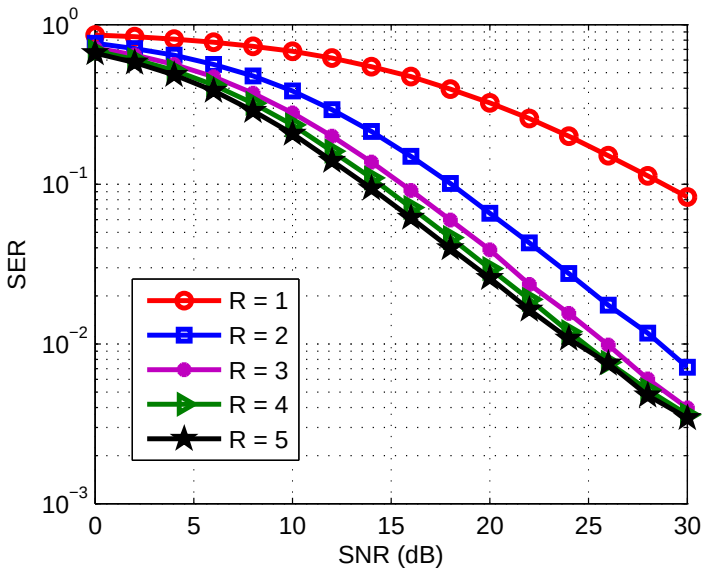

Figure 4.2: SER versus SNR performance of the proposed receiver for a different number of relays on the system with multiuser interference considered at the relays.

fading with path loss exponent equal to 3, the base station antenna array is composed by K antennas, 16-QAM modulation is used and Hadamard orthogonal codes are considered for spreading sequences. The signals transmitted by the relays of a given user arrive at the destination with the same angle of arrival and the angle spread is zero. Also, the number of multipaths $L_{r,m}^{(RD)}$ was considered 30. The symbol error rate (SER), bit error rate (BER) and channel's normalized mean square error (NMSE) curves are shown in function of the signal-to-noise ratio (SNR) of the RD link. The mean results were obtained by 10000 independent Monte Carlo samples with each run corresponding to a different realization of channel's gains, spatial signatures, modulation symbols and noise. The AF gain used at simulations is given by (3.40).

Figure 4.2 shows the SER performance versus SNR for the proposed receiver of this chapter with $P = 8$ chips, a datablock of $N = 16$ symbols, $K = 3$ receive antennas, a training sequence of length $W = 4$ and $M = 4$ users, for various values of R (number of relays on the cluster). From Fig. 4.2 we can observe a better SER performance when we increase the number of relays on the system from 1 to 3. This happens because when the number of relays is augmented, the model turns to a more cooperative scenario, exploiting cooperative diversity and resulting in better link quality. When we increase the relay count from 3 to 5, there is a small change on the SER. This is due to the fact that increasing the

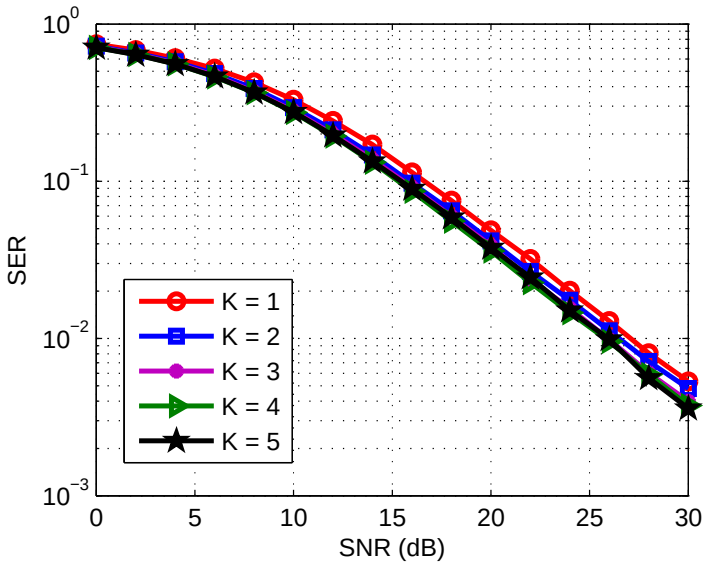

Figure 4.3: SER versus SNR performance of the proposed receiver for different values of K (number of receive antennas) with multiuser interference considered at the relays.

number of relays also increase multiuser interference, since a user's relays also receive the signals from the other users. Comparing Fig 4.2 with Fig. 3.8 we can see an increase on the overall SER in Fig. 4.2. This increase in the error rate results from the fact that multiuser interference is now considered at the relays.

In Fig. 4.3, we assume a datablock of $N = 16$ symbols, $M = 4$ users, $P = 8$ chips, a training sequence of length $W = 4$ and $R = 3$ relays. This figure shows the performance of the SER of the proposed receiver of this chapter for different values of K (number of receive antennas). From this figure, it can be viewed that the SER performance has a small improvement when the number of antennas at the base station is increased. Comparing Figure 4.3 with Figure 3.7 we can also see an increase on the overall SER in Figure 4.3. The explanation for this is the same as for the comparison of Fig 4.2 and Fig 3.8, that is, the multiuser interference at the relays decreases the system performance.

For Figure 4.4, we have the SER performance of the proposed receiver for different values of M (users on the system), where we consider $P = 8$, $K = 3$, $R = 3$, $W = 8$ and $N = 16$. From Fig. 4.4, we can see that decreasing the number of users also decreases the SER. This can be explained by the fact that when M is increased, the multiuser interference is increased at the relays. Comparing Figure 4.4 with Figure 3.11 we can see that Figure 3.11 shows no change on the SER as we change the number of users, whereas in Figure 4.4 the SER changes.

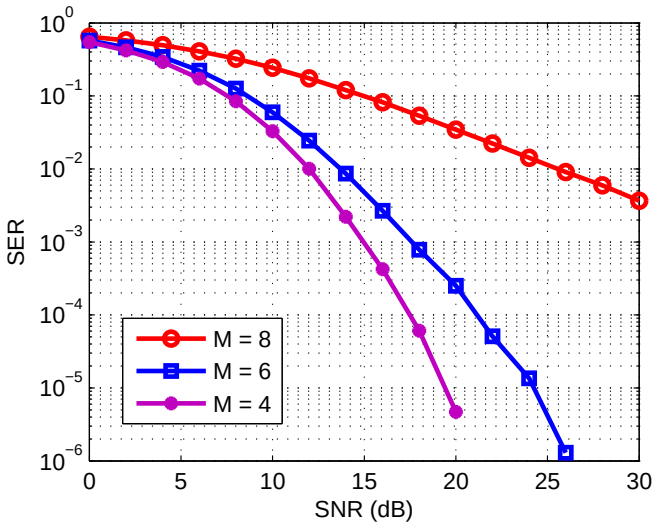

Figure 4.4: SER versus SNR performance of the proposed receiver for different values of M (users on the system) with multiuser interference considered at the relays.

Fig. 4.5 depicts the SER performance of the proposed receiver of this chapter for two values of the data block length N, where we have $P = 8$ chips, $K = 3$ receive antennas, $R = 3$ relays, $W = 4$ and $M = 4$ users. It is observed from Figure 4.5 that there is no change on the SER for a increase of the data block length from 2 to 128. As we already explained, the system does not exploit time diversity, thus we should not expect significant variations in the SER when the value of N is changed.

Figure 4.6 shows the influence of the spreading code length P on SER, where it is assumed $R = 3$ relays, $K = 2$ antennas, $N = 16$ symbols, a training sequence of length $W = 4$ and $M = 2$ users. In this figure, it is possible to see a small decrease in the SER as the length of the spreading code is augmented. The impact of the code length is not significant because the adopted system model does not exploit frequency diversity, due to the fact that frequency-flat fading is considered. By comparing Figure 4.6 with Figure 3.9, we can see that increasing P does not provides great changes on the SER for neither the system models. As multiuser interference at the relays is considered in this system model, CDMA codes are useful in the multiuser separation and also in exploiting the uniqueness properties of the PARAFAC decomposition with the parameter P.

In Figure 4.7, we compare the SER of the two proposed receivers: the one of Chapter 3 (semi-blind non-supervised case) and the one shown here in Chapter 4 (supervised case). We set the parameters as follows: $K = 3$, $R = 3$, $P = 8$, N

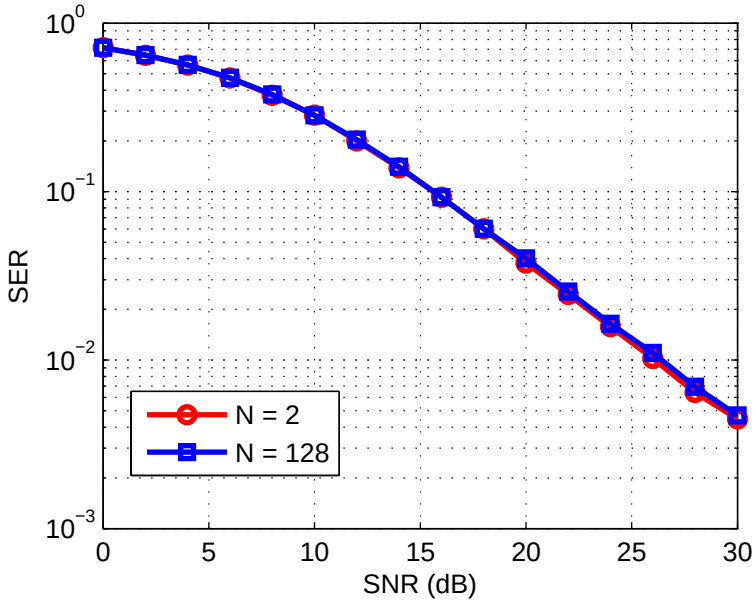

Figure 4.5: SER versus SNR performance of the proposed receiver for different values of N (data block length) with multiuser interference considered at the relays.

$= 16$, $W = 4$ and $M = 4$. From Figure 4.7, it is possible to see that the SER performance of the proposed semi-blind receiver of Chapter 3 (non-supervised) is better than the one of the receiver proposed in this chapter (supervised). This is due to the fact that the scenario of Chapter 3 does not consider multiuser interference at the relays whereas the scenario of Chapter 4 does. The multiuser interference at the relays, as shown in earlier results, increases the error rate, thus, explaining the worse performance of the supervised receiver.

Fig. 4.8 shows another comparison of the two proposed receivers, with the same configurations as for Figure 4.7. This time we increased the training sequence length W from 4 to 8. In Fig. 4.8, we can see that the supervised receiver (presented in this chapter) performs better than the receiver of Chapter 3. This is explained as follows: an increase on the training sequences length improves the estimation of data, thus, by increasing W we get better SER performance. This result shows that even with multiuser interference at the relays, the proposed receiver of this chapter can perform better than the semi-blind receiver of Chapter 3, where multiuser interference is not considered, as long as the training sequence is sufficient big.

In Figure 4.9, the impact of the training sequence length on the SER is shown. The parameters were set as: $R = 3$ relays, $K = 3$ antennas, $N = 16$ symbols, P

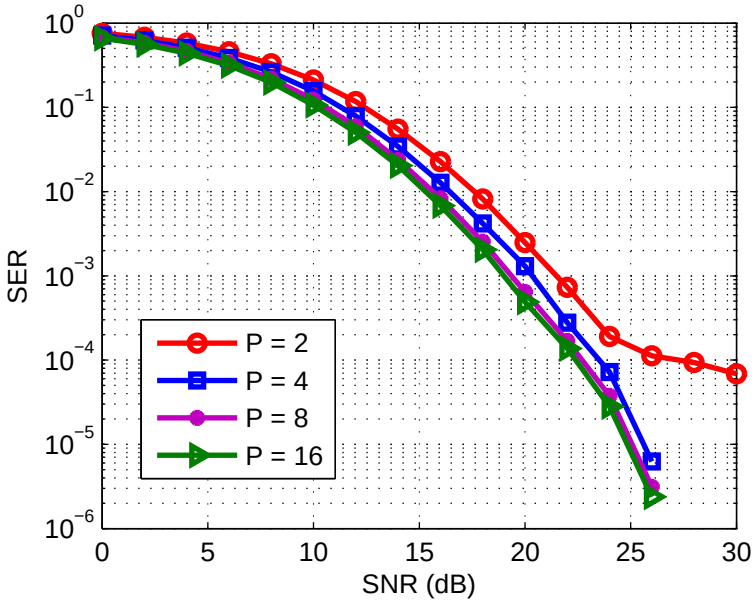

Figure 4.6: SER versus SNR performance of the proposed receiver for different values of P (spreading code length) with multiuser interference considered at the relays.

$= 8$ chips and $M = 4$ users. In Figure 4.9, it is possible to see a decrease in the SER as the length of the training sequence is augmented. As discussed earlier, by increasing the length of the training sequence, the estimations are more accurate, which diminishes the error rate during the second phase.

We show in the next figures the NMSE performance of the proposed receiver for the estimation of matrix $\mathbf{H}_2^G$, which can be obtained by:

$$NMSE_{\mathbf{HG2}} = \frac{1}{M_C}\left(\frac{1}{\|\mathbf{H}_{2(l)}^G\|_F^2}\left(\sum_{l=1}^{M_C}\|\mathbf{H}_{2(l)}^G - \hat{\mathbf{H}}_{2(l)}^G\|_F^2\right)\right), \tag{4.37}$$

where M_C is the number of Monte Carlo runs, $\mathbf{H}_{2(l)}^G$ is the matrix $\mathbf{H}_2^G$ obtained during the l-th Monte Carlo run and $\hat{\mathbf{H}}_{2(l)}^G$ represent the estimation of $\mathbf{H}_2^G$ on the l-th Monte Carlo run. In Figure 4.10, we have the NMSE of matrix $\mathbf{H}_2^G$ in function of the SNR for a variation in the number of users on the system. We set $K = 3$, $R = 3$, $P = 8$, $W = 8$ and $N = 16$. From Figure 4.10 we can see that decreasing the number of users on the system also decreases the NMSE. The explanation for this result is the same as for Figure 4.4 (increasing M also increases multiuser interference at the relays). Comparing Figure 4.10 with Figure 3.18 we can see that in Figure 3.18, variations in M did not change the NMSE of matrix $\mathbf{H}$. However, in 4.10, when we decrease M, we also decrease the NMSE of matrix

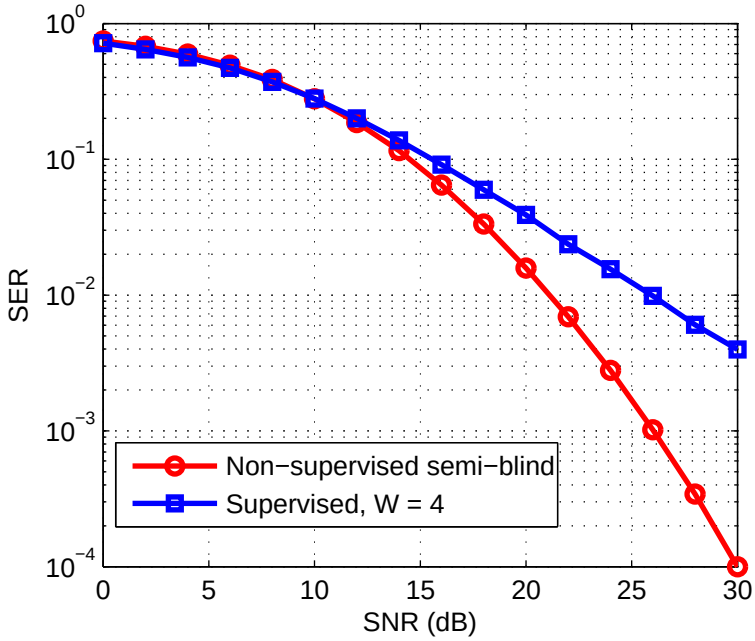

Figure 4.7: SER versus SNR performance for the two proposed receivers.

$\mathbf{H}_2^G$. The explanation for this is the same as for the comparison of Figure 4.4 and Figure 3.11.

Figure 4.11 shows the NMSE performance versus SNR of the matrix $\mathbf{H}_2^G$ for a variation of the number of relays on the system. For this result, we set $K = 3$, $P = 8$, $M = 4$, $W = 4$ and $N = 16$. As we can see from Figure 4.11, when we increase the number of relays, the NMSE of matrix $\mathbf{H}_2^G$ shows a small increase. The explanation for this behavior is the following. As we increase the number of relays, we take advantage of a higher degree of cooperative diversity, however, multiuser interference is also increased and we have more parameters to estimate, thus, we should not have significant changes by increasing or decreasing the number of relays.

The next result, depicted in Figure 4.12 shows the NMSEs of matrices $\mathbf{H}_2^G$ and $\mathbf{H}$ versus the SNR of the two proposed receivers: the one of Chapter 3 (semi-blind non-supervised) and the one shown here in Chapter 4 (supervised). We set the parameters as follows: $K = 3$, $R = 3$, $P = 8$, $N = 16$ and $M = 4$. From Figure 4.12, it is possible to see that the NMSE performance of the proposed semi-blind receiver of Chapter 3 (non-supervised) is better than the one of the receiver proposed in this chapter (supervised) when $W = 4$. When W is increased from 4 to 8, the supervised receiver provides better performance than the semi-blind receiver of Chapter 3. The explanation for this behavior is the same as for

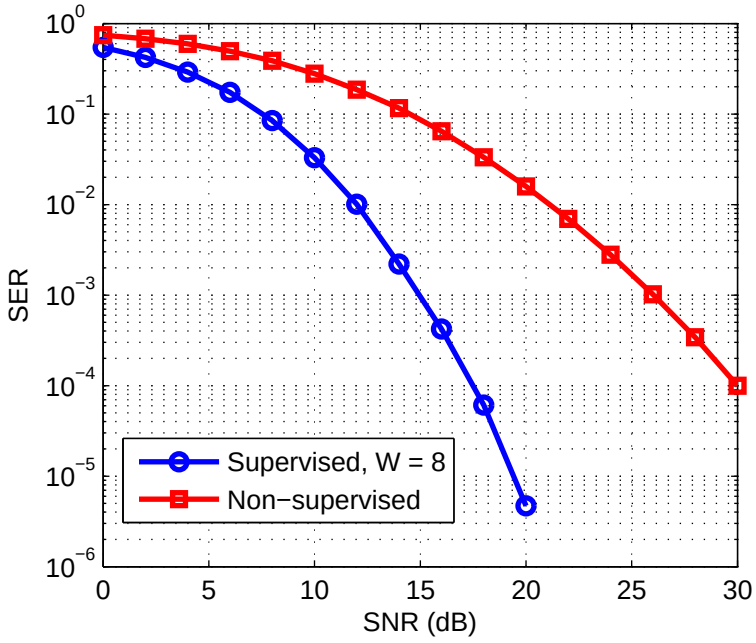

Figure 4.8: SER versus SNR performance for the two proposed receivers.

Figures 4.7, 4.8 and 4.9 (increasing the training sequence length provides more accurate estimations of matrix $\mathbf{H}_2^G$).

The next results shows the NMSE of matrix $\mathbf{A}$ versus the SNR. The NMSE of matrix $\mathbf{A}$ can be obtained by (3.42). In Fig. 4.13 whe have the NMSE performance for a variation on the number of relays. This result shows that increasing the relay count decreases the NMSE of matrix $\mathbf{A}$. When we increase the number of relays, we take advantage a higher degree of cooperative diversity but we also increase the interference, thus the explanation for the small performance improvement.

Figure 4.14 shows the NMSEs of matrices $\mathbf{A}$ versus the SNR of the two proposed receivers: the one of Chapter 3 (semi-blind non-supervised) and the one shown here in Chapter 4 (supervised). We set the parameters as follows: $K = 3$, $R = 3$, $P = 8$, $N = 16$, $W = 4$ and $M = 4$. We can see from Figure 4.14 that the NMSEs performance of the two proposed receivers are similar, with the one of the receiver proposed in this chapter (supervised) being better. The explanation for this behavior is because the estimation of $\mathbf{A}$ is done during the supervised stage, thus being more efficient than the estimation of the receiver proposed in Chapter 3.

As the results of this section showed, we can conclude that the multiuser interference considered at the relays caused overall SER and NMSE increase as some parameters, such as M, are augmented. Also, we could see that even with

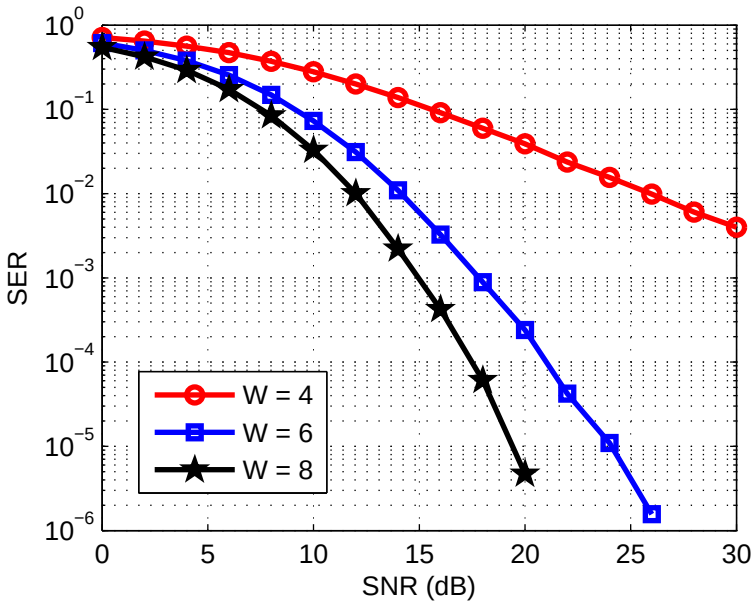

Figure 4.9: SER versus SNR performance of the proposed receiver for different values of W (training sequence length) with multiuser interference considered at the relays.

multiuser interference at the relays, with a sufficient length of training sequences, the proposed supervised receiver can perform better than the one of Chapter 3 (non-supervised semi-blind) and probably better than the ones of [2], [46] and [47].

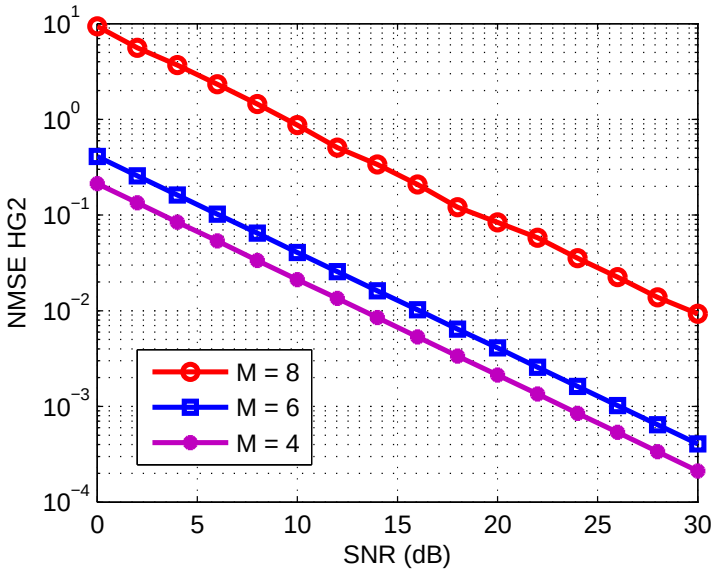

Figure 4.10: NMSE of matrix $\mathbf{H}_2^G$ versus SNR performance for a different number of users on the system, with multiuser interference considered at the relays.

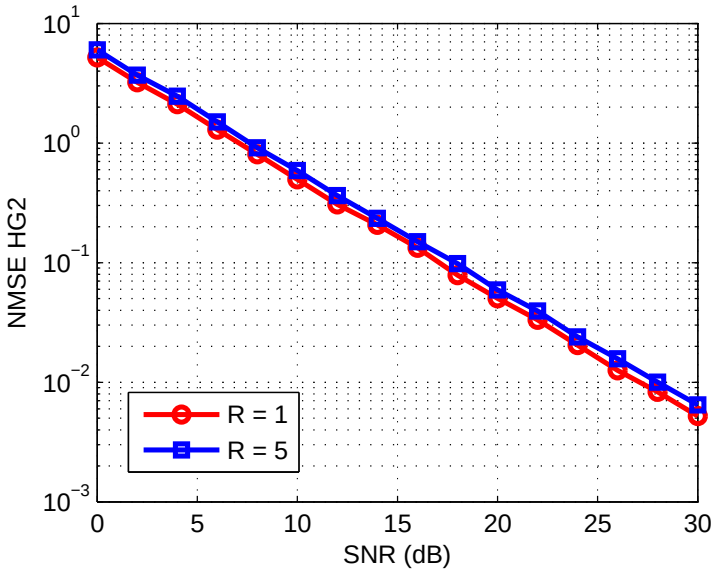

Figure 4.11: NMSE of matrix $\mathbf{H}_2^G$ versus SNR performance for a different number of relays on the system, with multiuser interference considered at the relays.

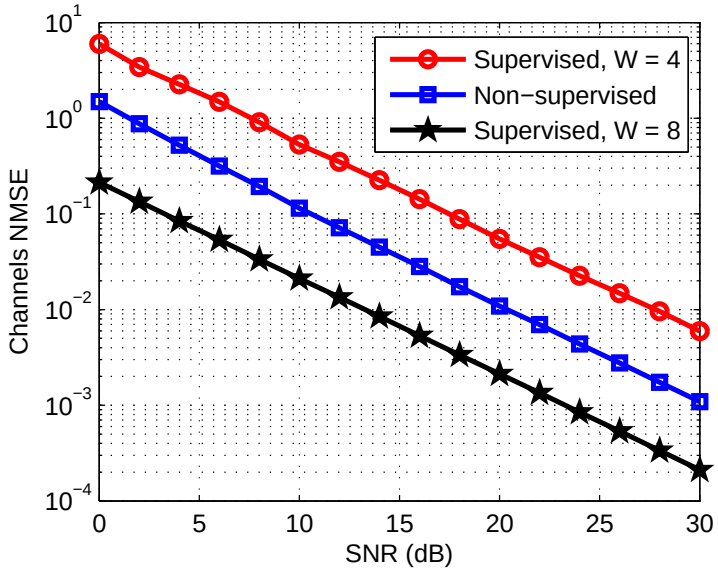

Figure 4.12: NMSE of Channel matrix versus SNR performance for the two proposed receivers.

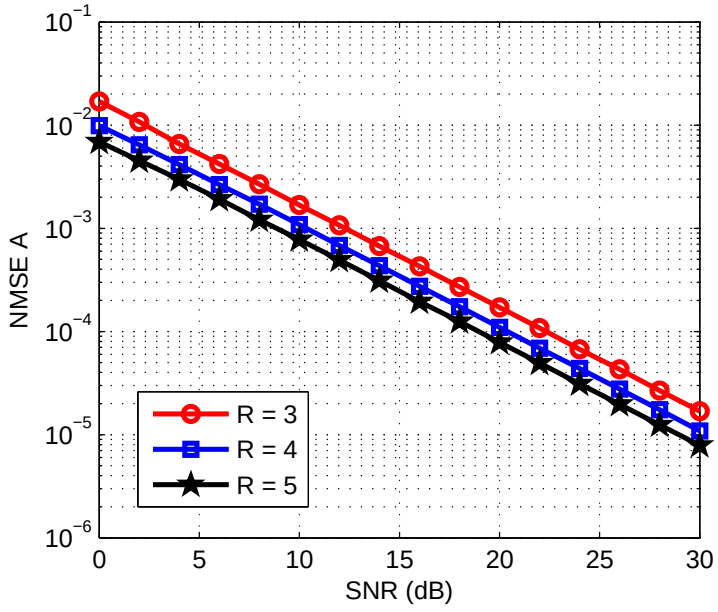

Figure 4.13: NMSE of matrix $\mathbf{A}$ versus SNR performance for a different number of relays on the system, with multiuser interference considered at the relays.

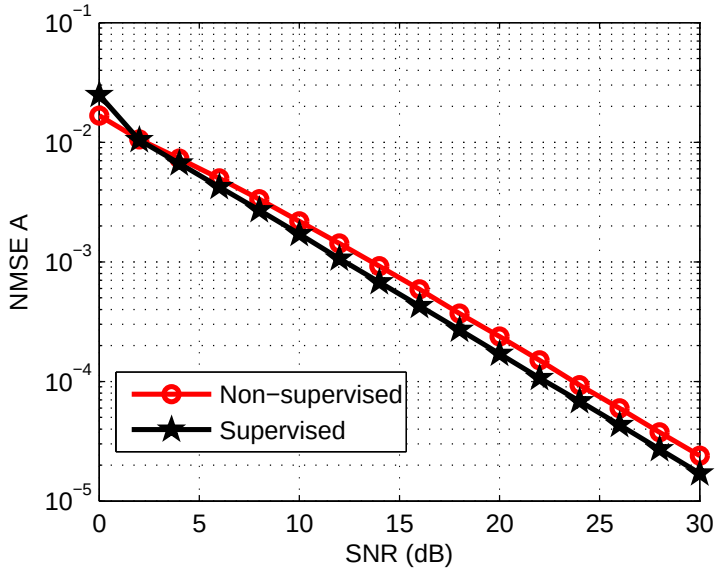

Figure 4.14: NMSE of matrix **A** versus SNR performance for the two proposed receivers.

Chapter 5

Conclusion

In this dissertation, we have considered two system models. Both are based on a cooperative DS-CDMA AF relay-aided scenario where direct-sequence spreading is used at the relays and an antenna array is employed at the destination. The presented system models take advantage of cooperative and spatial diversities and both systems consist in a wireless uplink, with users transmitting towards a base station and with the help of relay-aided links. In the first scenario, which was considered in Chapter 3, multiuser interference between users is not considered at the relays. The second scenario, which was used in Chapter 4, is similar to the previous one, however, multiuser interference is assumed at the relays, giving us a more realistic scenario. Based on these two system models, we proposed two receivers, one for each model.

Blind separation of signals arriving on an antenna array is of great importance in telecommunication applications. Semi-blind receivers are well motivated because they mitigate unknown multipath effects while avoiding bandwidth consuming with large training sequences. The proposed receivers can jointly and semi-blindly estimate parameters of the presented system models. The proposed receivers are based on the PARAFAC decomposition and, in the context of signal processing, they can semi-blindly estimate the channel gains, antenna array responses and transmitted symbols. The receivers are called semi-blind because it is assumed knowledge of a few transmitted symbols in order to remove scaling ambiguity. With the possibility of semi-blind estimation, the proposed receivers brings many advantages, as the followings:

- Use of less pilot symbols;
- Better spectral efficiency;

- No need of CSI at the transmitter.

The semi-blind receiver of the first system model is based on a quadrilinear PARAFAC decomposition. The estimation consists in fitting the tensor model to the received data using the ALS algorithm. The estimation that the proposed receiver is able to do is only possible because the powerful uniqueness property of the PARAFAC decomposition. This property allows some flexibility in choosing the parameters of the system, as the number of relays, number of antennas at the base station, spreading codes or data block length, as described in the previous chapters. Thus we are able to cover lots of practical scenarios as: less sensors and relays than users, more users than spreading gain and a short data block. It is possible that, depending of the parameters (K, R and P), the adopted system model of Chapter 3 turns into the system models of [46], [47] and [45]. Then, we can state that the presented system model of Chapter 3 generalizes [46], [47] and [45].

The system model of Chapter 4 also brings important contributions. The adopted system model considers multiuser interference at the relays, which is a challenging scenario. The receiver proposed in Chapter 4 is based on a trilinear PARAFAC decomposition by joining the users symbols dimension with the channel gains dimension. Then, we reduce the number of dimensions of the PARAFAC decomposition present in Chapter 3 by one. The second receiver estimate the data in two phases. During the first phase (a supervised stage), all users send a training sequence known at the receiver, thus the receiver is able to estimate the channel gains and spatial signatures of all users. Then, during the second phase, the receiver is able to estimate the users symbols using the previous channel estimations in a non-supervised stage. Moreover, the tensor modelings of Chapters 3 and 4 are also valid when the DS-CDMA spread carried out by the relays is replaced by a DKRST coding scheme.

The results sections of Chapters 3 and 4 showed us the performance of the proposed receivers for variations of parameters K, R, N and P. From the Chapter 3 results, we could see that the proposed receiver performs well in comparison to the receivers described in [2], [47], [46] and the ZF receiver. This shows that the quadrilinear PARAFAC model proposed has significant relevance to the area of cooperative communications and signal processing. Also, the results of Chapter 4 showed us that the receiver operating in two phases (supervised stage and non-supervised stage) obtained considerable results even with multiuser interference at the relays. However, as some results of Chapter 4 showed, the semi-blind

receiver o Chapter 3 proved to perform better in comparison to the receiver proposed in Chapter 4 when the training sequence is not sufficient large. This result is expected as no multiuser interference at the relays is considered in Chapter 3. By increasing the training sequence length, the supervised receiver of Chapter 4 can outperform the semi-blind receiver of Chapter 3 and much probably the ones of [2], [46] and [47].

Hence, the most relevant contributions presented in this dissertation are the two PARAFAC decompositions proposed for the two system models, the two proposed receivers and the simulations results showing the performance of the receivers.

This work may be extended by considering other fitting algorithms instead of the ALS, as in [45] where the Levenberg-Marquardt (LM) was used, or by the LS-KF (Least Squares - Khatri-rao Factorization), which can be accomplished using (3.25) and (4.18). Also, frequency-flat fading could be changed to frequency-selective fading, which is more realist in DS-CDMA scenarios. There are some topics that were not covered in this dissertation that could be covered in future works or extensions of this work, as, for instance: the impact of the length of training sequences in the spectral efficiency of the system. We end this dissertation with perspectives of studying the complexity of the presented algorithms in future works.

Appendix A

SBrT 2017 Paper

Paper accepted on the XXXV Simpósio Brasileiro de Telecomunicações e Processamento de Sinais (SBrT 2017).

Title: "Tensor-Based Multiuser Detection for Uplink DS-CDMA Systems with Cooperative Diversity"

Authors: Antonio Augusto T. Peixoto, Carlos Alexandre R. Fernandes

Tensor-Based Multiuser Detection for Uplink DS-CDMA Systems with Cooperative Diversity

Antonio Augusto Teixeira Peixoto and Carlos Alexandre Rolim Fernandes

***Abstract*— In the present paper, a semi-blind receiver for a multiuser uplink DS-CDMA (Direct-Sequence Code-Division Multiple-Access) system based on relay aided cooperative communications is proposed. For the received signal, a quadrilinear Parallel Factor (PARAFAC) tensor decomposition is adopted, such that the proposed receiver can semi-blindly estimate the transmitted symbols, channel gains and spatial signatures of all users. The estimation is done by fitting the tensor model using the Alternating Least Squares (ALS) algorithm. With computational simulations, we provide the performance evaluation of the proposed receiver for various scenarios.**

***Keywords*— Semi-blind receiver, DS-CDMA, Cooperative communications, PARAFAC, Tensor model, Alternating least squares.**

I. Introduction

Cooperative diversity is a new way for granting better data rates, capacity, fading mitigation, spatial diversity and coverage in wireless networks [1], so that, its promising characteristics have put it into research interest lately. The basic idea behind it is making the network nodes help each other, allowing an improvement in the throughput without increasing the power at the transmitter, similarly to multiple-input multiple-output (MIMO) systems. There are some cooperative protocols available, like the amplify-and-foward (AF) and the decode-and-foward (DF) [2]. In means of simplicity, the AF protocol is of good choice because the relay node will just amplify the user's signals and fowards it to the destination. Latency and complexity are then keep small on this protocol.

An important mathematical tool used in this work is tensor based models. An advantage of using tensors in comparison to matrices is the fact that tensors allows us the use of multidimensional data, allowing a better understanding and precision for a multidimensional perspective. Due to its powerful signal processing capabilities, tensors can be found applied to many fields, for example, in chemometrics and others [3].

The Parallel Factor (PARAFAC) decomposition [3], [4] was first used in wireless communications systems in [5], where a blind receiver was proposed for a DS-CDMA system and a tensor was used to model the received signal as a multidimensional variable. After, many other works using tensor decompostions in telecommunications were developed. Wireless MIMO systems had also been proposed with tensor approaches, which led to the development of new tensor models, as in [6], where a constrained factor decomposition was proposed, and in [7], where a new constrained tensor model called PARATUCK was proposed. An overview of some of these tensor models can be found in [8].

There are other examples of tensor decompositions in wireless cooperative communications like in [9], where a receiver was proposed for a two-way AF relaying system with multiple antennas at the relay nodes adopting tensor based estimation. In [10], an unified multiuser receiver based on a trilinear tensor model was proposed for uplink multiuser cooperative diversity systems employing an antenna array at the destination node. There are also recent works, as [11], where a two-hop MIMO relaying system was proposed adopting two tensor approaches (PARAFAC and PARATUCK), and in [12], where a one-way two-hop MIMO AF cooperative scheme was employed with a nested tensor approach. In [13], receivers were based on a trilinear decomposition on a cooperative scenario exploiting spreading diversity at the relays. In [14], a similar scenario was proposed without spreading, but with different time-slots for each relay transmission. [15] presented a new tensor decomposition called nested Tucker decomposition (NTD), applied to an one-way two-hop MIMO relay communication system.

In contrast to the works earlier mentioned, which are based on trilinear tensor models, we move to a quadrilinear PARAFAC decomposition in this paper. Indeed, we propose a semi-blind multiuser receiver able to jointly estimate the channel gains, antenna responses and transmitted symbols, exploiting the uniqueness properties of a fourth order tensor. More specifically, we are considering a cooperative AF relay aided scenario where direct-sequence spreading is used at the relays, thus, taking advantage of cooperative and spreading diversity.

This work extends [5] by considering a cooperative link with R relays. Moreover, in comparisson to [10] and [14], our work admits spreading at the relays by using orthogonal codes, and, in contrast to [13], the proposed system considers the relays transmitting in different time-slots instead of all relays transmitting simultaneously to the base station. An advantage of the proposed work, with respect to the previous ones, is its greater flexibility on the choice of some system parameters. By choosing the system parameters, such as the number of relays or the spreading code length, we get the models from [5], [10], [13] and [14]. It is also worth mentioning that the proposed receiver explores spatial and cooperative diversities.

The present work is structured as follows. Section II lays out the adopted system model, including the cooperative scenario and environment assumptions. Section III shows the quadrilinear tensor model used, Section IV presents the proposed receiver, Section V shows the simulations results and Section

Antonio Augusto Teixeira Peixoto and Carlos Alexandre Rolim Fernandes, Computer Engineering, Federal University of Ceará, *campus* de Sobral, CE, Brazil, E-mails: augusto.peixoto@outlook.com, alexandre_ufc@yahoo.com.br.

VI summarizes the conclusions.

The notation used in this paper is presented here. Scalars are denoted by italic Roman letters (a,b,...), vectors as lower-case boldface letters (**a**,**b**,...), matrices as upper-case boldface letters (**A**,**B**,...) and tensors as calligraphic letters ($\mathcal{A}$,$\mathcal{B}$,...). To retrieve the element (*i*,*j*) of **A**, we use $[\mathbf{A}_{i,j}]$.$\mathbf{A}^T$ and $\mathbf{A}^\dagger$ stands for the transpose and the pseudo-inverse of **A** respectively. The operator $diag_j[\mathbf{A}]$ is the diagonal matrix formed by the *j*-th row of **A**. The operator $\circ$ denotes the outer product of two vectors and $\diamond$ denotes the Khatri-Rao product between $\mathbf{A} \in \mathbb{C}^{I\times R}$ and $\mathbf{B} \in \mathbb{C}^{J\times R}$, resulting in $\mathbf{A} \diamond \mathbf{B} = [a_1 \otimes b_1, ..., a_R \otimes \mathbf{B}_R] \in \mathbb{C}^{IJ\times R}$.

II. System Model

The system model considered in this work is a DS-CDMA uplink with *M* users transmitting to a base station with the help of relay-aided links using the AF protocol. The links between a given user and one relay are called source-relay (SR) and the ones between a relay and the base station are called relay-destination (RD). The base station has an uniform linear array of *K* antennas. Each of the *M* users will transmit to its *R* associated AF relays. The *R* relays of a given user use direct-sequence spreading on the user signal, with a spreading code of length *P*, where the same code is used by all relays of a given user. Also, the relays and users are single antenna devices operating in half-duplex mode.

It is assumed perfect synchronization at the symbol level to avoid intersymbol interference, frequency-flat fading is considered and all channels are independent. We consider that each user communicates with its *R* associated relays and that each relay fowards the signal using a different time-slot. We also assume that an user and its relays are all located inside a cluster, such that, the signal received at a relay located within the cluster of the *m*-th user contains no significant interference from the other users, as Fig. 1 shows. This assumption was also made in [10] and in [14]. An interpretation of this assumption is that a user and its relays are located in a cell, while the other users and their associated relays are located in other cells, modeled as co-channel interferers.

The signal received by the *r*-th relay of the *m*-th user is given by:

$$u_{r,m,n}^{(SR)} = h_{r,m}^{(SR)} s_{n,m} + v_{r,m,n}^{(SR)}, \quad (1)$$

where $h_{r,m}^{(SR)}$ is the channel coefficient between the *m*-th user and its *r*-th relay, $s_{n,m}$ is the *n*-th symbol of the *m*-th user and $v_{r,m,n}^{(SR)}$ is the additive white gaussian noise (AWGN) component. All the data symbols $s_{n,m}$ are independent and identically distributed, with $1 \leq m \leq M$, and uniformly distributed over a Quadrature Amplitude Modulation (QAM) or a Phase-Shift Keying (PSK) alphabet.

The signal received at the *k*-th antenna of the base station, trough the *r*-th time slot, on the *n*-th symbol period and *p*-th chip of the spreading code, on the RD link is given by:

$$x_{k,r,n,p}^{(RD)} = \sum_{m=1}^{M} h_{k,r,m}^{(RD)} g_{r,m} u_{r,m,n}^{(SR)} c_{p,m} + v_{k,r,n,p}^{(RD)}, \quad (2)$$

where $h_{k,r,m}^{(RD)}$ is the channel coefficient between the *k*-th receive antenna and the *r*-th relay associated with the *m*-th user, $v_{k,r,n,p}^{(RD)}$ is the corresponding noise of the RD link, $g_{r,m}$ is the amplification factor applied by the *r*-th relay of the *m*-th user and $c_{p,m}$ is the *p*-th chip of the spreading code of the *m*-th user. Substituting (1) into (2), we get:

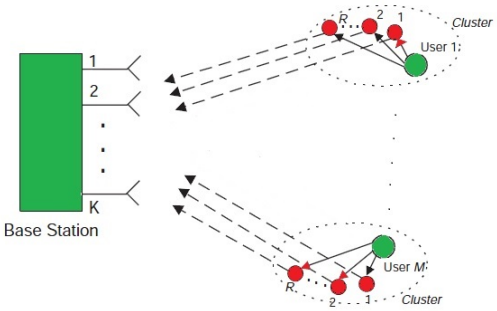

Fig. 1. System model - Uplink for multiuser cooperative scenario.

$$x_{k,r,n,p}^{(RD)} = \sum_{m=1}^{M} h_{k,r,m}^{(RD)} h_{r,m}^{(SR)} g_{r,m} s_{n,m} c_{p,m} + v_{k,r,n,p}^{(SRD)}, \quad (3)$$

$$v_{k,r,n,p}^{(SRD)} = \sum_{m=1}^{M} h_{k,r,m}^{(RD)} g_{r,m} v_{r,m,n}^{(SR)} c_{p,m} + v_{k,r,n,p}^{(RD)}. \quad (4)$$

The term $v_{k,r,n,p}^{(SRD)}$ is the total noise component through the source-relay-destination (SRD) link, from an user to the base station.

Regarding the propagation scenario adopted in the system model, let us also consider the following assumption. All links are subject to multipath propagation and all possible scatters are located far away from the base station, so that all the signals transmitted by the relays arrive at the destination with approximatively the same angle of arrival. The angle spread is small compared to the spatial resolution of the antenna array at the base station. This is truly valid when the user and its relays are close to each other and the base station experiences no scattering around its antennas. This is very common in suburban areas where the base station is placed on the top of a tall building or in a tower [16]. The channel coefficient $h_{k,r,m}^{(RD)}$ may be defined as:

$$h_{k,r,m}^{(RD)} = \sum_{l=1}^{L_{r,m}^{(RD)}} a_k(\theta_m) \beta_{l,r,m}^{(RD)}, \quad (5)$$

where θ_m is the mean angle of arrival of the *m*-th scattering cluster, $a_k(\theta_m)$ is the response of the *k*-th antenna of the *m*-th scattering cluster, defined as $a_k(\theta_m)$ = exp(jθ_m), where θ_m is an uniform random variable with zero mean and variance of 2π, $\beta_{l,r,m}^{(RD)}$ is the fading envelope of the *l*-th path between the *r*-th relay of the *m*-th user and the base station. $L_{r,m}$ is the total number of multipaths. (5) can be approximated as follows:

$$h_{k,r,m}^{(RD)} \approx a_k(\theta_m) \gamma_{r,m}^{(RD)}, \quad (6)$$

where $\gamma_{r,m}^{(RD)}$ is defined as $\gamma_{r,m}^{(RD)} = \sum_{l=1}^{L_{r,m}^{(RD)}} \beta_{l,r,m}^{(RD)}$. Now, by

substituting (6) into (3), we get:

$$x_{k,r,n,p}^{(RD)} = \sum_{m=1}^{M} a_k(\theta_m)\gamma_{r,m}^{(RD)} h_{r,m}^{(SR)} g_{r,m} s_{n,m} c_{p,m} + v_{k,r,n,p}^{(SD)} \tag{7}$$

and again, substituting (6) into (4), we get:

$$v_{k,r,n,p}^{(SRD)} = \sum_{m=1}^{M} a_k(\theta_m)\gamma_{r,m}^{(RD)} g_{r,m} v_{r,m,n}^{(SR)} c_{p,m} + v_{k,r,n,p}^{(RD)}. \tag{8}$$

The transmission rate for each user is given by 1/(*R*+1), thus, the total transmission rate on the system is *M*/(*R*+1).

III. Proposed Tensor Model

The model above described for the RD links can be viewed as a four-way array with its dimensions directly related to space (receive antennas at the base station), cooperative slots (cooperative channels), time (symbols) and spreading codes (chip). In this section, we model the received signal as a 4-th order tensor using a PARAFAC decomposition as shown in [8] and in [17]. Let $\mathcal{Y}$ be a *M*-component, quadrilinear PARAFAC model, so that $\mathcal{Y} \in \mathbb{C}^{K\times R\times N\times P}$ is a 4-th order tensor collecting the baseband RD data signals at the base station:

$$[\mathcal{Y}]_{k,r,n,p} = x_{k,r,n,p}^{(RD)} \tag{9}$$

for *k* = 1,...,*K*, *r* = 1,...,*R*, *n* = 1,...,*N* and *p* = 1,...,*P*.

In order to simplify the presentation, we omit the AWGN terms and assume that the channel is constant for *N* symbol periods throughout the rest of this section. A typical element of $\mathcal{Y}$, denoted by $y_{k,r,n,p} = [\mathcal{Y}_{k,r,n,p}]$ is given by:

$$y_{k,r,n,p} = \sum_{m=1}^{M} a_k(\theta_m) h_{r,m} s_{n,m} c_{p,m}. \tag{10}$$

The channel coefficient $h_{r,m}$ is defined as:

$$h_{r,m} = \gamma_{r,m}^{(RD)} h_{r,m}^{(SR)} g_{r,m}. \tag{11}$$

(10) corresponds to a PARAFAC decomposition with spatial, cooperative slots, time and code indices, in other words, a quadrilinear data tensor. The data tensor $\mathcal{Y}$ can be expressed as:

$$\mathcal{Y} = \sum_{m=1}^{M} \mathbf{A}_{.,m} \circ \mathbf{H}_{.,m} \circ \mathbf{S}_{.,m} \circ \mathbf{C}_{.,m}, \tag{12}$$

where $\circ$ denotes the outer product, $\mathbf{A} \in \mathbb{C}^{K\times M}$ is the antenna array response matrix with $[\mathbf{A}]_{k,m} = a_k(\theta_m)$, $\mathbf{H} \in \mathbb{C}^{R\times M}$ is the channel matrix with $[\mathbf{H}]_{r,m} = h_{r,m}$, $\mathbf{S} \in \mathbb{C}^{N\times M}$ is the symbol matrix with $[\mathbf{S}]_{n,m} = s_{n,m}$ and $\mathbf{C} \in \mathbb{C}^{P\times M}$ is the spreading codes matrix with $[\mathbf{C}]_{p,m} = c_{p,m}$. In (12), we have the PARAFAC decomposition of the data tensor $\mathcal{Y}$ as a sum of *M* rank-1 components.

A. Unfolding Matrices

We can also rewrite (12) in an unfolding matricial form. Let $\mathbf{Y}_1 \in \mathbb{C}^{KRN\times P}$ be defined as the tensor $\mathcal{Y} \in \mathbb{C}^{K\times R\times N\times P}$ unfolded into a matrix, as follows:

$$\mathbf{Y}_1 = (\mathbf{A} \diamond \mathbf{H} \diamond \mathbf{S})\mathbf{C}^T, \tag{13}$$

where $\diamond$ denotes the Khatri-Rao product (column-wise Kronecker product) [4]. There are also other unfolded matrices, as, for instance:

$$\mathbf{Y}_2 = (\mathbf{C} \diamond \mathbf{A} \diamond \mathbf{H})\mathbf{S}^T, \tag{14}$$

$$\mathbf{Y}_3 = (\mathbf{S} \diamond \mathbf{C} \diamond \mathbf{A})\mathbf{H}^T, \tag{15}$$

$$\mathbf{Y}_4 = (\mathbf{H} \diamond \mathbf{S} \diamond \mathbf{C})\mathbf{A}^T, \tag{16}$$

with $\mathbf{Y}_2 \in \mathbb{C}^{PKR\times N}$, $\mathbf{Y}_3 \in \mathbb{C}^{NPK\times R}$ and $\mathbf{Y}_4 \in \mathbb{C}^{RNP\times K}$.

B. Uniqueness Properties

One of the most important properties of the tensor model obtained in (10) and (12) is its essential uniqueness under certain conditions [17], [18]. The uniqueness property of the quadrilinear PARAFAC decomposition by Kruskal's condition described in [17], [18], and in [19], is given as follows:

$$\kappa_{\mathbf{A}} + \kappa_{\mathbf{H}} + \kappa_{\mathbf{S}} + \kappa_{\mathbf{C}} \geq 2M + 3, \tag{17}$$

where $\kappa_{\mathbf{A}}$ is the Kruskal rank of the matrix **A**, (similarly to **H**, **S** and **C**). The Kruskal rank of a matrix corresponds to the greatest integer κ, such that every set of κ columns of the matrix is linearly independent. If the condition (17) is satisfied, the factor matrices **A**, **H**, **S** and **C** are essentially unique, hence, each factor matrix can be determined up to column scaling and permutation. This uniqueness properties of the PARAFAC decomposition means that any other set of matrices ($\mathbf{A}'$, $\mathbf{H}'$, $\mathbf{C}'$ and $\mathbf{S}'$) that satisfies (11) is related with the original matrix set (**A**, **H**, **C** and **S**) by $\mathbf{A}' = \mathbf{A}\Pi\Delta_{\mathbf{A}}$, $\mathbf{H}' = \mathbf{H}\Pi\Delta_{\mathbf{H}}$, $\mathbf{C}' = \mathbf{C}\Pi\Delta_{\mathbf{C}}$ and $\mathbf{S}' = \mathbf{S}\Pi\Delta_{\mathbf{S}}$, where $\Pi \in \mathbb{C}^{M\times M}$ is a permutation matrix and $\Delta_{\mathbf{A}}$, $\Delta_{\mathbf{H}}$, $\Delta_{\mathbf{C}}$ and $\Delta_{\mathbf{S}}$ are diagonal matrices that meet $\Delta_{\mathbf{A}}\Delta_{\mathbf{H}}\Delta_{\mathbf{C}}\Delta_{\mathbf{S}} = \mathbf{I}$.

Now, let us assume that **A**, **H**, **C** and **S** are all full κ-rank (a matrix is said to have full κ-rank if its κ-rank is equal to the minimum between the number of rows and columns), where the κ-rank denotes the Kruskal rank of a matrix, thus (17) becomes:

$$min(K, M) + min(R, M) + min(N, M) + min(P, M) \geq 2M + 3. \tag{18}$$

Given that a matrix whose columns are drawn independently from an absolutely continuous distribution has full rank with probability one [5], then matrix **H** has full κ-rank with probability one. Also, the matrix **A** is full κ-rank because we model it as a Vandermonde matrix with distinc generators, as the user signals arrive at the base station array with different angles of arrival. The symbols matrix **S** is full κ-rank with high probability if *N* is sufficiently large in comparison to the modulation cardinality and the number of users. At last, for the matrix **C**, full κ-rank is possible if a certain length of spreading codes is used.

With the assumptions above, we can determine some parameters of the adopted system, for example, the number of users that the proposed receiver can handle and the minimum acceptable parameters (number of antennas at base station, length of the spreading codes, number of relays or the data block length) that matches a target number of user channels to be detected. Hence, we will have flexibility when choosing *K*, *R*, *N* and *P*, which is the one of the main reasons for

Algorithm 1 ALS FITTING

1)*Initialization* : *Set* $i = 0$; *Initialize* $\hat{\mathbf{A}}_{(i=0)}$ *and* $\hat{\mathbf{H}}_{(i=0)}$;
2)$i = i + 1$;
3)$\hat{\mathbf{S}}_{(i)}^{T} = (\mathbf{C} \diamond \hat{\mathbf{A}}_{(i-1)} \diamond \hat{\mathbf{H}}_{(i-1)})^{\dagger}\tilde{\mathbf{Y}}_2$;
4)$\hat{\mathbf{H}}_{(i)}^{T} = (\hat{\mathbf{S}}_{(i)} \diamond \mathbf{C} \diamond \hat{\mathbf{A}}_{(i-1)})^{\dagger}\tilde{\mathbf{Y}}_3$;
5)$\hat{\mathbf{A}}_{(i)}^{T} = (\hat{\mathbf{H}}_{(i)} \diamond \hat{\mathbf{S}}_{(i)} \diamond \mathbf{C})^{\dagger}\tilde{\mathbf{Y}}_4$;
6)*Repeat steps* $2-5$ *until convergence*;

considering the tensor approach. It provides different tradeoffs for our system based on the parameters. Indeed, we have from (18):

- If $P \geq M$, $N \geq M$ (typical DS-CDMA scenario), then, min(*K*,*M*) + min(*R*,*M*) $\geq$ 3. For example, let K = 2 and R = 1, we satisfy (18) and at least 1 relay and 2 antennas are sufficient for M users.
- If $P \geq M$, $N \geq M$ and $K \leq M$, then, R can be 0 if K = 3, giving us the model described in [3], a noncooperative DS-CDMA uplink.
- If $K \geq M$, $N \geq M$, $P \leq M$ and $R \leq M$, then for R = 2, P = 1 chip is sufficient for M users, therefore we get [14] (the same can be achieved if R = 3, thus P can be zero).
- If $K \geq M$, $P \geq M$, $R \leq M$ and $N \leq M$, then, for R = 1, N = 2 symbols are enough to guarantee uniqueness. It means that a short block length is sufficient for detection.

Based on the assumptions above, we can conclude that the proposed tensor model gives us flexibility about many parameters and diversity tradeoff.

IV. Receiver Algorithm

Assuming that there is no channel information at the receiver or transmitter, the receiver algorithm presented in this section is based on the ALS (Alternating Least Squares) method, which consists in fitting the quadriliear model to the received data tensor [20]. The idea behind the ALS procedure is very simple: each time, update one of the factor matrices by using the least squares estimation technique with the previous estimations of the other factor matrices. Each factor matrix is estimated, in an alternate way, always using the previous estimations of the other factor matrices. This procedure is repeated until convergence. The unfolding matrices in (13)-(16) are used to estimate $\mathbf{A}$, $\mathbf{H}$ and $\mathbf{S}$, where we assume knowledge of the spreading codes (matrix $\mathbf{C}$) at the receiver.

The Quadrilinear ALS algorithm is shown in Algorithm 1. The measured error at the end of the i-th iteration is given by $e(i) = \|\tilde{\mathbf{Y}}_1 - (\hat{\mathbf{A}}_{(i)} \diamond \hat{\mathbf{H}}_{(i)} \diamond \hat{\mathbf{S}}_{(i)})\mathbf{C}^T\|_F$, where $\|.\|_F$ denotes the Frobenius norm, $\tilde{\mathbf{Y}}_1$, $\tilde{\mathbf{Y}}_2$, $\tilde{\mathbf{Y}}_3$ and $\tilde{\mathbf{Y}}_4$ are the noisy unfolding matrices and $\hat{\mathbf{A}}_{(i)}, \hat{\mathbf{H}}_{(i)}$ and $\hat{\mathbf{S}}_{(i)}$) are the estimates of the factor matrices at the i-th iteration. The convergence of the algorithm is obtained when $|e(i) - e(i-1)| < 10^{-6}$.

After obtaining the estimation of $\mathbf{A}$, $\mathbf{H}$ and $\mathbf{S}$, it is necessary to remove the scaling ambiguity. The scaling ambiguity of $\hat{\mathbf{A}}$ is removed by considering that the first row of $\mathbf{A}$ is known, which is possible because $\mathbf{A}$ is a vandermonde matrix. The same can be done to remove the scaling ambiguity from $\hat{\mathbf{S}}$. It is assumed that the first row of $\mathbf{S}$ is known and the scaling ambiguity is removed by dividing the first row of $\hat{\mathbf{S}}$ by the first row of $\mathbf{S}$. After obtaining the scaling matrix of $\hat{\mathbf{A}}$ and $\hat{\mathbf{S}}$, we can find the scaling matrix $\Delta_{\mathbf{H}}$ of $\hat{\mathbf{H}}$ with $\Delta_{\mathbf{A}}\Delta_{\mathbf{S}}\Delta_{\mathbf{H}} = \mathbf{I}$.

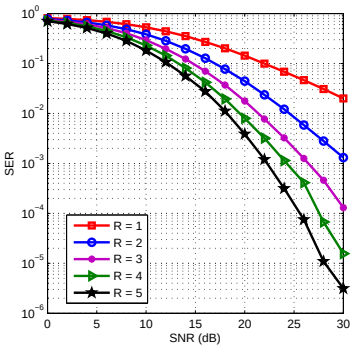

Fig. 2. SER versus SNR performance of the proposed receiver for a different number of relays.

V. Simulation Results

This section presents computer simulations results for performance evaluation purposes with the following scenario. The wireless links have frequency-flat Rayleigh fading with path loss expoent equal to 3, the base station antenna array is composed by K antennas, 16-QAM modulation is used and Hadamard codes are considered for spreading sequences. The symbol error rate (SER) curves are shown as a function of the signal-to-noise ratio (SNR) of the RD link. The mean results were obtained by 10000 independent Monte Carlo samples. The AF relays have variable gains and the source power P_s and the relay power P_r were considered as unitary.

Figure 2 shows the SER versus SNR for the proposed technique with P = 8 chips, a datablock of N = 16 symbols, K = 2 receive antennas and M = 4 users. Then we have curves for various values of R (number of relays on the cluster). From Fig. 2, we can observe a better performance when we increase the number of relays on the system. This happens because when the number of relays is augmented, the model turns to a more cooperative scenario, exploiting cooperative diversity and resulting in better link quality.

Now, we compare the SER of the proposed receiver with the ones of the: Zero Forcing (ZF) receiver, that works under complete knowledge of $\mathbf{A}$, $\mathbf{H}$ and $\mathbf{C}$, the semi-blind DS-CDMA receiver proposed in [5] (non-cooperative DS-CDMA), the receiver proposed in [10] using AF (same cenario of the present work, but without spreading codes) and the receiver shown in [13], where the relays transmit at the same time.

For Figure 3, we set N = 16, P = 4, M = 4, K = 3 and R = 1 for both the ZF and the proposed receiver. For the receiver proposed in [10], only one relay is used and we set K = 3, N = 16 and M = 2. For [13], we set N = 16, P = 2, M = 4, K = 3 and R = 1. For the receiver of [5], we set P = 4, K = 3, N = 16 and M = 4. These simulations parameters were chosen to give us the same or similar spectral efficiency for all the receivers. The direct link between user

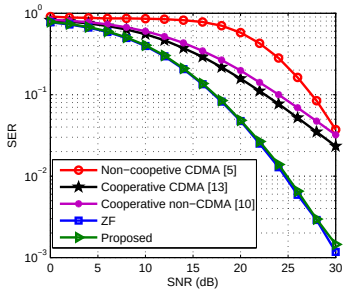

Fig. 3. SER versus SNR performance for different receivers.

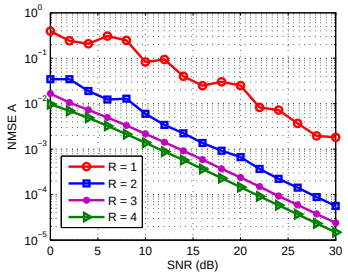

Fig. 4. NMSE of matrix **A** versus SNR for a different number of relays.

and base station (used in [5]) has three times the distance than the SR link, with path loss coeffiecient equal to 3.7. We see that the ZF receiver performed almost equal in comparison to the proposed receiver. This proves that the proposed receiver can operate without knowing the factor matrices (**A**, **H**) and still provide good performance. Both the ZF and the proposed receiver performed better than the non-cooperative semi-blind receiver described in [5], the receiver of [10] and the one of [13].

The addition of spreading makes the proposed receiver obtain better performance in comparison to [10]. The proposed receiver also went better than [5] because of the cooperative scenario (short relay-aided links instead of extended direct links). The espectral efficiency for each configuration is: $M\,/\,(RP{+}1)$ for the proposed receiver and the ZF, $M\,/\,(R{+}1)$ for the receiver described in [10], $M\,/\,P$ for [5] and $M\,/\,2P$ for [13].

Fig. 4 depicts the Normalized Mean Square Error (NMSE) of the matrix **A**. This figure shows us the capacity of the proposed receiver to satisfactorily estimate spatial signatures. It is observed a linear decrease in the NMSE as a function of the SNR, as expected. Moreover, a small gain is observed when R is increased, for the same reasons above explained.

VI. Conclusions

In this paper, we have proposed a tensor-based receiver that can jointly and semi-blindly estimate some parameters of the system (a cooperative DS-CDMA uplink): channel gains, antenna array responses and transmitted symbols. The estimation consists in fitting a PARAFAC tensor model to the received data using the ALS algorithm. Another characteristic of the proposed receiver is its powerful uniqueness property that allows some flexibility in choosing the parameters of the system, like the number of relays, number of antennas at the base station, spreading codes or data block length. Thus, we are able to cover lots of pratical scenarios. The results showed us that the proposed receiver performs well in comparison to the receivers described in [5], [10], [13] and the ZF receiver. This work may be extendend by using another algorithm instead of the ALS, as in [14]. Also, the frequency-flat fading could be changed to frequency-selective fading.

References

[1] Fitzek, F. H., & Katz, M. D. (2006). *Cooperation in wireless networks: principles and applications* (pp. 421-461). New York: Springer.

[2] Nosratinia, A., Hunter, T. E., & Hedayat, A. (2004). Cooperative communication in wireless networks. *IEEE communications Magazine, 42*(10), 74-80.

[3] Bro, R. (1997). PARAFAC. Tutorial and applications. *Chemometrics and intelligent laboratory systems, 38*(2), 149-171.

[4] Kolda, T. G., & Bader, B. W. (2009). Tensor decompositions and applications. *SIAM review, 51*(3), 455-500.

[5] Sidiropoulos, N. D., Giannakis, G. B., & Bro, R. (2000). Blind PARAFAC receivers for DS-CDMA systems. *IEEE Transactions on Signal Processing, 48*(3), 810-823.

[6] de Almeida, A. L., Favier, G., & Mota, J. C. M. (2008). A constrained factor decomposition with application to MIMO antenna systems. *IEEE Transactions on Signal Processing, 56*(6), 2429-2442.

[7] Favier, G., Da Costa, M. N., De Almeida, A. L., & Romano, J. M. T. (2012). Tensor space-time (TST) coding for MIMO wireless communication systems. *Signal Processing, 92*(4), 1079-1092.

[8] Favier, G., & de Almeida, A. L. (2014). Overview of constrained PARAFAC models. *EURASIP Journal on Advances in Signal Processing, 2014*(1), 142.

[9] Roemer, F., & Haardt, M. (2010). Tensor-based channel estimation and iterative refinements for two-way relaying with multiple antennas and spatial reuse. *IEEE Transactions on Signal Processing, 58*(11), 5720-5735.

[10] Fernandes, C. A. R., de Almeida, A. L. F., & da Costa, D. B. (2012). Unified tensor modeling for blind receivers in multiuser uplink cooperative systems. *IEEE Signal Processing Letters, 19*(5), 247-250.

[11] Ximenes, L. R., Favier, G., de Almeida, A. L., & Silva, Y. C. (2014). PARAFAC-PARATUCK semi-blind receivers for two-hop cooperative MIMO relay systems. *IEEE Trans. Signal Process, 62*(14), 3604-3615

[12] Ximenes, L. R., Favier, G., & de Almeida, A. L. (2015). Semi-blind receivers for non-regenerative cooperative MIMO communications based on nested PARAFAC modeling. *IEEE transactions on signal processing, 63*(18), 4985-4998.

[13] de Almeida, A. L., Fernandes, C. A., & da Costa, D. B. (2013). Multiuser detection for uplink DS-CDMA amplify-and-forward relaying systems. *IEEE Signal Processing Letters, 20*(7), 697-700.

[14] Fernandes, A. R., de Almeida, A. L., & da Costa, D. B. (2011, June). Blind receiver for amplify-and-forward cooperative diversity scheme. In *Signal Processing Advances in Wireless Communications (SPAWC), 2011 IEEE 12th International Workshop on* (pp. 546-550). IEEE.

[15] Favier, G., Fernandes, C. A. R., & de Almeida, A. L. (2016). Nested Tucker tensor decomposition with application to MIMO relay systems using tensor space?time coding (TSTC). *Signal Processing, 128*, 318-331.

[16] Ertel, R. B., Cardieri, P., Sowerby, K. W., Rappaport, T. S., & Reed, J. H. (1998). Overview of spatial channel models for antenna array communication systems. *IEEE Personal Communications, 5*(1), 10-22.

[17] Sidiropoulos, N. D., & Bro, R. (2000). On communication diversity for blind identifiability and the uniqueness of low-rank decomposition of N-way arrays. In *Acoustics, Speech, and Signal Processing, 2000. ICASSP'00. Proceedings. 2000 IEEE International Conference on* (Vol. 5, pp. 2449-2452). IEEE.

[18] Stegeman, A., & Sidiropoulos, N. D. (2007). On Kruskal's uniqueness condition for the Candecomp/Parafac decomposition. *Linear Algebra and its applications, 420*(2-3), 540-552.

[19] Kruskal, J. B. Rank, decomposition, and uniqueness for 3-way and N-way arrays. *Multiway data analysis*. North-Holland Publishing Co., 1989.

[20] Comon, P., Luciani, X., & De Almeida, A. L. (2009). Tensor decompositions, alternating least squares and other tales. *Journal of chemometrics, 23*(7-8), 393-405.

Bibliography

[1] A. De Almeida, *Tensor modeling and signal processing for wireless communication systems*. PhD thesis, Université de Nice Sophia Antipolis, 2007.

[2] N. D. Sidiropoulos, G. B. Giannakis, and R. Bro, "Blind parafac receivers for ds-cdma systems," *IEEE Transactions on Signal Processing*, vol. 48, no. 3, pp. 810–823, 2000.

[3] K. R. Liu, *Cooperative communications and networking*. Cambridge university press, 2009.

[4] J. N. Laneman, *Cooperative diversity in wireless networks: Algorithms and architectures*. PhD thesis, Citeseer, 2002.

[5] S. W. Peters and R. W. Heath Jr, "The future of wimax: Multihop relaying with ieee 802.16 j," *IEEE Communications Magazine*, vol. 47, no. 1, pp. 104–111, 2009.

[6] P. Herhold, E. Zimmermann, and G. Fettweis, "On the performance of cooperative amplify-and-forward relay networks," *ITG FACHBERICHT*, vol. 2, pp. 451–458, 2004.

[7] Y. Han, A. Pandharipande, and S. H. Ting, "Cooperative decode-and-forward relaying for secondary spectrum access," *IEEE Transactions on Wireless Communications*, vol. 8, no. 10, 2009.

[8] W. Su, A. K. Sadek, and K. Ray Liu, "Cooperative communication protocols in wireless networks: Performance analysis and optimum power allocation," *Wireless Personal Communications*, vol. 44, no. 2, pp. 181–217, 2008.

[9] A. J. Paulraj, D. A. Gore, R. U. Nabar, and H. Bolcskei, "An overview of mimo communications-a key to gigabit wireless," *Proceedings of the IEEE*, vol. 92, no. 2, pp. 198–218, 2004.

[10] G. J. Foschini and M. J. Gans, "On limits of wireless communications in a fading environment when using multiple antennas," *Wireless personal communications*, vol. 6, no. 3, pp. 311–335, 1998.

[11] A. Goldsmith, S. A. Jafar, N. Jindal, and S. Vishwanath, "Capacity limits of mimo channels," *IEEE Journal on selected areas in Communications*, vol. 21, no. 5, pp. 684–702, 2003.

[12] S. M. Alamouti, "A simple transmit diversity technique for wireless communications," *IEEE Journal on selected areas in communications*, vol. 16, no. 8, pp. 1451–1458, 1998.

[13] B. Vucetic and J. Yuan, *Space-time coding*. John Wiley & Sons, 2003.

[14] V. Tarokh, N. Seshadri, and A. R. Calderbank, "Space-time codes for high data rate wireless communication: Performance criterion and code construction," *IEEE transactions on information theory*, vol. 44, no. 2, pp. 744–765, 1998.

[15] N. D. Sidiropoulos and R. S. Budampati, "Khatri-rao space-time codes," *IEEE Transactions on Signal Processing*, vol. 50, no. 10, pp. 2396–2407, 2002.

[16] A. J. Viterbi, *CDMA: principles of spread spectrum communication*. Addison Wesley Longman Publishing Co., Inc., 1995.

[17] T. S. Rappaport *et al.*, *Wireless communications: principles and practice*, vol. 2. Prentice Hall PTR New Jersey, 1996.

[18] A. Goldsmith, *Wireless communications*. Cambridge university press, 2005.

[19] B. Hochwald, T. L. Marzetta, and C. B. Papadias, "A transmitter diversity scheme for wideband cdma systems based on space-time spreading," *IEEE Journal on selected areas in communications*, vol. 19, no. 1, pp. 48–60, 2001.

[20] H. Huang, H. Viswanathan, and G. J. Foschini, "Multiple antennas in cellular cdma systems: transmission, detection, and spectral efficiency," *IEEE Transactions on Wireless Communications*, vol. 1, no. 3, pp. 383–392, 2002.

[21] L. De Lathauwer, *Signal processing based on multilinear algebra*. Katholieke Universiteit Leuven, 1997.

[22] T. G. Kolda and B. W. Bader, "Tensor decompositions and applications," *SIAM review*, vol. 51, no. 3, pp. 455–500, 2009.

[23] P. Comon, "Tensors: a brief introduction," *IEEE Signal Processing Magazine*, vol. 31, no. 3, pp. 44–53, 2014.

[24] A. Cichocki, "Era of big data processing: a new approach via tensor networks and tensor decompositions," *arXiv preprint arXiv:1403.2048*, 2014.

[25] D. Muti and S. Bourennane, "Multidimensional filtering based on a tensor approach," *Signal Processing*, vol. 85, no. 12, pp. 2338–2353, 2005.

[26] A. L. F. de Almeida, G. Favier, J. C. M. Mota, and J. da Costa, "Overview of tensor decompositions with applications to communications," 2016.

[27] R. A. Harshman, "Foundations of the parafac procedure: Models and conditions for an" explanatory" multi-modal factor analysis," *UCLA Working Papers in Phonetics*, vol. 16, pp. 1–84, 1970.

[28] J. D. Carroll and J.-J. Chang, "Analysis of individual differences in multidimensional scaling via an n-way generalization of "eckart-young" decomposition," *Psychometrika*, vol. 35, no. 3, pp. 283–319, 1970.

[29] R. Bro, "Parafac. tutorial and applications," *Chemometrics and intelligent laboratory systems*, vol. 38, no. 2, pp. 149–171, 1997.

[30] A. Smilde, R. Bro, and P. Geladi, *Multi-way analysis: applications in the chemical sciences*. John Wiley & Sons, 2005.

[31] D. Nion, K. N. Mokios, N. D. Sidiropoulos, and A. Potamianos, "Batch and adaptive parafac-based blind separation of convolutive speech mixtures," *Audio, Speech, and Language Processing, IEEE Transactions on*, vol. 18, no. 6, pp. 1193–1207, 2010.

[32] L. De Lathauwer and J. Castaing, "Tensor-based techniques for the blind separation of ds–cdma signals," *Signal Processing*, vol. 87, no. 2, pp. 322–336, 2007.

[33] N. D. Sidiropoulos, R. Bro, and G. B. Giannakis, "Parallel factor analysis in sensor array processing," *IEEE transactions on Signal Processing*, vol. 48, no. 8, pp. 2377–2388, 2000.

[34] N. D. Sidiropoulos and G. Z. Dimic, "Blind multiuser detection in w-cdma systems with large delay spread," *IEEE Signal Processing Letters*, vol. 8, no. 3, pp. 87–89, 2001.

[35] T. Jiang and N. D. Sidiropoulos, "A direct blind receiver for simo and mimo ofdm systems subject to unknown frequency offset and multipath," in *Signal Processing Advances in Wireless Communications, 2003. SPAWC 2003. 4th IEEE Workshop on*, pp. 358–362, IEEE, 2003.

[36] Y. Rong, S. A. Vorobyov, A. B. Gershman, and N. D. Sidiropoulos, "Blind spatial signature estimation via time-varying user power loading and parallel factor analysis," *IEEE Transactions on Signal Processing*, vol. 53, no. 5, pp. 1697–1710, 2005.

[37] A. L. de Almeida, G. Favier, and J. C. M. Mota, "Parafac models for wireless communication systems," in *Proceedings of the International Conference on Physics in Signal and Image Processing (PSIP), Toulouse, France*, 2005.

[38] A. L. de Almeida, G. Favier, and J. C. M. Mota, "Parafac-based unified tensor modeling for wireless communication systems with application to blind multiuser equalization," *Signal Processing*, vol. 87, no. 2, pp. 337–351, 2007.

[39] C. E. R. Fernandes, G. Favier, and J. C. M. Mota, "Blind channel identification algorithms based on the parafac decomposition of cumulant tensors: the single and multiuser cases," *Signal Processing*, vol. 88, no. 6, pp. 1382–1401, 2008.

[40] A. de Baynast, L. De Lathauwer, and B. Aazhang, "Blind parafac receivers for multiple access-multiple antenna systems," in *Vehicular Technology Conference, 2003. VTC 2003-Fall. 2003 IEEE 58th*, vol. 2, pp. 1128–1132, IEEE, 2003.

[41] A. L. de Almeida, G. Favier, and J. C. M. Mota, "A constrained factor decomposition with application to mimo antenna systems," *IEEE Transactions on Signal Processing*, vol. 56, no. 6, pp. 2429–2442, 2008.

[42] G. Favier, M. N. Da Costa, A. L. De Almeida, and J. M. T. Romano, "Tensor space–time (tst) coding for mimo wireless communication systems," *Signal Processing*, vol. 92, no. 4, pp. 1079–1092, 2012.

[43] G. Favier and A. L. de Almeida, "Overview of constrained parafac models," *EURASIP Journal on Advances in Signal Processing*, vol. 2014, no. 1, p. 142, 2014.

[44] F. Roemer and M. Haardt, "Tensor-based channel estimation and iterative refinements for two-way relaying with multiple antennas and spatial reuse," *IEEE Transactions on Signal Processing*, vol. 58, no. 11, pp. 5720–5735, 2010.

[45] A. R. Fernandes, A. L. de Almeida, and D. B. da Costa, "Blind receiver for amplify-and-forward cooperative diversity scheme," in *Signal Processing Advances in Wireless Communications (SPAWC), 2011 IEEE 12th International Workshop on*, pp. 546–550, IEEE, 2011.

[46] C. A. R. Fernandes, A. L. F. de Almeida, and D. B. da Costa, "Unified tensor modeling for blind receivers in multiuser uplink cooperative systems," *IEEE Signal Processing Letters*, vol. 19, no. 5, pp. 247–250, 2012.

[47] A. L. de Almeida, C. A. Fernandes, and D. B. da Costa, "Multiuser detection for uplink ds-cdma amplify-and-forward relaying systems," *IEEE Signal Processing Letters*, vol. 20, no. 7, pp. 697–700, 2013.

[48] L. R. Ximenes, G. Favier, A. L. de Almeida, and Y. C. Silva, "Parafac-paratuck semi-blind receivers for two-hop cooperative mimo relay systems," *IEEE Trans. Signal Process*, vol. 62, no. 14, pp. 3604–3615, 2014.

[49] G. Favier, C. A. R. Fernandes, and A. L. de Almeida, "Nested tucker tensor decomposition with application to mimo relay systems using tensor space–time coding (tstc)," *Signal Processing*, vol. 128, pp. 318–331, 2016.

[50] A. A. Teixeira Peixoto and A. Fernandes, "Tensor-Based multiuser detection for uplink DS-CDMA systems with cooperative diversity," in *XXXV Simpósio Brasileiro de Telecomunicações e Processamento de Sinais (SBrT 2017)*, (São Pedro, Brazil), Sept. 2017.

[51] P. M. Ramos Oliveira and A. Fernandes, "Paratuck-3 semi-blind receivers for three-hop cooperative mimo relay systems," in *XXXV Simpósio Brasileiro de Telecomunicações e Processamento de Sinais (SBrT 2017)*, (São Pedro, Brazil), Sept. 2017.

[52] A. Y. Kibangou and A. L. de Almeida, "Distributed khatri-rao space-time coding and decoding for cooperative networks," in *Signal Processing Conference, 2011 19th European*, pp. 809–813, IEEE, 2011.

[53] J. B. Kruskal, "Three-way arrays: rank and uniqueness of trilinear decompositions, with application to arithmetic complexity and statistics," *Linear algebra and its applications*, vol. 18, no. 2, pp. 95–138, 1977.

[54] L. R. Tucker, "Some mathematical notes on three-mode factor analysis," *Psychometrika*, vol. 31, no. 3, pp. 279–311, 1966.

[55] R. A. Harshman and M. E. Lundy, "The parafac model for three-way factor analysis and multidimensional scaling," *Research methods for multimode data analysis*, vol. 46, pp. 122–215, 1984.

[56] A. Stegeman and N. D. Sidiropoulos, "On kruskal's uniqueness condition for the candecomp/parafac decomposition," *Linear Algebra and its applications*, vol. 420, no. 2-3, pp. 540–552, 2007.

[57] N. D. Sidiropoulos and R. Bro, "On the uniqueness of multilinear decomposition of n-way arrays," *Journal of chemometrics*, vol. 14, no. 3, pp. 229–239, 2000.

[58] L. De Lathauwer, "A link between the canonical decomposition in multilinear algebra and simultaneous matrix diagonalization," *SIAM journal on Matrix Analysis and Applications*, vol. 28, no. 3, pp. 642–666, 2006.

[59] L. De Lathauwer, B. De Moor, and J. Vandewalle, "An introduction to independent component analysis," *Journal of chemometrics*, vol. 14, no. 3, pp. 123–149, 2000.

[60] S. Choi, A. Cichocki, H.-M. Park, and S.-Y. Lee, "Blind source separation and independent component analysis: A review," *Neural Information Processing-Letters and Reviews*, vol. 6, no. 1, pp. 1–57, 2005.

[61] J. M. Lattin, J. D. Carroll, and P. E. Green, *Analyzing multivariate data*. Thomson Brooks/Cole Pacific Grove, CA, 2003.

[62] P. M. Kroonenberg, *Three-mode principal component analysis: Theory and applications*, vol. 2. DSWO press, 1983.

[63] I. Jolliffe, *Principal component analysis*. Wiley Online Library, 2002.

[64] P. M. Kroonenberg and J. De Leeuw, "Principal component analysis of three-mode data by means of alternating least squares algorithms," *Psychometrika*, vol. 45, no. 1, pp. 69–97, 1980.

[65] E. Acar, C. Aykut-Bingol, H. Bingol, R. Bro, and B. Yener, "Multiway analysis of epilepsy tensors," *Bioinformatics*, vol. 23, no. 13, pp. i10–i18, 2007.

[66] L. N. Ribeiro, A. R. Hidalgo-Muñoz, G. Favier, J. C. M. Mota, A. L. De Almeida, and V. Zarzoso, "A tensor decomposition approach to noninvasive atrial activity extraction in atrial fibrillation ecg," in *Signal Processing Conference (EUSIPCO), 2015 23rd European*, pp. 2576–2580, IEEE, 2015.

[67] D. A. Fleisch, *A student's guide to vectors and tensors*. Cambridge University Press, 2011.

[68] L. N. Ribeiro, "On supervised multilinear filtering: applications to system identification and antenna beamforming," 2016.

[69] X. Zhang and D. Xu, "Blind parafac receiver for space-time block-coded cdma system," in *Communications, Circuits and Systems Proceedings, 2006 International Conference on*, vol. 2, pp. 675–678, IEEE, 2006.

[70] A. Y. Kibangou and A. De Almeida, "Distributed parafac based ds-cdma blind receiver for wireless sensor networks," in *Signal Processing Advances in Wireless Communications (SPAWC), 2010 IEEE Eleventh International Workshop on*, pp. 1–5, IEEE, 2010.

[71] S. Liu and G. Trenkler, "Hadamard, khatri-rao, kronecker and other matrix products," *Int. J. Inform. Syst. Sci*, vol. 4, no. 1, pp. 160–177, 2008.

[72] R. A. Harshman, "Determination and proof of minimum uniqueness conditions for parafac1," *UCLA Working Papers in phonetics*, vol. 22, no. 111-117, p. 3, 1972.

[73] N. D. Sidiropoulos and R. Bro, "On communication diversity for blind identifiability and the uniqueness of low-rank decomposition of n-way arrays," in *Acoustics, Speech, and Signal Processing, 2000. ICASSP'00. Proceedings. 2000 IEEE International Conference on*, vol. 5, pp. 2449–2452, IEEE, 2000.

[74] T. Jiang and N. D. Sidiropoulos, "Kruskal's permutation lemma and the identification of candecomp/parafac and bilinear models with constant modulus constraints," *IEEE Transactions on Signal Processing*, vol. 52, no. 9, pp. 2625–2636, 2004.

[75] P. Comon, X. Luciani, and A. L. De Almeida, "Tensor decompositions, alternating least squares and other tales," *Journal of chemometrics*, vol. 23, no. 7-8, pp. 393–405, 2009.

[76] W. A. Syafei, Y. Nagao, M. Kurosaki, B. Sai, and H. Ochi, "A gigabit mimo wlan system with international standardization strategy," in *Intelligent Signal Processing and Communication Systems, 2009. ISPACS 2009. International Symposium on*, pp. 228–231, IEEE, 2009.

[77] V. Chande, H. Sun, P. K. Vitthaladevuni, J. Hou, and B. Mohanty, "Performance analysis of 64-qam and mimo in release 7 wcdma (hspa+) systems," in *Vehicular Technology Conference (VTC 2010-Spring), 2010 IEEE 71st*, pp. 1–5, IEEE, 2010.

[78] Q. Li, G. Li, W. Lee, M.-i. Lee, D. Mazzarese, B. Clerckx, and Z. Li, "Mimo techniques in wimax and lte: a feature overview," *IEEE Communications magazine*, vol. 48, no. 5, 2010.

[79] R. H. Roy III and B. Ottersten, "Spatial division multiple access wireless communication systems," May 7 1996. US Patent 5,515,378.

[80] A. J. Paulraj and T. Kailath, "Increasing capacity in wireless broadcast systems using distributed transmission/directional reception (dtdr)," Sept. 6 1994. US Patent 5,345,599.

[81] A. Nosratinia, T. E. Hunter, and A. Hedayat, "Cooperative communication in wireless networks," *IEEE communications Magazine*, vol. 42, no. 10, pp. 74–80, 2004.

[82] G. Kaur and P. P. Bhattacharya, "A survey on cooperative diversity and its applications in various wireless networks," *arXiv preprint arXiv:1112.2248*, 2011.

[83] R. B. Ertel, P. Cardieri, K. W. Sowerby, T. S. Rappaport, and J. H. Reed, "Overview of spatial channel models for antenna array communication systems," *IEEE personal communications*, vol. 5, no. 1, pp. 10–22, 1998.

[84] F. S. Gutleber, "Orthogonal cdma system utilizing direct sequence pseudo noise codes," July 17 1984. US Patent 4,460,992.

[85] S. R. Kim, Y. G. Jeong, and I.-K. Choi, "A constrained mmse receiver for ds/cdma systems in fading channels," *IEEE Transactions on communications*, vol. 48, no. 11, pp. 1793–1796, 2000.